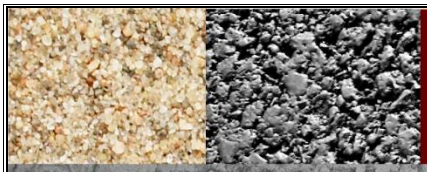

Civil and Environmental Engineering Department

Columbus Mississippi Field Aging and Laboratory Conditioning Study: Plant Mixed and Field Compacted Asphalt Test Sections

Report Written and Performed By:

Braden T. Smith – Mississippi State University

Isaac L. Howard – Mississippi State University

Robert A. Moore – Mississippi State University

Final Report

FHWA/MS-DOT-RD-18-266/270-Volume 2

December 2018

Mississippi State University

CMRC

Construction Materials Research Center

An Industry, Agency & University Partnership

Technical Report Documentation Page

1. Report No. FHWA/MS-DOT-RD-18-266/270-Volume 2	2. Government Accession No.	3. Recipient's Catalog No.
4. Title and Subtitle Columbus Mississippi Field Aging and Laboratory Conditioning Study: Plant Mixed and Field Compacted Asphalt Test Sections		5. Report Date December 2018
		6. Performing Organization Code
7. Author(s) *Braden T. Smith*, Alumni, MSU *Isaac L. Howard*, Materials and Construction Industries Chair, MSU *Robert A. Moore*, Alumni, MSU		8. Performing Organization Report No.
9. Performing Organization Name and Address Mississippi State University (MSU) Civil and Environmental Engineering Department 501 Hardy Road: P.O. Box 9546 Mississippi State, MS 39762		10. Work Unit No. (TRAIS)
		11. Contract or Grant No.
12. Sponsoring Agency Name and Address Mississippi Department of Transportation (MDOT) Research Division P.O. Box 1850 Jackson, MS 39215-1850		13. Type of Report and Period Covered Final Report March 2013 to June 2018
		14. Sponsoring Agency Code

Supplementary Notes: Work was performed under Mississippi State University projects titled: Asphalt Mixture Field Aging Study Preliminary Testing (Project No. 106526 101000), Field Aging Effects on Asphalt Mixed at Different Temperatures and Hauled Different Distances (State Study 266), and Laboratory Conditioning and Field Aging of Asphalt Mixtures (State Study 270). All work performed for this report was under principal investigator Isaac L. Howard. Two additional reports were performed as part of Project 106526 101000, State Study 266, and State Study 270, which were designated FHWA/MS-DOT-RD-18-266/270-Volume 1 and FHWA/MS-DOT-RD-18-266/270-Volume 3. Both additional volumes deal with field aging of asphalt mixtures and all three reports complement each other.

16. Abstract

The main objective of this report was to characterize the effects of short and long term aging for a full-scale and non-trafficked asphalt test section originally built as part of an emergency paving demonstration. The primary data sets collected for this overall body of work are from full-scale constructed test sections where cores were collected over time (Volume 2), and from plant mixed asphalt containing warm mix technology that was field aged for four years or laboratory conditioned (Volume 3). Approximately 5,100 mixture specimens were tested as part of this three volume set of reports. When rounded to the nearest hundred mixture specimens, 300 were tested for Volume 1, 3,400 were tested for Volume 2, and 1,400 were tested for Volume 3. Binder testing was also performed in support of mixture testing. One recommendation from this work was to rely on ASTM D7227 to remove moisture induced during short exposure periods more so than to remove moisture induced during long exposure periods such as years of field aging. Cantabro Mass Loss (CML) testing is recommended when paired with a laboratory conditioning protocol to assess the effects field aging has on asphalt pavement. The default recommendation is to expose a specimen to 5 days of 85 ºC air, followed by 14 days submerged in 64 ºC water, and 1 freeze-thaw cycle before testing for CML, which was able to simulate around 4 to 5 years of exposure to the Mississippi climate. Testing binder sampled during construction in a pressure aging vessel (PAV) in conjunction with binder recovered at the surface and at depth in the test sections showed roughly 11 hours of PAV conditioning was needed to simulate one year of the Mississippi climate on the pavement surface, while 3 hours of PAV conditioning simulated one year at depth.

17. Key Words WMA, Aging, Cantabro, Evotherm, Foam, Fracture Energy, Hamburg		18. Distribution Statement No distribution restrictions.	
19. Security Classif. (of this report) Unclassified	20. Security Classif. (of this page) Unclassified	21. No. of Pages 122	22. Price

Form DOT F 1700.7 (8-72) **Reproduction of completed page authorized**

NOTICE

The contents of this report reflect the views of the author, who is responsible for the facts and accuracy of the data presented herein. The contents do not necessarily reflect the views or policies of the Mississippi Department of Transportation or the Federal Highway Administration. This report does not constitute a standard, specification, or regulation.

This document is disseminated under the sponsorship of the Department of Transportation in the interest of information exchange. The United States Government and the State of Mississippi assume no liability for its contents or use thereof.

The United States Government and the State of Mississippi do not endorse products or manufacturers. Trade or manufacturer's names appear herein solely because they are considered essential to the object of this report.

TABLE OF CONTENTS

LIST OF FIGURES

LIST OF TABLES

ACKNOWLEDGEMENTS

Thanks are due to many for the successful completion of this report. The MDOT Research Division is owed special thanks for funding State Study 266 and State Study 270, both of which followed Project No. 106526 101000. James Watkins served as State Research Engineer at the beginning of this project, with Cindy Smith serving as State Research Engineer at the conclusion of this project. The MDOT Project Engineer was Alex Middleton.

APAC Mississippi supported the field aging test section. The Ergon Asphalt & Emulsions Student Support Initiative in Construction Materials was also beneficial for asphalt activities during a portion of the time frame of this project. Paragon Technical Services, Inc (PTSi) supported all binder testing activities. Several current and former Mississippi State University (MSU) students assisted this project in a variety of manners, mostly as research assistants.

Individuals deserving thanks for the work of Project No. 106526 101000, State Study 266, and State Study 270 include: Thomas Allard, Anna Baglan, Gaylon Baumgardner, Rabeea Bazuhair, Mike Bogue, Justin Cooper, Brittni Cooper, Ben Cox, Will Crawley, Codrin Daranga, Web Floyd, Westin Graves, Bradley Hansen, Mike Hemsley, Chase Hopkins, Amanda Hufft, Chase Hopkins, Trey Jordan, Patrick Kuykendall, Garrison Lipscomb, Rae Ann Otts (Lawrence), Carl Pittman, Matt Roddy, Sonia Serna, Cody Smith, and Abby Sparks.

LIST OF SYMBOLS AND ACRONYMS

a	Inside Cross-Sectional Area of Permeameter Standpipe
A	Cross-Sectional Contact Area
AAPT	Association of Asphalt Paving Technologists
Abs_P	Absorbance Peak
Abs	Aggregate Absorption
AFB	Air Force Base
ANOVA	Analysis of Variance
ARB	As-Received Binder
Avg	Average
BBF	Bending Beam Fatigue
BBR	Bending Beam Rheometer
BBR_S	Bending Beam Rheometer Stiffness Criteria
BBR_m	Bending Beam Rheometer *m*-value Criteria
BMD	Balanced Mix Design
CDD	Cumulative Degree Days
CDD_{high}	High Temperature Cumulative Degree Days
$CD_{fluctuation}$	Cumulative Days of Temperature Fluctuation
CI	Carbonyl Index
CFI	Cumulative Freezing Index
CML	Cantabro Mass Loss
COV	Coefficient of Variation
CP	Conditioning Protocol
CPPC	Cyclic Pore Pressure Conditioning
D	Diameter
DCT	Disc-Shaped Compact
DDC	Deformation Differential Curve
DGA	Dense Graded Asphalt
d2s	Limit for Acceptable Difference Between Two Test Results
DSR	Dynamic Shear Rheometer
DSR_8	Dynamic Shear Rheometer Test Using 8 mm Plates
DSR_{25}	Dynamic Shear Rheometer Test Using 25 mm Plates
ECS	Environmental Conditioning System
ESAL	Equivalent Single Axle Load
FCB	Field Core Binder
FCB_0	Field Core Binder Recovered from 0 to 1.3 cm Below Pavement Surface
FCB_5	Field Core Binder Recovered from 5 to 6.3 cm Below Pavement Surface
FDO	Forced Draft Oven
FDOA	Forced Draft Oven Aging
FE	Fracture Energy
FE_{+20C}	Fracture Energy at 20°C
FE_{-10C}	Fracture Energy at -10°C
FI	Freezing Index
FL	Full Layer

FT	Freeze-Thaw
FTIR	Fourier Transformation Infrared Spectroscopy
G^*	Complex Shear Modulus
GAS	Global Aging System
GLWT	Georgia Loaded Wheel Tester
G_{mb}	Bulk Specific Gravity of Mix
ΔG_{mm}	Increase in Maximum Specific Gravity
G_{mm}	Maximum Specific Gravity
G_{sa}	Apparent Specific Gravity of Aggregate
G_{sb}	Bulk Specific Gravity of Aggregate
GTR	Ground Tire Rubber
h_1	Initial Head Across the Test Specimen
h_2	Final Head Across the Test Specimen
HLWT	Hamburg Loaded Wheel Test
HMA	Hot-Mix Asphalt
ΔHT	Haul Time Increase
HT	Haul Time
h_t	Specimen Height
IA-DT	Iowa Durability Test
IDT	Indirect Tensile Strength
Inf	Infiltration Rate
LCPC	French Wheel Tracker
LMLC	Laboratory Mixed and Laboratory Compacted
LPO	Low Pressure Oxidation
LTOA	Long Term Oven Aging
Maat	Mean Annual Air Temperature
MDOT	Mississippi Department of Transportation
M_1	Initial Specimen Mass
M_2	Final Specimen Mass
M_{core}	Core Mass
ΔML_{CI}	95% Confidence Interval for Difference Between ML_f and ML_l
ML	Mass Loss
$ML_{(Tbl\ 7.1)}$	Mass Loss Prediction Based on Table 7.1 (5 years of aging)
$ML_{(Tbl\ 9.1)}$	Mass Loss Prediction Based on Table 9.1 (6 years of aging)
ML_f	Mass Loss of Field Aged Core
ML_l	Mass Loss of Laboratory Conditioned Core
MLR	Mass Loss Ratio
MMLS3	Model Mobile Load Simulator
M_R	Resilient Modulus
MSP	Mississippi Permeameter
n	Number of Specimens Tested
n_o	Number of Outliers Removed
n_{pairs}	Number of Pairs Considered
NDG	Nuclear Density Gauge
NMAS	Nominal Maximum Aggregate Size
OGFC	Open Graded Friction Course

P_{200}	Percent of Material Finer than 0.075 mm
PAV	Pressure Aging Vessel
PAVi	Pressure Aging Vessel Time
P_b	Asphalt Binder Content
$P_{ba(mix)}$	Absorbed Asphalt Binder Content by Mixture Mass
P_{be}	Effective Asphalt Binder Content
Pen	Penetration
P/F	Pass/Fail
PG	Performance Grade
PL	Permeability Locations
P_{max}	Ultimate Load
PMFC	Plant Mixed and Field Compacted
PMLC	Plant Mixed and Laboratory Compacted
PTSi	Paragon Technical Services, Inc.
PURWheel	Purdue University Laboratory Wheel Tracking Device
p-value	Probability of Non-significance
R^2	Coefficient of Determination
R^2_{adj}	Adjusted Coefficient of Determination
RAP	Reclaimed Asphalt Pavement
RAS	Reclaimed Asphalt Shingles
RD_{HLWT}	Rut Depth after 20,000 Hamburg Passes
REOB	Recycled Engine Oil Bottoms
RRP	Rutting Resistance Parameter
RTFO	Rolling Thin Film Oven
S	Stiffness
SAS	Single Aggregate Source
SCB	Semicircular Bend
SGC	Superpave Gyratory Compacted
SHRP	Strategic Highway Research Program
SIDT	Superpave Indirect Tension
SI	Sulfoxide Index
SIP	Stripping Inflection Point
SMA	Stone Matrix Asphalt
SS266	State Study 266
SS270	State Study 270
S_t	Indirect Tensile Strength
$S_{t\ (Tbl\ 7.1)}$	Indirect Tensile Strength Predicted Based on Table 7.1
STOA	Short Term Oven Aging
S_tR	Indirect Tensile Strength Ratio
S-VECD	Simplified Viscoelastic Continuum Damage
ΔT_c	Difference Between Stiffness and m-value based BBR Critical Temperatures
T_c	Critical Temperature
T_{design}	Mixture Design Temperature
T_{dlow}	Minimum Daily Temperature
T_{dmax}	Maximum Daily Temperature
TFOT	Thin Film Oven Test

T_{pre}	Mix Temperature Before Hauling
$T_{production}$	Mixture Production Temperature
T_R	Temperature in Rankine
TSR	Tensile Strength Ratio
TSRST	Thermal Stress Restrained Specimen Test
TxDOT	Texas Department of Transportation
TXOT	Texas Overlay Test
$t_{warm-up}$	Time to re-heat water
t_F	Time in the field measured in years
V_a	Air Voids
V_{aic}	Inter-Connected Air Void Volumes
V_{anc}	Non-Connected Air Void Volumes
$V_{a-\Delta o}$	Observed Error in V_a Measurement
V_{be}	Volume of Effective Binder
$V_{Gsa-Gse}$	Volume in aggregate pores not filled with asphalt binder
VMA	Voids in Mineral Aggregates
WMA	Warm Mixed Asphalt
Z	Pavement Depth
ε_{ult}	Peak Stress
δ	Phase Angle
η	Viscosity
η_{orig}	Original Viscosity
$\eta_{t=0}$	As-Constructed Viscosity
η_{aged}	Aged Viscosity

CHAPTER 1-INTRODUCTION

1.1 General and Background Information

It is generally accepted that Strategic Highway Research Program (SHRP) activities reduced asphalt pavement rutting from levels that were often problematic to levels that are often not the most problematic distress. In present day, durability and cracking distresses are often governing pavement life. This is partly due to the success of the SHRP program, but is also being contributed to by the ever-increasing emphasis on sustainability and virgin binder prices. Increased emphasis on using reclaimed asphalt pavement (RAP), ground tire rubber (GTR), bituminous shingles, and similar generally results in more rut resistant pavements that have brittleness potential. Methods capable of assessing durability and cracking distresses (i.e. longer term performance distresses) are arguably more important than at any other time in the history of the asphalt paving industry.

Laboratory conditioning protocols to better simulate environmental effects over a several year period would be useful to capture brittle behaviors associated with asphalt mixtures during the design and material selection phases. There has been a widespread discussion of asphalt pavement aging throughout the industry in recent years, and a key point of discussion has been that asphalt aging has not been accurately simulated for a wide range of materials and a wide range of environments using a single laboratory conditioning protocol.

A pavement test section constructed as part of Howard et al. (2012) has been closely monitored since its construction in 2011 and offered a somewhat unique opportunity to evaluate changes to asphalt mixture performance as a result of short and long term aging in Mississippi. This test section is the focus of this report.

1.2 Objectives and Scope

This report is part of a three volume series that investigated: 1) the effects field aging has on asphalt concrete produced at hot mix temperatures and hauled long distances; and 2) the effects field aging has on asphalt concrete produced at different mixing temperatures and hauled a moderate distance. This research effort utilized laboratory and field testing of asphalt mixtures and binders, literature review, and data analysis. The research program was funded by MDOT through Project 106526 101000, State Study 266 (SS266), and State Study 270 (SS270). The three report volumes do not coincide with MDOT funding mechanisms, rather are divided according to technical content. Collectively, these three reports contain all deliverables for these three funded endeavors (1 through Materials Division, 2 through Research Division).

Volume 1 (FHWA/MS-DOT-RD-18-266/270-Volume 1) includes data and analysis of reference mixtures that are intended largely for benchmarking and interpretation of Volume 2 and Volume 3 data. Volume 2 (FHWA/MS-DOT-RD-18-266/270-Volume 2) focused most of its effort on the effects field aging has on asphalt concrete produced at hot mix temperatures and hauled long distances. Volume 3 (FHWA/MS-DOT-RD-18-266/270-Volume 3) focused most of its efforts on the effects field aging has on asphalt concrete produced at different mixing temperatures and hauled a moderate distance.

The main objective of this report (Volume 2) was to characterize the effects of short and long term aging for a full-scale and non-trafficked asphalt test section originally built as part of an emergency paving demonstration documented in Howard et al. (2012). Volume 2 focuses on field aging and laboratory conditioning of plant mixed and field compacted (PMFC) asphalt within a test section constructed at APAC Mississippi, Inc's Columbus facility. The majority of the testing conducted for this report was performed on cores or plant mixed and laboratory compacted (PMLC) specimens produced from mixtures sampled during construction, though some evaluations were conducted on asphalt binders sampled the same day as construction. There was no data collected from laboratory mixed and laboratory compacted (LMLC) specimens in this portion of the effort.

Remaining chapters in this document report the findings of this investigation relative to the full-scale pavement test section in Columbus, MS. Chapter 2 presents a literature review. Chapter 3 describes the pavement test section and experimental program. The remaining chapters provide test results and analysis.

1.3 Summary of Asphalt Mixtures Considered

There were a total of 20 asphalt mixtures (M01 to M20) tested as part of this research program (Project 106526 101000, SS266, and SS270). This section is repeated in all three volumes for clarity, and an asphalt mixture is defined as a unique combination of ingredients at consistent proportions. A single mixture could be produced in different ways and at different points in time using the same aggregate and asphalt binder sources at consistent proportions. For example, one mixture could be plant-mixed and field compacted (PMFC), plant-mixed and laboratory compacted (PMLC), or laboratory-mixed and laboratory compacted (LMLC). M01 to M13 were the focus of Volume 1 as an investigation of single aggregate source (SAS) and Air Force Base (AFB) mixtures which were often field aged on the full-scale test section described in Chapter 3 of Volume 2. M14 to M16 were the focus of this report (Volume 2) which considers the full-scale and non-trafficked test section described in Chapter 3 of this report. Volume 3 relies on results from M17 to M20 which were also field aged on the full-scale test section. Tables 1.1 to 1.3 provide mixture design volumetric information, ingredient source information, and gradations, respectively. All terms used in Tables 1.1 to 1.3 are provided in the list of symbols.

Table 1.2 describes constituent materials in M01 to M20 by type, source, and sample (where documented). M01 to M10 were lab mixed from constituent materials and M11 to M20 were plant mixed. Aggregate sources which were sampled in more than one paving season are differentiated by year, and sample number differentiates binder samples. Notice that a single sample of asphalt binder was used for M01 to M10 and M17 to M20.

Table 1.1. Mixture Volumetric Properties Utilized During Research Program

Mix ID	T_{design} (°C)	$T_{production}$ (°C)	G_{mm}	G_{sb}	G_{se}	G_{sa}	P_b (%)	P_{be} (%)	$P_{ba\ (mix)}$ (%)	VMA (%)	Design V_a (%)	V_{be} (%)	P_{200} (%)	NMAS (mm)
M01	163	163	2.250	2.385	2.520	2.651	8.3	6.2	2.3	16.9	4	12.9	6.0	12.5
M02	163	163	2.250	2.385	2.520	2.651	8.3	6.2	2.3	16.9	4	12.9	6.0	12.5
M03	163	163	2.250	2.385	2.520	2.651	8.3	6.2	2.3	16.9	4	12.9	6.0	12.5
M04	129	129	2.248	2.385	2.505	2.651	8.0	6.1	2.1	16.8	4	12.8	6.0	12.5
M05	129	129	2.248	2.385	2.505	2.651	8.0	6.1	2.1	16.8	4	12.8	6.0	12.5
M06	129	129	2.248	2.385	2.505	2.651	8.0	6.1	2.1	16.8	4	12.8	6.0	12.5
M07	163	163	2.479	2.694	2.733	2.743	6.2	5.7	0.5	17.2	4	13.2	5.9	12.5
M08	129	129	2.481	2.694	2.735	2.743	6.2	5.7	0.5	17.0	4	13.0	5.9	12.5
M09	163	163	2.123	2.248	2.362	2.507	8.7	6.7	2.2	17.2	4	13.2	6.2	12.5
M10	129	129	2.125	2.248	2.351	2.507	8.3	6.5	2.0	16.8	4	12.8	6.2	12.5
M11	150	150	2.531	2.693	2.753	2.811	5.2	4.4	0.8	14.1	4	10.1	4.5	12.5
M12	166	160	2.370	2.484	2.560	2.653	6.0	4.8	1.2	14.3	4	10.3	4.0	12.5
M13	177	160	2.381	2.481	2.556	2.607	5.9	4.8	1.2	14.3	4	10.3	4.5	12.5
M14	160	164	2.378[A]	2.515	2.567	2.663	5.4	4.6	0.8	14.1	4	10.1	5.9	12.5
M15	160	153	2.378[A]	2.515	2.567	2.663	5.4	4.6	0.8	14.1	4	10.1	5.9	12.5
M16	160	148	2.378[A]	2.515	2.567	2.663	5.4	4.6	0.8	14.1	4	10.1	5.9	12.5
M17	143	143	2.461	2.609	2.668	2.688	5.3	4.5	0.8	14.3	4	10.3	4.9	12.5
M18	129	132	2.461	2.609	2.668	2.688	5.3	4.5	0.8	14.3	4	10.3	4.9	12.5
M19	129	132	2.461	2.609	2.668	2.688	5.3	4.5	0.8	14.3	4	10.3	4.9	12.5
M20	129	132	2.461	2.609	2.668	2.688	5.3	4.5	0.8	14.3	4	10.3	4.9	12.5

A: Mix design values are shown – other values were used such as those sampled from the paver in most areas throughout the work.

Table 1.2. Mixture Components Information Utilized During Research Program

Mix ID	Aggregates								Asphalt Binder			
	Gravel		Limestone		Sand		RAP	HL	PG		Warm Mix	
	Source	(%)	Source	(%)	Source	(%)	(%)	(%)	Grade	Source	Technology	Sample
M01	Hamilton, MS (’13)	100	---	---	---	---	---	---	67-22	Vicksburg, MS	---	1
M02	Hamilton, MS (’13)	100	---	---	---	---	---	---	67-22	Vicksburg, MS	0.5% Evo.	1
M03	Hamilton, MS (’13)	100	---	---	---	---	---	---	67-22	Vicksburg, MS	1.5% Sasobit	1
M04	Hamilton, MS (’13)	100	---	---	---	---	---	---	67-22	Vicksburg, MS	---	1
M05	Hamilton, MS (’13)	100	---	---	---	---	---	---	67-22	Vicksburg, MS	0.5% Evo.	1
M06	Hamilton, MS (’13)	100	---	---	---	---	---	---	67-22	Vicksburg, MS	1.5% Sasobit	1
M07	---	---	Tuscaloosa, AL (’13)	100	---	---	---	---	67-22	Vicksburg, MS	---	1
M08	---	---	Tuscaloosa, AL (’13)	100	---	---	---	---	67-22	Vicksburg, MS	---	1
M09	Creede, CO	100	---	---	---	---	---	---	67-22	Vicksburg, MS	---	1
M10	Creede, CO	100	---	---	---	---	---	---	67-22	Vicksburg, MS	---	1
M11	---	---	California	100	---	---	---	---	70-10	California	---	1
M12	Hamilton, MS (’13)	51	Tuscaloosa, AL (‘13)	33	Hamilton, MS (’13)	15	---	1	76-22	Memphis, TN	---	1
M13	Hamilton, MS (’13)	41	Tuscaloosa, AL (‘13)	25	Hamilton, MS (’13)	13	20	1	70-22	Memphis, TN	---	1
M14	Hamilton, MS (’11)	39	Tuscaloosa, AL (‘11)	35	Hamilton, MS (’11)	10	15	1	67-22	Vicksburg, MS	---	2
M15	Hamilton, MS (’11)	39	Tuscaloosa, AL (‘11)	35	Hamilton, MS (’11)	10	15	1	67-22	Vicksburg, MS	Foamed	2
M16	Hamilton, MS (’11)	39	Tuscaloosa, AL (‘11)	35	Hamilton, MS (’11)	10	15	1	67-22	Vicksburg, MS	0.5% Evo.	2
M17	Undocumented	25	Calera, AL	60	Undocumented	15	---	---	67-22	Vicksburg, MS	---	1
M18	Undocumented	25	Calera, AL	60	Undocumented	15	---	---	67-22	Vicksburg, MS	Foamed	1
M19	Undocumented	25	Calera, AL	60	Undocumented	15	---	---	67-22	Vicksburg, MS	0.5% Evo.	1
M20	Undocumented	25	Calera, AL	60	Undocumented	15	---	---	67-22	Vicksburg, MS	1.5% Sasobit	1

Hydrated Lime (HL); Reclaimed Asphalt Pavement (RAP); Evotherm 3G™ (Evo.)

Table 1.3. Mixture Gradations Utilized During Research Program

Mix ID	Percent Passing (%)										
	25 mm	**19 mm**	**12.5 mm**	**9.5 mm**	**No. 4**	**No. 8**	**No. 16**	**No. 30**	**No. 50**	**No. 100**	**No. 200**
M01	100	100	96	88	70	53	37	27	14	7.6	6.0
M02	100	100	96	88	70	53	37	27	14	7.6	6.0
M03	100	100	96	88	70	53	37	27	14	7.6	6.0
M04	100	100	96	88	70	53	37	27	14	7.6	6.0
M05	100	100	96	88	70	53	37	27	14	7.6	6.0
M06	100	100	96	88	70	53	37	27	14	7.6	6.0
M07	100	100	96	87	67	48	25	17	12	8.4	5.9
M08	100	100	96	87	67	48	25	17	12	8.4	5.9
M09	100	100	96	87	67	48	29	17	12	8.6	6.2
M10	100	100	96	87	67	48	29	17	12	8.6	6.2
M11	100	100	95	83	64	49	33	22	13	7.0	4.5
M12	100	100	96	88	61	44	31	22	11	6.0	4.0
M13	100	100	93	85	57	38	27	21	11	6.0	4.5
M14	100	100	95	85	54	36	25	19	11	7.5	5.9
M15	100	100	95	85	54	36	25	19	11	7.5	5.9
M16	100	100	95	85	54	36	25	19	11	7.5	5.9
M17	100	100	96	85	68	54	38	28	15	6.8	4.9
M18	100	100	96	85	68	54	38	28	15	6.8	4.9
M19	100	100	96	85	68	54	38	28	15	6.8	4.9
M20	100	100	96	85	68	54	38	28	15	6.8	4.9

CHAPTER 2 – LITERATURE REVIEW

2.1 Overview of Literature Review

Asphalt pavement durability and methods for simulating field aging of pavements to a condition where behaviors of non-durable pavements can begin to be commonly encountered are of primary interest within this literature review. Several investigations are first referenced to identify pavement behaviors associated with durable and non-durable pavements and factors related to poor or increased durability (Section 2.2). Industry changes to methods for measuring air voids (V_a), the most frequently discussed pavement performance property, are then discussed from the 1920s to current day (Section 2.3).

Section 2.4 presents a review of literature discussing investigations for the effects of short-term aging (i.e., period involving mixture production, storage, hauling, laydown, compaction, and cooling). The effects of long term aging (i.e., period beginning immediately after pavements have cooled) and methods for simulating long term aging are discussed in Section 2.5. Note that this investigation only uses "aging" to describe effects produced by the natural environment and uses "conditioning" to describe any laboratory methods to simulate aging. The last two sections of this chapter discuss methods for measuring pavement mixture performance (Section 2.6) and asphalt binder characteristics (Section 2.7).

2.2 Pavement Durability

In ideal circumstances, asphalt mixtures are designed to maximize durability performance while minimizing the potential for rutting. Rutting and durability distresses have been a primary topic of discussion since the early days of asphalt paving. Rutting is a pavement distress usually observed early during pavement service, if at all. Asphalt durability, however, can be more elusive with multiple types of later-age pavement distresses contributing to what is generally referred to as pavement durability. The remainder of this section provides a review of literature relative to defining asphalt pavement durability, identifying mixture properties associated with durable mixtures, and describing the current state of the industry with respect to durability.

2.2.1 Definitions and Factors of Pavement Durability

The definition of asphalt pavement durability has evolved multiple times with the progression of time but key principles are generally maintained over time. Hveem (1943) described cracking and raveling as durability issues. Over a decade later, Vallerga et al. (1957) stated that durable asphalt mixtures were "resistant to the effects of weathering and the abrasive action of traffic over a period of years." Finn (1967) described durability as the long-term "resistance to weathering, including aging, and the abrasive action of traffic" and the "ability of materials to resist change during weathering." Twenty years ago, Copas and Pennock (1979) defined durability as the "resistance of asphalt pavement surface to change during service."

Several mixture properties have been identified to affect pavement durability. A literature review presented in Cox et al. (2017) provides literature identifying initial pavement mixture properties associated with improved durability (Table 2.1).

Table 2.1. Pavement Durability Factors

Pavement Durability Factor	Reference(s)
High Binder Content	Finn, 1967; Hubbard and Gollomb, 1937
Softest Non-Rutting Binder Grade	Hubbard and Gollamb, 1937
Dense Aggregate Gradation	Finn, 1967
Lowest Reasonable Mixing Temperature	Hubbard and Gollamb, 1937
Decreased In-place V_a	Finn, 1967; Copas and Pennock, 1979; Hubbard and Gollomb, 1937; Kandhal and Koehler, 1984

2.2.2 Effects of In-Place Density

Increased pavement density (or decreased V_a) has been discussed most frequently as a driver of pavement performance including durability over the past five decades. Table 2.2 provides a summary of V_a relationships, and the following paragraphs provides discussion of each investigation.

Table 2.2 Air Void Relationships to Pavement Durability Factors

Reference(s)	Finding
Epps and Monismith (1969)	↑V_a produces ↓Fatigue Life
Kandhal and Koehler (1984)	V_a was closest indicator of performance when compared with penetration, viscosity (60°C), and ductility (16°C)
Santucci et al. (1985)	↑V_a produces ↑ aged viscosity (60°C) and ↓ aged pen.
Epps et al. (2002) and Monismith et al. (2004)	↑V_a from 5% to 9% produced non-linear ↓Fatigue Life by 75%.
Hekmatfare et al. (2015)	A modified mixture design producing specimens with equal V_{be} at 5% performed as well or better than mixtures designed to 4% V_a, which were expected to achieve approximately 7% V_a in-place.

Epps and Monismith (1969) investigated mixtures in controlled-stress flexural fatigue tests. While fatigue performance is different from the current investigation, in that it considers the effects of traffic loading, some of the factors considered in fatigue performance can also be related to durability. Epps and Monismith (1969) considered the effects of loading type, asphalt properties, asphalt content, aggregate type, aggregate gradation, specimen stiffness, and V_a. Original asphalt properties consisted of penetration at 25°C, viscosity at 60°C and 135°C, and flash point. Penetration at 25°C and softening point were also considered for asphalt materials recovered from mixtures used in the study. Asphalt binder contents varied from 4.4% to 7.7% by mixture mass, and there were three asphalt binders used (40-50, 60-70, 85-100). Four aggregate types (crushed basalt, crushed limestone, crushed granite, and crushed gravel) were evaluated in conjunction with four aggregate gradations with a 12.5 mm nominal maximum aggregate size (NMAS). The study concluded that increasing V_a reduced fatigue life and mixture stiffness, the effects of aggregate type were unclear, asphalt type influenced fatigue life, and asphalt content produced a noticeable change in fatigue performance.

Kandhal and Koehler (1984) presented an investigation of several pavements in Pennsylvania during a period when many state DOTs were conducting durability investigations. Three separate durability studies were summarized, and pavement performance

was related to V_a, penetration at 25°C , viscosity at 60°C, and ductility at 16°C. In cases where V_a was considered, V_a was the primary pavement property indicative of performance with increased performance associated with decreased V_a.

Santucci et al. (1985) evaluated the effects of moisture and the level of compaction achieved in-place with respect to raveling and stripping resistance for several pavements in Oregon. Most pavements were between two and five years old when evaluated. While the authors evaluated field aged properties, and there were some conditioning methods utilized (e.g., the Lottman (1982a) procedure and rolling thin film oven), the key contribution of the paper was to identify variables of early failure – not to address aging over time. Through mixture (i.e., resilient modulus) and binder (i.e., viscosity, ductility, and penetration) property evaluation, the study concluded that moisture induced damage and increased V_a can lead to accelerated pavement failure. Further, two phases of moisture induced damage were identified, moisture retained during construction and moisture exposure during service. For a collection of pavements which were between three and five years old, there was an increasing linear relationship developed between V_a and viscosity at 60°C and a decreasing non-linear relationship between V_a and percentage of retained penetration.

A performance related specification for HMA construction was suggested in Epps et al. (2002) based on results of WesTrack, a multimillion dollar test road project which considered the effects of V_a. Test sections in WesTrack were constructed at one of three target V_a levels (4%, 8%, or 12%). Information collected during WesTrack was utilized in Monismith et al. (2004) to develop a method for determining performance-based pay factors in asphalt construction. Performance models therein considered failure modes of rutting and fatigue cracking. Rutting variables considered were V_a, asphalt content, and aggregate gradation. Aggregate gradation factors considered in rutting performance models were P_{200}, and the fraction which passes the No. 8 sieve but is retained on the No. 200 sieve. Variables considered in fatigue evaluations were V_a, asphalt content, and asphalt concrete thickness. Simulations performed therein indicated that an increase in V_a from 5% to 9% produced a decrease in the number of ESALs prior to fatigue failure of 75% in a non-linear relationship. Rutting simulations indicated that V_a also played a critical role in the number of ESALs to be experienced prior to rutting to 15 mm or more. The recommended performance-based pay factor approach also considered pavement performance in a holistic manner rather than by weighting individual variables (e.g. V_a).

Hekmatfare et al. (2015) performed a field investigation in Indiana with the attempt to decrease in-place air voids and subsequently increase pavement resistance to oxidation. The field investigation modified gradations of Superpave mixtures originally designed to 4% V_a and 100 gyrations. Subsequent mixtures were designed with equal volume of effective binder (V_{be}) at 5% V_a using compaction levels of 30, 50, and 75 gyrations. Laboratory investigations considered specimens that were compacted to expected field densities of 7% or 5% V_a for traditional and re-designed mixtures, respectively. These comparisons were considered reasonable since they had equal V_{be} and were representative of targeted compaction levels in-place. Dynamic modulus and flow number tests were conducted to characterize mixture stiffness and in-service rutting, respectively. Laboratory results indicated that the re-designed mixtures at decreased V_a, but equal binder volume representative of in-service density, performed as well or better than mixtures designed and placed using traditional methods. Further, a field trial indicated that the re-designed mixtures were able to produce in-place V_a of roughly 5%.

2.2.3 Current State of Asphalt Paving Industry

While the asphalt paving industry has evaluated factors related to pavement durability for several decades, industry transitions in recent years have produced even more need for improved controls on mixture durability. The 2016 Annual Meeting of the Association of Asphalt Paving Technologists (AAPT) included a symposium on balanced mix design (BMD) and a leading-edge workshop on asphalt cracking test methods. This subsection presents a review of information from the aspects of material changes, design modifications, and mixture test methods discussed at the 2016 Annual Meeting of AAPT.

It is generally accepted that one of the primary contributions of the Strategic Highway Research Program (SHRP) was the Superpave mix design method. Further, it is generally accepted that the Superpave mix design method reduced the occurrence of rutting (i.e., a primary accomplishment of Superpave) by generally decreasing binder contents and increasing aggregate angularity. These changes are discussed in Buchanan (2016) where the presenter discussed results of a survey conducted within Oldcastle® materials companies. The survey results indicated that durability related distresses were the predominate forms of pavement distress encountered by the 40 companies surveyed. SHRP activities focused on reducing rutting, and generally speaking increased the potential for pavements to crack. Also, material modifications in recent years seem to have compounded this tendency. Increased use of post-consumer materials (e.g., RAP, RAS, REOB, etc.) have introduced complexities in volumetric principles while most likely increasing the cracking potential of constituent materials. As discussed in Howard et al. (2016), industry transitions away from predominately virgin mixtures utilized in the early 1990's timeframe of SHRP have increased the need for performance controls in mix design and acceptance.

The balanced mix design (BMD) symposium conducted during the 2016 Annual Meeting of AAPT included five presentations discussing the concept. Buchanan (2016) suggested that a performance test could be beneficial, but suggested that a surrogate test might also be beneficial. Zhou (2016) discussed the development and implementation of BMD in Texas. The three implementation challenges mentioned where: a cracking test, longer design times, and higher costs. Bennert (2016) provided information on New Jersey's implementation of BMD. Bennert (2016) suggested using balanced mix design approaches (e.g., asphalt pavement analyzer (APA) for rutting and NJ DOT Overlay Tester for cracking) to develop improved volumetric design requirements. Mohammed (2016) discussed development of BMD specifications in Louisiana, which predominately utilizes the semicircular bend (SCB) test. The overarching theme of the BMD symposium was the need for implementable performance tests for utilization in tandem with existing volumetric principles.

Howard et al. (2016) provided an in-depth review of industry transitions leading to the need for BMD approaches and cracking performance tests discussed at the annual meeting. Therein, the authors note that 17 of the 24 (71%) of the papers presented at the 2016 Annual Meeting of AAPT utilized cracking performance tests in some way. While the current investigation makes use of the Superpave Indirect Tension Test (SIDT) (Section 2.6.4), there are multiple methods considered for cracking performance evaluation discussed in Howard et al. (2016). Other categories of cracking performance testing discussed at the 2016 AM include: Semi-Circular Bend (SCB), Disc-Shaped Compact Tension (DCT), Bending Beam Fatigue (BBF), Texas Overlay Test (TXOT), and Simplified Viscoelastic Continuum Damage (S-VECD).

2.3 Pavement Density Measurement

Although the importance of achieving high pavement density is well documented, methods of measuring pavement density have evolved over the past several years. Three key developments in pavement density measurement have been: improved methods for measuring density of compacted specimens, the development of non-destructive in-place density gauges, and rapid drying techniques that are non-destructive.

Approaches for measuring density of compacted specimens have varied from dimensional measurements in the early twentieth century to vacuum sealing (i.e., CoreLok) in more recent years. Hubbard and Field (1926) evaluated voids in mineral aggregate, implying that air voids were characterized in some way. In-place density was measured for both the WASHO (Highway Research Board, 1953) and AASHO (Highway Research Board, 1962) road tests in the 1950s and 1960s on cubical specimens that were sliced from pavement sections. Beginning in 1978, the Virginia DOT used a method where specimens were dry sawn from pavement sections and Archimedes principle was applied without accounting for moisture absorption during density measurement (Hughes, 1986). Hughes (1986) suggested density measurements that accounted for moisture absorbed during density measurement was a more accurate approach. The density measurement approach suggested by Hughes (1986) is essentially a modified version of AASHTO T166, which was the most widely used method for measuring pavement density by a considerable margin in the early 2000s (Crouch et al., 2002).

While, AASHTO T166-13 remains a predominately used method for measuring compacted density of asphalt mixtures, there have been alternative methods for density measurement considered. Two forms of density measurement which encapsulate specimens in another material prior to density measurement by submerging in water are CoreLok (i.e., AASHTO T331-13) and coating specimens in paraffin wax (i.e., AASHTO T275-07). Santucci et al. (1985) reported that wax-coated measurement was a more consistent measurement of density than surface dry measurement (i.e., T166). Howard and Doyle (2014) evaluated 2,400 data points over a broad collection of mixture properties and concluded that T331 was the most accurate and versatile method for measuring pavement density for varying materials and conditions. Buchanan (2000) evaluated multiple methods of compacted density measurement and concluded that vacuum sealing (i.e., T331) was the most versatile method for measuring density of open graded friction course (OGFC), stone matrix asphalt (SMA), coarse graded Superpave, or fine graded Superpave mixtures.

There have been multiple in-place density gauges developed in attempts to measure pavement density in non-destructive methods. Two density gauges used during the construction of the pavement test section used in this investigation were a Troxler Model 3440 nuclear density gauge (NDG) and a PQI model 301 (Howard et al., 2012). Based on Howard et al. (2012), the Troxler Model 3440 NDG was the more reliable density gauge used therein. This finding somewhat agrees with information presented in Williams et al. (2011), Kandhal and Koehler (1984), and Brown (1990). Williams et al. (2011) concluded that NDG measurements correlate well with T166 measurements, but with a reasonable amount of scatter. Kandhal and Koehler (1984) performed NDG measurements and core density measurements on a series of eight projects. Four projects reported higher NDG measurement than core density measurement, and three projects reported higher core density measurement than NDG measurement. Brown (1990) suggested that NDG was a useful tool but that cores should be taken for in-place density acceptance.

A topic of discussion throughout multiple investigations has been the tendency of moisture retained in asphalt specimens to artificially increase the measured density. Hughes (1986) discussed the influence of sampling technique (i.e., wet vs. dry coring) and the implications of moisture retained from wet coring. The study concluded that the two techniques provided comparable results if wet cored specimens were sufficiently dried prior to determining a specimen mass in air. Brown (1990) stated that density measurements with cores was the most accurate density method but stated that failure to allow cores sufficient time to dry sometimes occurred. The most recent version of AASHTO T166-13 includes a method for rapidly determining specimen density by measuring specimen volume in a partially saturated state and oven drying sufficiently to determine specimen mass in air.

Bae et al. (2012) performed a lab investigation of multiple devices manufactured by Instrotek and evaluated the ability of ASTM D7227 (i.e., CoreDry) to sufficiently remove moisture from field aged cores. Specimens were oven dried to constant mass and subsequently soaked for 2 hours. After soaking, specimens were dried using a CoreDry apparatus and tested using T166. After T166 testing, specimens were re-submerged for 2 hours, oven dried at 52°C for 16 hours, and re-tested using T166. A one to one comparison between bulk density determined after CoreDry and oven drying indicated that the CoreDry was sufficient at removing moisture absorbed during a two-hour submersion period. The results of Bae et al. (2012) suggest that ASTM D7227 is sufficient at removing moisture acquired during coring or any laboratory activities. However, the investigation did not consider moisture absorbed during field aging over long periods of time.

2.4 Short Term Mixture Aging

It has long been understood that asphalt mixtures undergo property changes when exposed to elevated temperatures and oxygen experienced during construction (e.g., Bateman and Lehmann, 1929). Some methods simulate this exposure to elevated temperatures with short-term oven conditioning. However, there is still room for improvement relative to understanding the effects on mixture performance when short-term aging environments are modified or when constituent materials are changed (e.g., RAP, GTR, RAS, etc.). While the predominate theme of this section is conditioning and aging of asphalt mixtures, currently practiced binder conditioning protocols within the performance grading system (i.e., AASHTO M320-10) are also discussed. Key findings to subsequent chapters are presented in Table 2.3, and the following subsections are divided by investigations prior to the 1990s, methods implemented in the 1990s, and investigations conducted since the implementation of Superpave.

Table 2.3. Summary of Short-Term Aging Findings

Reference(s)	Investigation Type	Findings or Developments
Heithaus and Johnson (1958)	Field Test Section	– Binder content and gradation not related to short-term binder hardening. – Binder hardening during construction was ≈ 140% of that achieved in the microfilm durability test.
Wright and Paquette (1966)	Haul Effects	– ↑ haul time (HT) produced ↑ asphalt hardening – ↑ mixing temperature (149°C to 160°C) produced statistically significant, but practically little effect on hardening. – Noticeable gradients in asphalt binder hardening existed within a single truck-load of material. – Additional binder hardening from increased haul time is evident after 3 years of field aging.
Kari (1982)	Silo Storage Effects	– ↑ Storage time produced ↑ binder viscosity
Lund and Wilson (1984, 1986)	Multiple Project Investigation	– Development of "C" value aging equation – Cases with "C" values greater than 30% indicated good performance.
Hveem et al. (1962)	Binder Conditioning	– Rolling Thin Film Oven
Bell et al. (1994a, 1994b); Bell and Sosnovske (1994)	Multiple Project Investigation	– Though extended mixing protocol produced more uniform aging, short term conditioning in forced draft ovens seemed most practical – Conditioning protocols for AASHTO R30
Howard et al. (2013)	Haul Effects	– There was no significant change in PG grade up to an 8 hour haul – Low temperature properties were better for binders in mixtures produced at lower temperatures – The majority of carbonyl and sulfoxide formation occurred during the initial 3 hr of haul time.
Yin et al. (2015)	Multiple Project Investigation	– Short-Term oven conditioning criteria of 2 hr at 135°C (HMA) or 116°C (WMA) is adequate – WMA technology, inclusion of recycled materials, aggregate absorption, and binder source shown to affect stiffness.
Jacques et al. (2016)	Silo Storage Effects	– Significant differences in aging of RAP and virgin mixes – Significant differences in low temperature cracking performance after 5 hr and 7.5 hr for virgin and RAP mixtures.

2.4.1 Short Term Aging Investigations Prior to the 1990s

Most short-term asphalt aging investigations prior to SHRP predominately considered the effects of short term damage on asphalt binder properties. This subsection presents a review of literature leading up to the SHRP where the effects of mixture production and handling were evaluated.

Heithaus and Johnson (1958) investigated four mixtures which were placed on an entrance road for a refinery in Wood River, Illinois. A key point of the investigation was to consider the microfilm durability test described in Griffin et al. (1957) against the effects of short-term aging and long term aging in the Illinois climate. Apparent viscosities of asphalt

cements were evaluated before mixing and on recovered binders soon after compaction and after 36 months of aging (see Section 2.5.1). The study concluded that asphalt content and aggregate gradation had no effect on short term aging of the asphalt cement, and the amount of asphalt hardening during construction was approximately 140% of the hardening produced in the microfilm durability test.

Wright and Paquette (1966) evaluated extracted binder properties for mixtures which had been hauled in trucks for 0, 1, 2, and 4 hr without the use of tarps. Asphalt property tests included absolute viscosity at temperatures of 60, 77, and 95°F, penetration, ductility, and a modest amount of FTIR analysis to support oxidation as a primary cause of hardening. Approximately 100 asphalt mixture samples were taken from ten haul trucks containing mixtures produced using 60-70 penetration grade asphalts from four different binder sources (Humble Oil, Charleston; Hunt Oil, Tuscaloosa; Shell Oil, Atlanta; and Shell Oil, Savannah). No aggregate source or gradation information was provided. Findings from Wright and Paquette (1966) are discussed in the following paragraph.

Wright and Paquette (1966) identified multiple factors that appreciably affect the amount of asphalt hardening experienced during hauling. As expected, asphalt source was identified to affect the degree and rate of asphalt hardening. Mixtures produced at 160°C were shown to have statistically higher absolute viscosity (i.e., approximately 20% higher) when compared to mixtures produced at 149°C, but this effect was deemed of little practical concern. Aging gradients experienced during transport were identified to meaningfully alter binder properties with binder viscosities sampled 30 cm below the material surface have viscosities elevated by 10, 27, and 69% when compared to material sampled from the material surface after 1, 2, and 4 hr of transport, respectively. Material sampled for the main portion of the experiment were quenched in water to accelerate the cooling process, and secondary evaluations showed that quenching with water produced noticeable differences in viscosity results. Ultimately, materials were sampled after field aging (up to 10 months), and comparisons were made between viscosity measurements with for mixtures which were hauled for less than 30 minutes or for 4 hours. Viscosity measured on binder from mixture hauled for 4 hours was consistently higher than mixtures hauled for up to 30 minutes. Viscosity measurements at the surface (i.e., average depth of 3 mm) were meaningfully higher than viscosities measured greater than 12.5 mm deep into the surface, which were relatively consistent. While viscosity measurements were relied upon much more heavily, penetration testing was conducted in many instances and the correlation presented in equation (2.1) was developed between absolute viscosity at 25°C and penetration.

$$\eta_{25°C}(\text{megapoises}) = 3591.3(\text{Pen})^{-1.719} \quad (2.1)$$

Investigations continued in the 1980s, when Kari (1982) provided extracted binder properties for samples collected from mixtures sampled immediately or after 16 hours of hot storage in silos. Viscosity and penetration measurements were used to show that mixtures aged for longer periods of time consistently hardened. Binder viscosities were reported as 1520, 3140, and 8810 Poise at 60°C for original, immediately after mixing, and after 16 hours of hot storage. A relative measure of toughness was shown by the amount of time necessary to penetrate 6.35 mm at 48.9°C. This process took 17 seconds for the binder sampled immediately after mixing and 60 seconds for the binder sampled after 16 hours of storage.

Lund and Wilson (1984, 1986) investigated short-term aging in asphalt plants in Oregon. The authors sampled asphalt mixtures from 29 field projects, and binder properties were determined for samples collected immediately before testing and for recovered binder samples collected from project paving sites. Binder samples were then evaluated as necessary to determine C values from equation (2.2). Lund and Wilson (1984) concluded that mixtures exhibiting C values greater than 30% had adequate performance.

$$C = \frac{R - A}{B - A}(100\%) \tag{2.2}$$

Where;
A = Absolute Viscosity of Original Asphalt
B = Absolute Viscosity of Rolling Thin Film Oven Residue
R = Absolute Viscosity of Asphalt Binder Recovered from Mixture

Lund and Wilson (1986) reported a field validation and discussed the results of implementing findings from the short-term aging information presented in Lund and Wilson (1984). After field validation, the authors concluded that "C" value acceptance specifications appeared to be a good measure of asphalt tenderness properties. The authors mentioned that several contractors with originally poor performance and low "C" values improved performance over the two years between the studies.

2.4.2 Short Term Conditioning Methods Implemented in the 1990s

A currently utilized protocol for short term aging of mixes is oven conditioning as described in AASHTO R30-02 (2010). AASHTO R30 subjects mixtures used for volumetric property measurement to 2 hr of forced draft oven (FDO) conditioning at compaction temperature and mixtures used for mechanical property testing to 4 hr of forced draft oven conditioning at 135°C. Both are on loose mix prior to compaction. R30 also includes a long-term conditioning protocol for compacted mixtures at 85°C for 5 days. These conditioning protocols were adopted from Bell et al. (1994a, 1994b) and Bell and Sosnovske (1994). This subsection discusses the development of the current short term conditioning protocols to simulate short-term field aging.

The Standard Specifications for Performance Graded Asphalt Binders (AASHTO M320-10) utilizes the Rolling Thin Film Oven (RTFO) test (ASTM D2872-12) to characterize the effects of short term binder aging produced during construction. While the performance grading system was originally adopted during the 1990's, the RTFO binder conditioning method was developed in Hveem et al. (1962) and was first approved by ASTM in 1970. The conditioning method claims to approximately change viscosity and other rheological properties as would be achieved during construction if mixing temperatures near 150°C were maintained (ASTM D2872-12). Further, there have been multiple investigations to support that ASTM D2872 reasonably simulates short-term aging effects on binder. A series of equality plots in Jemison et al. (1991) suggest that the RTFO test produces approximately equal aging with respect to binders aged in hot mixed asphalts when considering infrared carbonyl areas, viscosity at 135°C, and viscosity at 60°C. However, oven conditioning methods produced

noticeably more stiffening when considering penetration and produced fewer carbonyl areas from percent larger molecular size.

Bell et al. (1994a) considered two primary approaches for short-term conditioning as part of SHRP. The first approach, was loose mixture conditioning in a FDO at temperatures of 135°C and 163°C for periods of 0, 6, or 15 hr. A secondary approach considered an extended mixing approach, which utilized a modified version of the rolling thin film oven (RTFO) that conditioned loose mixtures for 0, 10, 120, and 360 min at 135°C or 163°C. After conditioning, mixtures were compacted into specimens and tested for resilient modulus, dynamic modulus, and indirect tensile tests. Resilient modulus was the primary performance property evaluated by the authors for short-term conditioned mixtures by comparing non-conditioned mixture resilient modulus to the resilient modulus of conditioned mixtures. Both conditioning protocols produced noticeable increases in resilient modulus ratio, and the extended mixing approach produced more uniform data. However, the study concluded that FDO conditioning was likely the more feasible option for short-term conditioning where laboratory productivity was a concern. The FDO short-term conditioning protocol was supported in Bell and Sosnovske (1994) and Bell et al. (1994b).

2.4.3 Short Term Aging Investigations After Superpave

In the two decades since the implementation of Superpave, there have been multiple investigations to the effects of short-term aging on asphalt pavements. The majority of these investigations have focused predominately on mixture performance characteristics with supplementation from binder properties.

Howard et al. (2013) describes effects on asphalt mixture and binder properties because of varying haul time (HT). One asphalt mix design with three varying binder types (i.e., neat, foamed, and with chemical additive) were mixed at a single plant in Columbus, MS, sampled immediately after mixing, and after haul times of 1.0 to 10.5 hr. Materials testing relevant to short-term aging consisted of asphalt volumetric, Superpave performance grading on binders extracted from hauled mixtures, and Fourier Transform Infrared Spectroscopy (FTIR). Maximum specific gravity (G_{mm}) testing revealed that asphalt binders gradually absorbed further into aggregate pores for increased HT (e.g., G_{mm} increased on average by 0.016 over 1 hr hauls and 0.018 for 6 hr hauls). Performance grading of extracted binders (note: there was no RTFO aging applied to mixtures subjected for plant mixing and subsequent hauls) indicated that there was no significant change in performance grade between 1 and 8 hr of haul time. FTIR outputs were used to determine calculate carbonyl and sulfoxide indices as an aging index, and most chemical aging was evident within the first 3 hr of HT.

Yin et al. (2015) performed a short-term aging investigation of nine field projects in drastically different regions where mixtures were evaluated in three states: LMLC specimens produced from raw materials sampled during construction, PMLC specimens compacted at the plant during construction, and PMFC cores that were collected soon after construction. Mixtures were evaluated using PMLC specimens and LMLC specimens to evaluate the accuracy of current short-term oven aging (STOA) criteria to simulate volumetric property changes that occur during plant production. Compacted specimens were tested for resilient modulus, dynamic modulus, and using the Hamburg Loaded Wheel Test (HLWT). Findings from the study are discussed in the following paragraph.

The study found that current STOA criteria for HMA (2 hours at 135°C) and warm mixed asphalt (WMA) (2 hours at 116°C) mixtures were adequate to simulate changes to volumetric properties (i.e. asphalt absorption) and performance criteria (i.e. M_R, E*, and HLWT parameters) that occur during plant production. However, the authors observed differences between HLWT behaviors of laboratory compacted and field compacted specimens. This was suspected to be the result of thin asphalt lifts that required plaster spacers.

Other factors studied by Yin et al. (2015) were: WMA technology, production temperature, plant type, inclusion of recycled materials, aggregate absorption, and binder source. The only factors from the six aforementioned factors that did not produce a noticeable difference in MR stiffness were plant production type and production temperature. Limited HLWT test data indicated that WMA technology, inclusion of recycled materials, and aggregate absorption produced noticeable differences in mixture performance, but there was not sufficient data to evaluate many of the factors evaluated using resilient dynamic moduli.

Jacques et al. (2016) performed an investigation of variations of short-term aging by extending silo storage time. A virgin asphalt mixture and a mixture containing 25% RAP, both with a 12.5 mm NMAS, were sampled from silo storage after storage times of 0 to 7.5 hours and 0 to 10 hours for the virgin and RAP mixtures, respectively. Extracted binder evaluations and mixture tests were conducted on aged materials to characterize the effects of increasing short-term aging, and a series of modified rolling thin film oven (RTFO) conditioning protocols were conducted for the binders used during mixture production to evaluate the current short-term conditioning of asphalt binders.

Binder test results from Jacques et al. (2016) indicated that there were noticeable differences in binder properties because of varying silo storage time and that current RTFO conditioning protocols do not accurately represent short-term aging in current practice. High temperature dynamic shear rheometer (DSR) pass/fail (P/F) temperatures increased by 0.39°C/hr and 0.53°C/hr for the virgin and RAP mixture binders, respectively. Intermediate temperature DSR P/F temperatures increased by 0.2°C/hr in the virgin mixture with no observable trend for the RAP mixture. Bending beam rheometer (BBR) results indicated that low temperature P/F temperatures increased by 0.14°C/hr and 0.21°C/hr for the virgin and RAP mixtures, respectively. BBR test results were m-value controlled. Rheological indices analysis using R-values with crossover frequency and the Glover-Rowe method indicated that there were meaningful changes in binder aging as a function of silo storage time. When overlaying rheological indices of laboratory conditioned binders, RTFO conditioning times of up to 135 minutes did not seem to produce rheological changes similar to that of plant mixed materials.

Mixture tests in Jacques et al. (2016) consisted of dynamic modulus testing, simplified viscoelastic continuum model (S-VECD) testing, and the thermal stress restrained specimen test (TSRST). Dynamic modulus master curves were developed for the virgin and RAP mixtures at a reference temperature of 21.1°C. The authors presented average dynamic modulus ratios for each master curve developed (one per mix per silo storage time) using mixtures sampled immediately as a baseline. Results indicated that the RAP mixture stiffened at a faster rate than the virgin mixture with the average dynamic modulus ratio for the RAP mixture after 2.5 hr of storage being similar to that of the virgin mixture after 7.5 hr of storage. S-VECD analysis indicated that mixtures stored for longer times had higher pseudo-stiffness than mixtures sampled sooner. TSRST testing indicated statistically significant differences in

critical cracking temperature after 5 hr and 7.5 hr of storage time for virgin and RAP mixtures, respectively.

2.5 Long Term Mixture Aging

The degrading effects of the environment on asphalt paving mixtures has been a topic discussed for several decades (e.g., Lang and Thomas, 1939), and there have since been many pieces of information added to the collection of knowledge. Table 2.4 provides key points identified in this section while dividing studies into three categories: 1) long-term mixture aging with no conditioning, 2) long-term mixture aging with binder conditioning, and 3) long-term mixture aging with mixture conditioning.

Table 2.4. Summary of Long Term Aging Findings

Investigation Category	Reference(s)	Findings or Developments
Long Term Aging with No Conditioning	Hveem (1955)	– Binder penetration decreased from 120 – 150 to an average of 36 after 1 yr
	Heithaus and Johnson (1958)	– V_a identified as primary aging factor – Majority of penetration lost in first 3 of service
	Mirza and Witczak (1995)	– The Global Aging System – Relationship between pen. and viscosity
Long Term Aging with Binder Conditioning	Lang and Thomas (1939)	– Mixing 22 hr at 82°C closest representation of 1 year
	Lee (1977)	– Iowa Durability Test (IA-DT) – 46 hr in IA-DT representative of 5 years
	Kemp and Predoehl (1981)	– Lab specimen aging more aggressive than field pavement aging (2 yr compared to 32 months) – Modified RTFO conditioning (California Test 374) for 7 days compared to 2 years in California desert
	Bahia and Anderson (1995)	– Pressure Aging Vessel (PAV) [AASHTO R28] – R28 compared to 5 to 10 years of service
	Glover et al. (2005)	– R28 not comparable to Texas performance – Recommended modified PAV protocol 3 times harsher than R28
Long Term Aging with Mixture Conditioning	Lottman (1978, 1982a, 1982b)	– Tensile Strength Ratio (TSR) [AASHTO T283] – Vacuum Saturation + F-T + 24 hr in 60°C water good predictor of moisture induced damage
	Bell et al. (1994a, 1994b) Bell and Sosnovske (1994)	– AASHTO R30 Long Term Oven Aging (LTOA) – 5 days at 85°C similar to 7 to 10 years of field service
	Terrel and Al-Swailmi (1994); Allen and Terrel (1994); Tandon et al. (2004); Alam et al. (1998); Tandon and Nazarian (2001)	– Environmental Conditioning System (ECS) – Field cores experience aging not simulated in ECS – Improvements made upon ECS
	Zou et al. (2013) Isola et al. (2014)	– Fracture Energy (FE) loss over time in Florida – Oven conditioning did not simulate Florida environment – Combination of oven conditioning and cyclic pore pressure conditioning (CPPC) capable of simulating field aging
	Yin et al. (2016)	– Field aging more damaging than R30 LTOA

2.5.1 Long Term Mixture Aging with No Conditioning

The effects of long term mixture aging have been documented many times. Hveem (1955) presented a case where asphalt binders recovered after one year of field aging reduced from 120 to 150 to an average penetration of 36. This subsection presents a review of literature from investigations where asphalt mixtures were field aged and evaluated over time without performing laboratory conditioning.

Heithaus and Johnson (1958) performed an evaluation of factors affecting short and long term binder aging over a three-year period in Wood River, IL. There were multiple components of long term aging evaluated based on changes to extracted binder apparent viscosity (see section 2.4.1 for short-term aging details). Air voids were the primary factor identified to affect long term aging of asphalt binders in mixtures. There was also evidence from four Midwestern pavements that the majority (about 60%) of the binder penetration lost during the first ten years of service occurred during the first three years of service for pavements with air voids ranging from 2% to 14%.

Mirza and Witczak (1995) presented the global aging system (GAS), which has been utilized by many other investigations, using a master data base extracted binder information containing 2,308 line entries from 40 field projects throughout North America and Europe. The investigation was separated into two phases of model development. The first focused on developing a model for short-term aging. The second developed a model for asphalt property changes due to long term age-hardening.

The aging model defines a constant for certain properties (e.g., penetration, viscosity, etc.) of asphalt binders prior to mixing and immediately after laydown. However, the model recognizes that there is an aging gradient with depth into the pavement surface over long term aging. Many of the line entries reported “surface” cores in the master data base, which the authors assumed to be 6.3 mm in to the pavement surface. Ultimately there were three primary models developed which predicted: short-term properties from original properties, long term properties from short-term properties at 6.3 mm deep, properties with depth relationships. An additional model also developed a way of considering the effects of V_a on aged properties. These four models are presented in Table 2.5.

Table 2.5. Global Aging System

Model Description	Equation
Short-Term Aging	$\log-\log\left(\eta_{t=0}\right)=0.054405+0.972035\ \log-\log\left(\eta_{orig}\right)$
Long-Term Aging	$\log-\log\left(\eta_{aged}\right)=\frac{\log-\log\left(\eta_{t=0}\right)+A\cdot t}{1+B\cdot t}$ $A=-0.004166+1.41213\,C+C\log(Maat)+D\log-\log\left(\eta_{t=0}\right)$ $B=0.197725+0.068384\log(C)$ $C=10^{274.4946-193.831\log\left(T_R\right)+33.9366\log\left(T_R\right)^2}$ $D=-14.5521+10.47622\log\left(T_R\right)-1.88161\log\left(T_R\right)^2$
Air Voids Long-Term Aging Factor	$F_V=\frac{1+1.0367\left(10^{-4}\right)V_a(t)}{1+6.1798\left(10^{-4}\right)t}$; $\log-\log\left(\eta'_{aged}\right)=F_V\left(\log-\log\left(\eta_{aged}\right)\right)$
Aged Viscosity with Depth	$\eta_{t,z}=\frac{\eta_t(4+E)-E\left(\eta_{t=0}\right)(1-4z)}{4(1+Ez)}$ $E=23.82\,Exp^{(-0.0308\,Maat)}$

-- Original Viscosity (η_{orig}); As-Constructed Viscosity ($\eta_{t=0}$); Aged Viscosity (η_{aged}); Mean Annual Air Temperature (*Maat*); Time in Months (t); Temperature in Rankine (T_R); Pavement Depth (Z)

Mirza and Witczak (1995) also developed a relationship between viscosity (η) and penetration (Pen). The η-Pen regression considered only 5 second 100 gm penetrations and viscosities measured at shear rates of 0.05 sec^{-1}. This relationship is presented in equation (2.3).

$$\log(\eta)=10.5012-2.2601\log(Pen)+0.00389\log(Pen)^2 \quad (2.3)$$

Where;
η = viscosity (poise)
Pen = penetration (dmm)

2.5.2 Long Term Mixture Aging with Binder Conditioning

Among the earliest publications on asphalt durability, Lang and Thomas (1939) investigated asphalt binder specifications which addressed the ability of an asphalt binder to cement aggregates together and maintain cementing qualities after weathering. While binder characterization was performed on binders extracted from weathered pavements, there was an emphasis on mixture performance tests. Mixture tests consisted of tensile strength and elongation, impact resistance, abrasion loss, and shear strength.

The abrasion test conducted in Lang and Thomas (1939) had some parallels to the Cantabro test described in Cox et al. (2017). Lang and Thomas (1939) compacted mixtures of 2% asphalt with 98% Ottawa sand in a laboratory environment to conduct a comparison of binder behaviors when in contact with a standard aggregate. There were four conditioning environments used to evaluate durability of each of the 24 asphalt binders considered, including: mixing for 22 hours in the presence of air, elevated temperature (180°F), and ultraviolet light; mixing for 22 hours in the presence of air at an elevated temperature (180°F);

mixing for 22 hours in the presence of nitrogen and elevated temperature (180°F); and natural weathering for one year in molded specimens. After weathering, the sand and asphalt mixtures were subjected to abrasion testing by subjecting ten cylindrical specimens (50 mm by 75 mm) to 500 revolutions in a Deval abrasion drum filled with 60°F water. The study concluded that mixing for 22 hours at 180°F in the presence of air and ultraviolet most nearly represented weathering that occurred over one year in compacted specimens.

Coons and Wright (1967) evaluated the effects of binder hardening in field cores which had been aged for 4 months to 12.5 years in Georgia. The primary factor considered was pavement core depth using five 6.5 mm (1/4 inch) slices cut from 0 to 44.5 mm (1 ¾ inch) deep. The study concluded that binder that was extracted from the top layer of field cores had approximately 50% higher viscosity than binder extracted from the layer below it, and there was little change over time in binder extracted from 12.5 mm (1/2 inch) to 38.1 mm (1 ½ inch) deep. Materials extracted from more than 38.1 mm below the pavement surface indicate little change in viscosity over time after an initial change during construction, and the relative viscosity of binders sampled from 38.1 mm or more below the surface are independent of original viscosity.

Lee (1977) reported an investigation for the Iowa State Highway Commission where eight pavements were monitored for changes to binder viscosity over a 48 month period. Initial pavement air voids ranged from 5.1% to 12.3% and binder contents ranged from 5.0 to 7.5%. Therein, the authors presented a figure of changes to measured air voids for all eight pavements with densities measured on cores taken from the wheel path and cores taken from between the wheel paths. There was no appreciable difference in "densification" for specimens cored from the wheel paths and cores taken from between the wheel paths. The authors suggested that this could have been a situation where moisture absorbed into aggregate pores may have caused measured densities to be higher than reality (see investigation in Chapter 4).

A key contribution of Lee (1977) was the Iowa durability test (IA-DT), which consisted of two binder conditioning phases: thin-film oven test (TFOT) and applying pressure oxidation for up to 1,000 hr in a TFOT residue film thickness of 3 mm at 150°F and 20 atm. Binder characterization to evaluate the IA-DT consisted primarily of rheological properties (penetration, softening point, flash and fire, ductility, specific gravity, spot test, and viscosity) with a small amount of chemical analysis (asphaltene precipitation and infrared spectroscopy). It was suggested that 46 hr in the IA-DT would produce the same amount of damage to asphalt cement as five years in Iowa pavements.

Kemp and Predoehl (1981) monitored environmental effects on asphalt durability in laboratory compacted specimens that were field aged for four years. The experiment considered three asphalt binders (low, high-moderate, and high susceptibility to temperature), three target air void levels (4±1%, 8±1%, and 11±1%), and two aggregate sources including absorbent or non-absorbent properties. Laboratory compacted specimens were field aged in four different climatic areas of California (Valley, Mountain, Coast, and Desert). Ultimately, there was a test road constructed in the desert area of California near the field aging location for the laboratory compacted specimens which used one of the asphalts from the study. The experiment involved a small amount of resilient modulus testing on original specimens that had been stored in a laboratory and specimens which were field aged for four years. After characterizing binder from field aged specimens, there were five binder conditioning procedures evaluated and a sixth binder conditioning procedure developed using penetration at 25°C, absolute viscosity at 60°C, and kinematic viscosity at 135°C.

The investigation concluded that high air temperatures (inducing thermal oxidation) was the most contributing factor of asphalt hardening rate with air voids and aggregate properties being meaningful contributors. The five pre-existing binder conditioning procedures produced noticeably less binder damage than 2 years in the California desert. However, the binder conditioning protocol that was developed simulated two years in the California desert over 7 days in a modified RTFO, and was available as California Test 374 from the California Department of Transportation. The effect of air voids was found to be consistent for all asphalt types, but aggregate porosity seemed to have a changing effect when volatile asphalts were used. Cores from the test road paved two years into the study indicated that 24 months of briquette weathering was similar to 32 months of road weathering. When evaluating binder properties of thinner slices from briquettes there was an obvious stiffening gradient with binder extracted from mix sampled more than 22 mm from the briquette surface having near uniform properties within a specimen for a given point in time.

The current version of the Superpave performance grading system for asphalt binders utilizes the Pressure Aging Vessel (PAV) as a conditioning method to consider the resistance of asphalt binders to age hardening. Bahia and Anderson (1995) discusses the development of the PAV which included a field validation study where binders were extracted from pavement cores of twelve test sections and compared to properties of original binders which had been TFOT and PAV conditioned. The study concluded that the PAV procedure was not developed to duplicate field conditions, but to provide a comparative measure of binder potential with respect to oxidative aging. However, AASHTO R28-12 claims to produce an amount of aging comparable to that experienced over 5 to 10 years of field aging.

Glover et al. (2005) conducted an asphalt binder durability study for the Texas Department of Transportation (TxDOT) to develop a method for detecting binders which are susceptible to early durability failure. Nineteen Texas pavements were studied to achieve a reasonable assessment of changes to asphalt binder properties over time. The study concluded that asphalt binders aged for one month in a room maintained at 60°C was approximately equal to the binder damage that would occur over 15 months of field aging in Texas pavements. A primary contribution of the investigation was the recommendation to modify PAV conditioning protocols to methods which produced approximately 3 times the amount of aging produced in R28 conditioning.

2.5.3 Long Term Mixture Aging with Mixture Conditioning

It is apparent that most pavement durability studies prior to the 1980s focused predominately on changes to asphalt cement over time. There were instances where abrasion (e.g., Lang and Thomas, 1939) or resilient modulus (e.g., Benson, 1976) testing was performed on mixtures of asphalt and aggregates. However, the authors could not identify any cases prior to 1978 where asphalt mixtures were laboratory conditioned in attempts to simulate field aging based on mixture performance. This sub-section discusses field aging investigations beginning in 1978 where mixtures were laboratory conditioned in attempts to simulate field aging.

A comprehensive study of moisture induced damage with considerations for laboratory conditioning and field aging is presented in Lottman (1978, 1982a, 1982b). Lottman (1978) was undertaken with the primary objective of developing a practical means for simulating the damage induced by moisture in asphalt concrete mixtures. A preliminary portion of the investigation evaluated six pavements from Arizona, Idaho, and Virginia. However, there were

ultimately nineteen pavements from fourteen states evaluated. States which participated in the investigation were asked to provide cores, representative aggregates, representative asphalt binder samples, and pertinent pavement data (e.g., gradations, air voids, and asphalt contents).

After producing representative laboratory specimens, compacted mixtures were subjected to vacuum saturation followed by freeze-thaw (F-T) cycles and hot water conditioning. Field cores were either tested immediately or after being vacuum saturated with water. Laboratory produced specimens were tested in three groups: non-conditioned, vacuum saturated, and after conditioning in a vacuum saturated state. The initial phase of Lottman (1978) considered multiple conditioning modes using hot water, freezing, and load applications. However, the second phase of Lottman (1978) considered only two forms of accelerated conditioning to simulate moisture induced aging: application of 18 cycles of thermal conditioning (0°F to 120°F) using freezers and a hot water bath and one 15 hr F-T cycle followed by 24 hr at 140°F. Mixtures were predominately evaluated in indirect tension at temperatures of 55°F or 73°F to determine tensile strength or elastic modulus. The study ultimately concluded that one F-T cycle after vacuum saturation followed by 24 hr of conditioning in 140°F water was the most reliable conditioning method considered for predicting moisture induced damage.

The current version of AASHTO R30 describes methods for short-term oven conditioning (described earlier in this chapter) and long term oven conditioning to simulate mixture changes which occur in the field. The specification claims that the long-term mixture conditioning "is designed to simulate the aging the compacted mixture will undergo during 7 to 10 years of service" (AASHTO R30-02). While there are several investigations which have called this claim in to question (e.g. Isola et al. 2014, Epps Martin et al. 2014, Yin et al. 2016), this section describes the efforts to develop the long term oven conditioning methods in R30.

Bell et al. (1994a), Bell and Sosnovske (1994), and Bell et al. (1994b) were three companion reports from SHRP which investigated laboratory conditioning to simulate field aging of asphalt mixtures. Bell et al. (1994a) identified potential protocols for conditioning compacted asphalt specimens to simulate field aging. Bell and Sosnovske (1994) evaluated the identified mixture conditioning approaches by evaluating conditioned mixture properties in comparison with expected mixture performance based on laboratory conditioned binder assessments. A field validation study was presented in Bell et al. (1994b) which considered multiple materials throughout multiple projects.

The long term conditioning approaches considered in Bell et al. (1994a) were forced draft oven aging (FDOA) at elevated temperatures, high pressure oxidation, and low pressure oxidation (LPO) using a triaxial cell. The original FDOA trials pre-conditioned specimens for two days before increasing oven temperature to 107°C for up to 7 days. The initial investigation found that oven conditioning produced changes in resilient modulus, but that the increased temperature should be decreased due to potential for specimen damage during conditioning. The high pressure oxidation methods were identified as problematic due to the potential for specimen volume change or damage during conditioning. Alternatively, LPO at 25°C and 60°C by forcing $0.11 m^3$/hr of oxygen or air through compacted specimens in a triaxial cell with confinement seemed promising. FDOA and LPO were identified as reasonable conditioning methods which produced increases in resilient modulus while not changing specimen geometry.

Bell and Sosnovske (1994) performed mixture conditioning through FDOA and LPO in triaxial cells and compared modulus results to binder property results from other SHRP

contractors. FDOA conditioning was conducted at 85°C for 5 days and 100°C for 2 days. LPO was conducted with the same flow rate identified in the previous paragraph, but at temperatures of 60°C and 85°C for 5 days. The investigation concluded that pure asphalt binder conditioning was inadequate for considering factors inherent for asphalt mixtures. FDOA conditioning of five days at 85°C was suggested for standard mixtures, and LPO conditioning at 85°C was suggested for mixtures which are susceptible to damage during conditioning (e.g., OGFC or mixtures containing soft binder).

Bell et al (1994b) presented a field validation study for the FDOA and LPO conditioning methods developed in Bell et al. (1994a) from projects in Arizona, California, France, Georgia, Michigan, Minnesota, Oregon, Washington, and Wisconsin. Laboratory specimens were produced using representative materials at gradations and binder contents determined from field cores prior to conditioning and comparing moduli to that of field cores. Field cores were sampled after periods of a few months to 19 years, with the majority of field projects sampled after less than 5 years. All cores collected from sites that were more than 5 years old were collected as part of a supplementary study that only considered pavements in Washington.

While there was evidence to support that 5 days of FDOA at 85°C produced an increase in pavement modulus similar to that of 9 years in the dry-freeze and 18 years in the wet-no freeze climatic zones of Washington, this relatively small geographical area does not suggest that the damage produced by FDOA successfully simulated field aging in other climatic regions. In fact, some of the conclusions from Bell et al. (1994b) claim that there was not sufficient evidence to recommend aging relationships based on climate.

The environmental conditioning system (ECS) was developed as a conditioning protocol to simulate moisture induced damage on asphalt mixtures. Though the ECS was able to identify specimens with decreased resistance to moisture induced damage (Terrel and Al-Swailmi, 1994), field cores appeared to experience long-term aging that was not simulated in the ECS system (Allen and Terrel, 1994). Later studies (e.g. Tandon et al., 2004; Alam et al., 1998; Tandon and Nazarian, 2001) evaluated modified versions of the ECS using simple performance tests (i.e. flow, creep, and dynamic modulus) rather than resilient modulus. However, the ECS was never implemented to the extent of AASHTO R30.

A more recent investigation by the University of Florida is discussed in the next two paragraphs. Zou et al. (2013) performed a field aging investigation of Superpave projects throughout Florida. A key material property evaluated over field aging periods of 6 to 12 years was fracture energy (FE). Therein, test sections which presented signs of moisture damage experienced reductions in FE of 46% to 76% while test sections with no signs of moisture damage experienced FE reductions of 25% to 56% (see Section 2.6.4 for FE test method). This observation was utilized in later investigations from the University of Florida to evaluate agreement between laboratory conditioning protocols and field aging.

Three types of laboratory conditioning were employed at the University of Florida to simulate the aging of asphalt pavement mixtures in comparison to the investigation described in the previous paragraph (Isola et al., 2014). The three protocols considered were: long term AASHTO R30, cyclic pore pressure conditioning (CPPC) to induce moisture damage, and a combination of the two. CPPC was conducted on compacted specimens which had been sliced and prepared for fracture energy testing described in Section 2.6.4 by placing them in a triaxial cell filled with water and subjecting specimens to pressure cycles. A primary objective of the study was to develop appropriate aging procedures which consider more effects than oxidation

to adequately assess asphalt mixture changes with time. Mixtures were evaluated using the instrumented indirect tension test described in Section 2.6.4 with further testing to consider resilient modulus (M_R) and creep compliance in addition to FE. The study concluded that long term R30 conditioning was inadequate in producing decreases in mixture performance documented in Florida and that a combination of R30 and CPPC most closely represented field aging.

Yin et al. (2016) performed a field aging investigation for seven projects where field cores were taken soon after construction and at least once after a period of field aging. There were also virgin materials (binder, aggregates, and recycled materials) taken during construction to produce lab mixed and lab compacted (LMLC) specimens. LMLC specimens were lab conditioned for 2 weeks at 60°C, 3 days at 85°C (only 2 mixtures), or 5 days at 85°C before conducting performance tests. Performance tests included M_R at 25°C according to ASTM D7369 with external LVDTs and the Hamburg Loaded Wheel Test (HLWT) according to AASHTO T324.

To account for variations in construction seasons and climates, Yin et al. (2016) utilized a cumulative degree days (CDD) with 32°F as a base temperature. The CDD variable was used to normalize the amount of aging between construction seasons and climates for the seven field projects monitored over time. Response variables (i.e. M_R and a HLWT rutting resistance parameter (RRP)) were normalized as ratios of M_R and RRP after aging to M_R and RRP soon after construction. Using the approach described in the previous two sentences, exponential functions were developed between M_R and RRP ratios over time in CDD with R^2 of 0.83 and 0.76 for M_R and RRP ratios, respectively.

When comparing the M_R ratio of LMLC specimens subjected to the three oven conditioning protocols described in Yin et al. (2016), none of the conditioning protocols produced more damage than what was seen over a 12 month period in warmer climates or a 23 month period in colder climates. Factors considered in analysis of mixture performance over time included: WMA technology, production temperature, plant type, inclusion of recycled materials, and aggregate absorption. Of the five factors considered in further analysis, the only factor to produce no meaningful effect on mixture performance was plant production type. However, production temperature was not produce a statistically significant effect on M_R.

2.6 Mixture Performance Tests

This section reviews the mixture performance tests utilized in this study. Mixture performance tests of interest are the Cantabro Mass Loss (CML) test, the indirect tensile (IDT) test, the Hamburg loaded wheel test (HLWT), and the Superpave instrumented IDT (SIDT) test. The four following sub-sections present relevant information organized by test method in the order previously stated.

2.6.1 Cantabro Mass Loss

The Cantabro Mass Loss (CML) test has been used as an index test method to characterize relative durability of OGFC mixtures for several years. The CML test utilizes a Los Angeles abrasion drum without steel sphere charges and subjects compacted specimens to 300 revolutions of abrasion. The ratio of mass change to initial specimen mass is reported as mass loss (*ML*). CML has wider acceptance for OGFC than for dense graded asphalt (DGA).

Multiple investigations involving MSU have used CML to characterize DGA mixtures in recent years. A comprehensive summary relative to CML findings from these investigations is provided in Cox et al. (2017) and is not repeated here for brevity.

There were several general trends presented in Cox et al. (2017) where *ML* was related to mixture properties generally accepted to affect mixture durability. *ML* consistently increased as high PG binder grades increased, until polymer modified binders were encountered. Replacing PG 67-22 binders with PG 76-22 binders produced by polymer modifying PG 67-22 binders decreased *ML*. CML detected the inclusion of post-consumer materials in mixtures produced with elevated RAP contents or ground tire rubber (GTR) rather than SBS polymer for binder modification. CML was also able to detect differences in asphalt mixture performance resulting from conditioning or aging. Increased Va was shown to produce higher *ML*, and increased Va accelerated the damaging effects of laboratory conditioning or field aging. The volume of effective binder (V_{be}) was also shown to correlate with *ML*.

2.6.2 Indirect Tensile Test

The indirect tensile test has been used for many years to evaluate asphalt pavement mixtures. The test is traditionally performed near 25°C with a load rate of 50 mm/min. IDT Strength (S_t) is determined at the maximum load carried by the specimen during testing throughout this investigation. The method most commonly referenced is AASHTO T283-14, which uses S_t from conditioned and non-conditioned specimens to determine tensile strength ratio (TSR) as a measure of resistance to moisture induced damage. Azari (2010) conducted an inter-laboratory study to investigate test variability for AASHTO T283. The study concluded, based on information collected from forty laboratories, that the test was very variable and an acceptable range for TSR values within a single laboratory and between two laboratories were 9% and 25%, respectively.

Non-instrumented IDT testing was conducted for some of the mixture aging investigations mentioned earlier in this literature review. Non-instrumented IDT test results were utilized by Lottman (1978, 1982a, and 1982b) where the ultimate tensile strength was related to mixture performance. Cox et al. (2017) presented relationships between CML data and non-instrumented IDT data.

2.6.3 Wheel Tracking Tests

While there are multiple methods of wheel tracking to determine resistance of a mixture to rutting, the Hamburg Loaded Wheel Test (HLWT) is of primary concern to the current investigation. Cooley et al. (2000) provided a state of the practice review for wheel tracking test methods used in conjunction with asphalt mixtures in the US. The six wheel tracking tests considered were the Georgia Loaded Wheel Tester (GLWT), Asphalt Pavement Analyzer (APA), Hamburg Loaded Wheel Test (HLWT), LCPC (French) Wheel Tracker, Purdue University Laboratory Wheel Tracking Device (PURWheel), and one-third scale Model Mobile Load Simulator (MMLS3).

The HLWT was developed in Hamburg, Germany and has been used as a relative measure for a mixture's resistance to moisture-induced damage (Aschenbrener, 1995). The test is typically conducted by submerging asphalt specimens in 50°C water and subjecting them to rolling steel wheels applying a 700 N force. AASHTO T324-14 specifies that a standard test

includes 20,000 passes of the steel wheels or up to 20 mm of deflection. The primary performance factors identified within the HLWT method include: creep slope, stripping inflection point (SIP), and stripping slope. Each of the performance factors are determined from relationships between deformation and wheel passes. The creep slope is determined using slope of the linear region of specimen deformation prior to stripping (in the event of stripping). The stripping slope is determined from the slope of specimen deformation after the on-set of stripping. The SIP defined as point during testing, defined by number of wheel passes, where the linear portions from creep and stripping behavior intersect. The SIP has been used by many as a reference of moisture susceptibility (e.g., Cooley et al., 2000; Williams et al., 2011). The HLWT has also been used in recent years for mixture aging investigations (e.g., Yin et al., 2015; Yin et al., 2016).

2.6.4 Instrumented Indirect Tensile Test

While the traditional IDT test methods described in Section 2.6.2 has been widely used for decades, there have been multiple investigations to present the improved capability of the Superpave IDT (SIDT) test. For brevity, this sub-section only presents literature relative to the SIDT method for determining fracture energy (FE).

Roque and Buttlar (1992) and Lytton et al. (1993) were seminal papers describing face-mounted instruments to characterize deformations during IDT testing. The papers compared the stress state at the center of an IDT specimen to that of typically loaded asphalt pavements (i.e., tensile stresses in the horizontal direction produced from vertical compression). Further, the authors discussed the tendency for asphaltic materials to approach elastic behaviors at mid-range to low temperatures (e.g. less than 30°C) and suggested that determining tensile behaviors produced from compressive forces is reasonable. A key contribution of Roque and Buttlar (1992) was the recommendation to utilize gage points mounted to the faces of IDT specimens during testing with a 38 mm gage length for 150 mm diameter specimens. This recommendation addressed a frequently reported problem of load strip damage when external deformation measurement was used (e.g. Molenaar et al., 2002).

While there have been investigations to discuss tensile strength (S_t) and horizontal strain at peak stress (ε_{ult}) as improved cracking performance characteristics, many have correlated fracture energy (FE) with field cracking (e.g., Kim and Wen, 2002; Zhang et al., 2001). Fracture energy from SIDT testing is equal to the area under the stress-strain curve between initial loading and fracture. The instant of fracture is identified within this system by determining the peak point on the deformation differential curve (DDC), or the difference between vertical and horizontal deformations. The instant of fracture should occur before the specimen peak load is experienced (Buttlar et al., 1996; Roque et al., 1997; Koh and Roque, 2010). Work by Koh and Roque (2010) produced a 1:1 relationship between FE determined by dog-bone direct tension and SIDT tests, which suggest FE as a fundamental mixture property not affected by specimen geometry.

2.7 Asphalt Binder Characterization

This section presents literature relative to the asphalt binder performance tests utilized in this study. Binder performance tests of interest include asphalt binder penetration, dynamic

shear rheometry, bending beam rheometry, and Fourier Transform Infrared Spectroscopy (FTIR). The following sub-sections present relevant information organized by test method.

2.7.1 Asphalt Binder Penetration

Asphalt binder penetration (ASTM D5) has been utilized as a relative measure of binder stiffness for several decades. The test records the distance that a 100 g weighted needle can penetrate into a sample of asphalt binder submerged in water typically conditioned to 25°C for a period of 5 seconds. Many investigations mentioned in earlier sections have made use of ASTM D5 as a relative measure of asphalt binder stiffness at normal temperature (e.g., Epps and Monismith, 1969; Kandhal and Koehler, 1984; Santucci et al., 1985; Wright and Paquette, 1966; Kari, 1982; Jemison et al., 1991; Hveem, 1955; Heithaus and Johnson, 1958; Mirza and Witczak, 1995; Lee, 1977; Kemp and Predoehl, 1981).

2.7.2 Superpave Binder Evaluations

The Performance Grade (PG) asphalt binder characterization system consists of multiple components, which are described in AASHTO M320-10. One factor that makes the PG system unique from prior binder grading systems is the consideration of binder properties at cold (i.e., Bending Beam Rheometer), intermediate (i.e., 8 mm DSR), and high (i.e., 25 mm DSR) temperatures. Petersen et al. (1994) provides discussion of each of the test methods considered in the PG grading system including data analysis and recommendations for test specifications.

2.7.3 Fourier Transform Infrared Spectroscopy

Infrared spectroscopy has been utilized for several years as a rapid method for identifying collections of complex functional groups of compounds found in samples of asphalt binder (Beitchman, 1959; Petersen, 1986). Some studies from literature identified to utilize FTIR analysis were Wright and Paquette (1966) and Howard et al. (2013). Wright and Paquette (1966) evaluated infrared spectra around the wavelengths of 2.9, 5.9, and 9.7 μm to evaluate hydroxyl, carbonyl and the carbon-oxygen-carbon band. Observations at these wavelengths were used to support a claim that oxidation was occurring for increased haul-times. Howard et al. (2013) followed recommendations of Glaser and Loveridge (2012) by considering peak heights of absorbance measurements in FTIR analysis. Howard et al. (2013) concentrated on the 1700 cm^{-1} (carbonyl) and 1031 cm^{-1} (sulfoxide) regions of the spectral output to determine carbonyl and sulfoxide indices, or the ratios between the 1375 cm^{-1} region (the representative asphalt peak) and the two previous regions.

CHAPTER 3 – EXPERIMENTAL PROGRAM

3.1 Overview of Experimental Program

This experimental program considers plant produced asphalt used during the emergency paving study of Howard et al. (2012). Many of the construction details for the test section are not repeated here for brevity. This chapter describes overall information of the test section (Section 3.2), materials and specimens tested (Section 3.3), field compacted specimen sampling and handling (Section 3.4), laboratory conditioning protocols (Section 3.5), mixture test methods (Section 3.6), and binder property evaluations (Section 3.7).

3.2 Field Test Section

The pavement test section evaluated herein consisted of twelve 3.3 m wide test strips which were placed as part of an emergency paving demonstration; construction details are available in Howard et al. (2012). Paving was performed November 1 to 3, 2011. The pavement was left in place to study field aging of asphalt pavements. Following construction, the test section was blocked off to traffic and monitored for property changes over a six year period (most evaluations occurred over a five year period). The following sub-sections provide construction and weather details for the pavement test section.

3.2.1 Construction Procedures

The twelve test strips were identical with respect to design aggregate blend and mix design. However, binder types were varied: neat PG 67-22 (strips 1 to 4), PG 67-22 foamed with 2% moisture (strips 5 to 8), and PG 67-22 dosed with 0.5% Evotherm 3G™ (strips 9 to 12). During construction, one mixture was produced per day and hauled for four different times. After a haul time of 1.0 to 10.5 hours, a single truck load would arrive to the pavement site and pave one of the twelve test strips. The three mixtures and respective haul times are described in Table 3.1.

Table 3.1. Test Strip Descriptions

Mix ID	Binder ID	Mix Description	Strip	Haul Time (hr)
M14	B1	HMA	1	1.0
			2	2.3
			3	5.8
			4	7.9
M15	B2	Foamed	5	1.1
			6	2.4
			7	5.6
			8	8.4
M16	B2	Evotherm 3G™	9	1.0
			10	5.7
			11	8.1
			12	10.5

-- Strips 9 to 11 are also referred to as M16a, and Strip 12 is referred to as M16b.

Compaction was performed with a single vibratory roller with varying amounts of static and vibratory passes within and between strips. Zone 1 and Zone 2 were 3.3 m long sections beginning 5.6 m and 24.2 m from the west end baseline of each test strip (Figure 3.1). During construction, compaction was monitored on-site using a PQI Model 301 and Troxler Model 3440 Nuclear Density Gauge (NDG) for identical locations in Zone 2 of each test strip. Following construction, one pavement core was removed from each strip for comparison with in-place density gauges.

a) Compaction

b) PQI Model 301

c) Troxler Model 3440

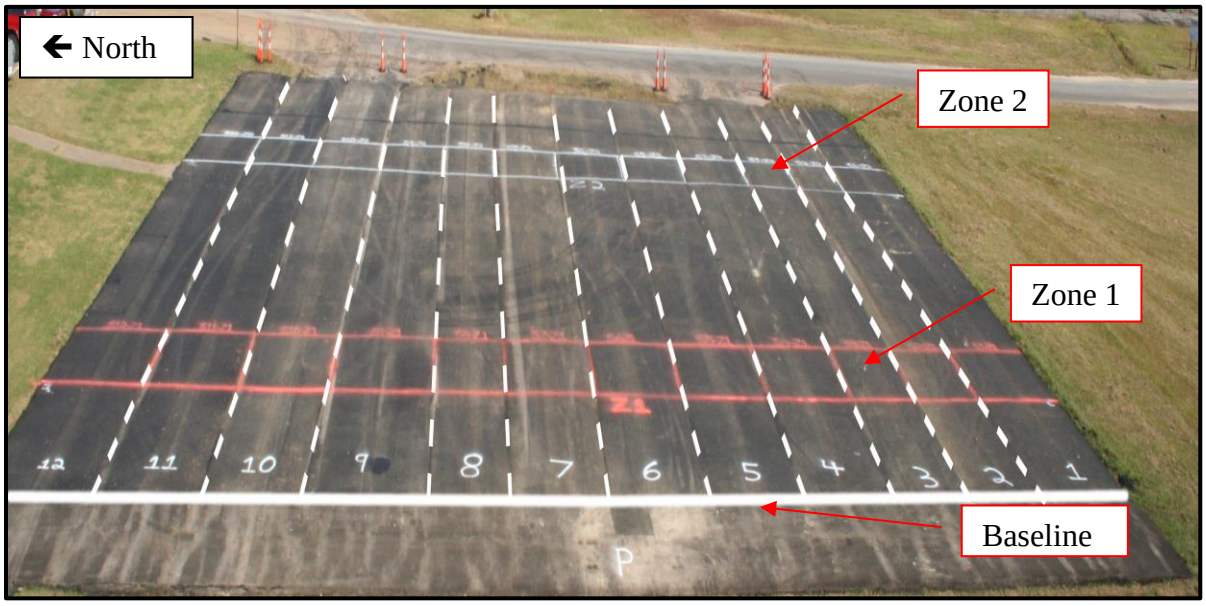

d) Overall Test Section

Figure 3.1. As Constructed Test Section

3.2.2 Field Aging Environment

Weather data reported from the Columbus Air Force Base, which is approximately 19 km from the test section, was recorded throughout this study. As shown in Tables 3.2 to 3.6, the Columbus Mississippi environment consists of relatively mild winters and hot summers. Further, the cumulative row for each table indicates averages weighted by day where appropriate. Weather was not monitored beyond year 5.

Table 3.2. Year 1 Weather Summary (November 2011 to October 2012)

		Avg. Daily Temp		High Daily Temp		Low Daily Temp		Rainfall		Relative Humidity	
Month	Days	Mean (°C)	St. Dev (°C)	Mean (°C)	St. Dev (°C)	Mean (°C)	St. Dev (°C)	Total (cm)	Days of 1.25 cm+	Mean (%)	St. Dev (%)
Nov-11	30	12.2	5.3	18.6	5.6	5.5	6.4	5.4	1	77.4	12.7
Dec-11	31	8.0	4.1	13.8	4.9	1.9	5.0	14.8	5	83.0	10.6
Jan-12	31	9.2	5.1	16.0	4.8	2.5	6.3	10.5	4	75.4	17.7
Feb-12	29	10.0	5.3	15.9	5.7	3.9	5.8	11.4	4	76.1	14.2
Mar-12	31	17.7	4.2	24.4	4.3	11.1	4.7	11.3	2	73.9	15.6
Apr-12	30	18.0	3.8	25.1	4.1	11.2	4.3	7.1	1	71.4	10.2
May-12	31	22.7	2.4	29.5	2.9	16.0	2.5	8.3	1	79.1	9.3
Jun-12	30	24.7	2.6	31.3	3.8	18.4	2.6	7.6	2	71.2	11.4
Jul-12	31	27.6	1.5	33.2	2.6	22.0	1.2	10.7	3	77.7	9.9
Aug-12	31	25.3	2.0	30.7	2.6	20.4	2.5	11.1	3	83.3	7.9
Sep-12	30	22.4	3.5	28.9	3.2	16.1	4.6	14.2	3	78.6	9.3
Oct-12	31	16.0	4.0	22.6	4.7	9.3	4.1	6.6	2	79.4	12.3
All	***366***	***17.8***	***7.6***	***24.2***	***7.7***	***11.6***	***8.1***	***119.1***	***31***	***77.2***	***12.5***

Table 3.3. Year 2 Weather Summary (November 2012 to October 2013)

		Avg. Daily Temp		High Daily Temp		Low Daily Temp		Rainfall		Relative Humidity	
Month	Days	Mean (°C)	St. Dev (°C)	Mean (°C)	St. Dev (°C)	Mean (°C)	St. Dev (°C)	Total (cm)	Days of 1.25 cm+	Mean (%)	St. Dev (%)
Nov-12	30	9.5	3.4	17.8	4.2	1.3	3.4	4.8	2	77.6	10.7
Dec-12	31	9.6	5.5	15.3	5.6	3.8	6.2	15.3	3	82.5	13.2
Jan-13	31	8.3	5.8	13.2	6.1	3.3	6.4	19.7	6	80.3	12.8
Feb-13	28	7.7	3.4	13.4	3.8	1.8	4.2	13.0	3	75.2	13.6
Mar-13	31	9.2	4.7	15.8	6.1	2.6	4.4	18.3	3	66.8	15.8
Apr-13	30	16.3	4.2	22.9	5.0	9.8	4.5	14.9	4	76.5	11.2
May-13	31	19.9	4.5	26.1	4.6	13.9	5.2	9.0	3	76.9	11.7
Jun-13	30	25.5	1.7	31.1	2.1	19.9	1.9	11.4	3	78.0	6.7
Jul-13	31	25.6	1.5	30.5	2.0	20.8	1.7	22.0	5	81.1	7.1
Aug-13	31	26.1	1.9	31.5	2.3	20.8	2.1	6.3	1	81.8	5.7
Sep-13	30	23.9	2.9	30.3	3.7	17.6	3.1	12.1	3	75.6	9.3
Oct-13	31	17.7	4.6	23.7	4.4	11.7	5.6	4.3	2	84.6	9.8
All	***365***	**16.7**	**8.1**	**22.7**	**8.2**	**10.7**	**8.7**	**151.1**	**39**	**78.1**	**11.7**

Table 3.4. Year 3 Weather Summary (November 2013 to October 2014)

		Avg. Daily Temp		High Daily Temp		Low Daily Temp		Rainfall		Relative Humidity	
Month	Days	Mean (°C)	St. Dev (°C)	Mean (°C)	St. Dev (°C)	Mean (°C)	St. Dev (°C)	Total (cm)	Days of 1.25 cm+	Mean (%)	St. Dev (%)
Nov-13	30	9.3	5.3	15.3	5.5	3.1	6.2	8.2	3	74.2	12.7
Dec-13	31	6.8	5.9	12.2	6.8	1.3	6.2	15.8	7	81.6	10.0
Jan-14	31	1.8	5.3	9.2	6.5	-5.7	5.2	5.2	1	60.4	16.2
Feb-14	28	6.6	5.1	12.4	6.8	0.7	4.6	9.2	2	75.6	11.8
Mar-14	31	10.4	4.4	17.7	5.7	3.0	4.2	9.0	2	71.8	14.1
Apr-14	30	16.5	4.0	23.3	4.5	9.7	4.5	20.2	4	74.9	13.7
May-14	31	21.2	3.4	28.0	3.7	14.8	4.3	11.2	3	72.9	11.2
Jun-14	30	25.4	1.5	30.7	2.3	20.4	1.3	15.2	3	80.6	7.0
Jul-14	31	24.6	2.3	30.1	2.8	19.2	2.4	9.5	3	78.5	8.7
Aug-14	31	26.3	1.7	32.4	2.0	20.3	2.0	7.7	1	77.1	8.3
Sep-14	30	24.3	2.6	30.4	2.4	18.4	3.4	4.1	2	76.9	6.7
Oct-14	31	18.1	4.2	25.3	4.1	11.0	5.2	11.4	3	80.5	9.7
All	***365***	**16.0**	**9.2**	**22.3**	**9.3**	**9.7**	**9.7**	**126.7**	**34**	**75.3**	**12.3**

Table 3.5. Year 4 Weather Summary (November 2014 to October 2015)

		Avg. Daily Temp		High Daily Temp		Low Daily Temp		Rainfall		Relative Humidity	
Month	Days	Mean (°C)	St. Dev (°C)	Mean (°C)	St. Dev (°C)	Mean (°C)	St. Dev (°C)	Total (cm)	Days of 1.25 cm+	Mean (%)	St. Dev (%)
Nov-14	30	8.2	5.5	14.9	6.0	1.5	6.0	10.7	2	70.6	11.3
Dec-14	31	8.4	3.8	13.3	4.1	3.2	4.4	18.2	5	85.0	10.0
Jan-15	31	4.9	4.7	11.3	5.9	-1.5	4.8	12.2	4	72.0	16.5
Feb-15	29	3.6	4.6	9.1	6.2	-2.2	4.2	37.9	3	65.2	17.3
Mar-15	31	13.1	5.2	18.7	6.3	7.4	5.9	15.6	5	82.6	12.9
Apr-15	30	18.1	3.2	24.1	3.5	12.3	4.2	18.9	4	79.2	13.9
May-15	31	22.5	2.9	29.7	2.9	15.5	4.2	11.2	4	73.8	14.0
Jun-15	30	25.9	2.2	31.7	2.5	20.2	2.4	2.0	0	77.2	6.0
Jul-15	31	27.9	1.9	33.8	2.6	22.2	1.4	6.2	3	76.1	7.2
Aug-15	31	26.0	2.3	31.8	2.7	20.4	2.7	12.0	4	77.8	9.0
Sep-15	30	23.4	2.8	29.9	3.0	17.1	3.8	2.2	0	76.9	6.4
Oct-15	31	17.8	3.7	24.7	4.9	11.2	5.1	40.6	1	76.4	11.8
All	***366***	**16.7**	**9.1**	**22.8**	**9.6**	**10.7**	**9.4**	**187.9**	**35**	**76.2**	**12.8**

Table 3.6. Year 5 Weather Summary (November 2015 to October 2016)

		Avg. Daily Temp		High Daily Temp		Low Daily Temp		Rainfall		Relative Humidity	
Month	**Days**	**Mean (°C)**	**St. Dev (°C)**	**Mean (°C)**	**St. Dev (°C)**	**Mean (°C)**	**St. Dev (°C)**	**Total (cm)**	**Days of 1.25 cm+**	**Mean (%)**	**St. Dev (%)**
Nov-15	30	14.1	4.8	19.8	3.7	8.3	6.6	7.4	1	83.2	11.0
Dec-15	31	12.5	5.5	17.9	4.7	7.0	7.3	0.0	0	85.9	11.0
Jan-16	31	5.2	4.3	10.8	5.2	-0.7	4.4	18.5	3	74.0	10.6
Feb-16	28	9.4	5.1	15.4	5.3	3.1	6.2	21.4	4	68.7	15.8
Mar-16	31	14.7	4.4	21.1	5.0	8.3	5.0	27.3	5	74.9	12.8
Apr-16	30	17.3	3.2	23.6	3.6	11.1	4.0	15.2	2	72.9	12.4
May-16	31	20.9	3.4	27.3	3.5	14.6	4.1	3.0	1	74.2	8.5
Jun-16	30	26.6	1.7	32.5	1.7	20.9	2.6	19.3	3	77.8	6.9
Jul-16	31	27.9	1.3	33.6	1.6	22.3	1.6	10.9	3	82.7	7.3
Aug-16	30	28.1	0.9	33.7	1.9	22.8	0.9	8.7	3.0	85.8	6.6
Sep-16	31	26.0	2.6	33.4	2.8	18.9	3.3	0.5	0.0	69.7	8.0
Oct-16	30	20.1	3.1	29.1	2.8	11.4	4.0	2.5	1.0	68.2	8.7
All	***365***	**18.6**	**8.2**	**24.8**	**8.4**	**12.3**	**8.6**	**134.7**	**26**	**76.6**	**11.9**

A few parameters used to describe the cumulative weather patterns over time are used throughout this effort. High temperature cumulative degree days (CDD_{high}) is used to describe the accumulation of high temperature days over time, and CDD_{high} is defined in Equation 3.1 (Figure 3.2a). For example, a single day with a maximum temperature of 30 °C with a 25 °C baseline would contribute 5 °C – days to CDD_{high} in Equation 3.1. Cumulative freezing index (CFI) is used to describe the accumulation of low temperature days over time and is defined in Equation 3.2 (Figure 3.2b). Cumulative days of temperature fluctuation ($CD_{fluctuation}$) describes the accumulation of days where the where the difference in maximum and minimum temperature is greater than a defined baseline. For example, the 18 °C baseline in Figure 3.2c reaches a maximum of 196 days with at least a 18 °C temperature fluctuation in a single day. Cumulative precipitation was also used to describe the cumulative rainfall over time (Figure 3.2d).

$$CDD_{high}(°C-\text{days}) = \sum(T_{dmax} - \text{Baseline})\ if\ T_{dmax} > \text{Baseline} \tag{3.1}$$

$$CFI(°C-\text{days}) = \sum(T_{dlow})\ if\ T_{dlow} < 0°C \tag{3.2}$$

Where,

T_{dlow} = Minimum Daily Temperature (°C)
T_{dmax} = Maximum Daily Temperature (°C)

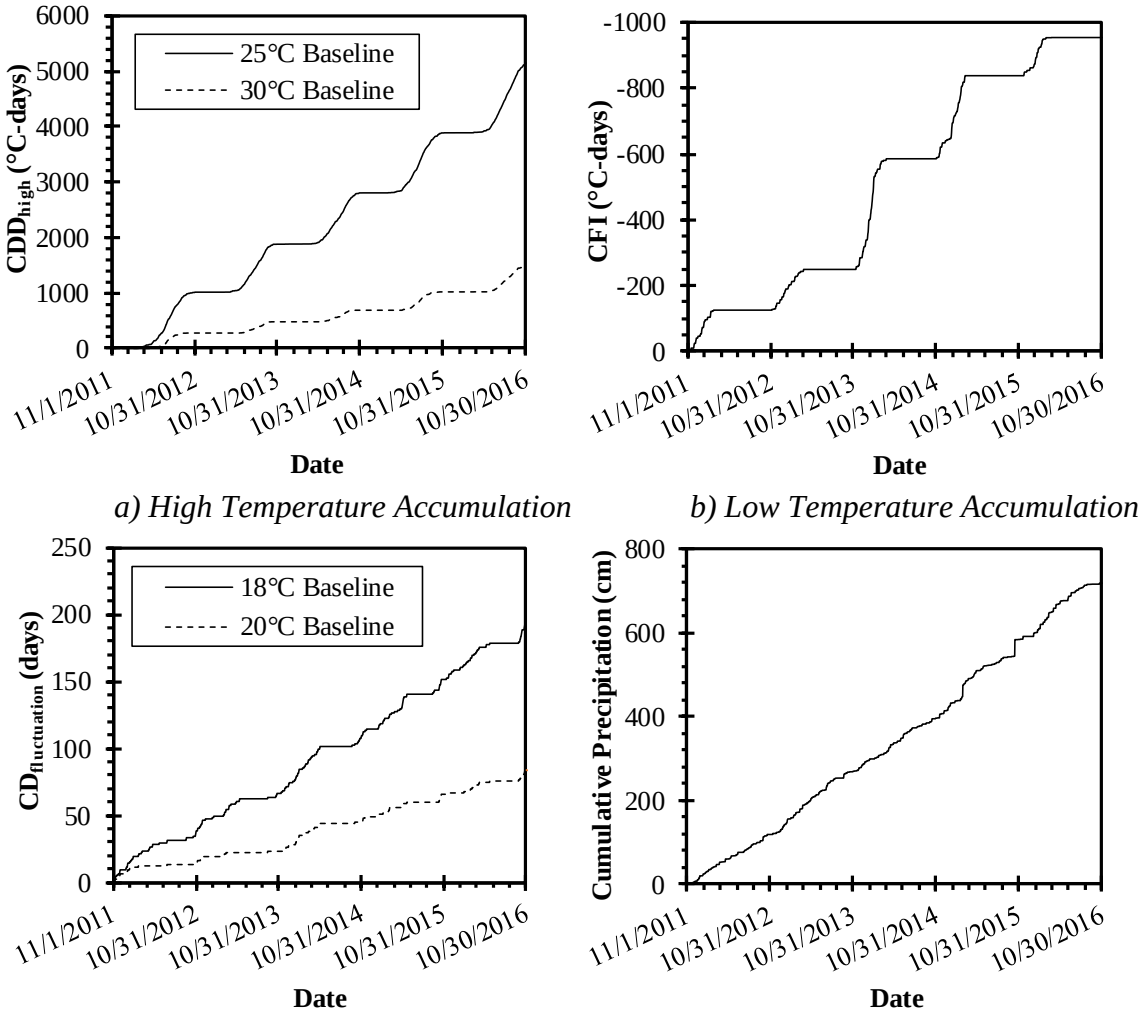

a) High Temperature Accumulation *b) Low Temperature Accumulation*

c) Temperature Fluctuation *d) Cumulative Precipitation*

Figure 3.2. Cumulative Weather Summary

3.3 Specimens Tested

Plant mixed materials were sampled and used to produce specimens in three stages: 1) during construction (395 plant mixed and laboratory compacted specimens were produced from re-heated loose mixture); 2) soon after construction (1,375 cores were taken prior to meaningful field aging); and 3) after field aging of 2 to 6 years (1,659 cores were taken and reported herein, and an additional 131 cores were taken that are not reported herein). The following sub-sections describe sampling and specimen preparation.

3.3.1 Plant Mixed and Laboratory Compacted Specimens

Plant mixed materials sampled during construction were re-heated and used to produce laboratory compacted specimens using a Pine AFGC 125X Superpave Gyratory Compactor (Figure 3.3b). Loose mix was sampled from trucks before leaving the asphalt plant or from the

paver during construction and stored in metal buckets for transportation back to the laboratory. Mixtures were re-heated to 146°C in individual pans for 150 mm specimens and in small groups (i.e. 2 to 4) for 100 mm specimens prior to compaction. Specimens were then compacted to one of three target air void levels in the laboratory: 4%, 7% or the average compacted air voids for the respective field test strip. A description of specimens available for this study from field mixed and laboratory compacted specimens is provided in Table 3.7.

Table 3.7. Lab Compacted Specimens Available for Study

Mix ID	Haul Time (hr)	Target Va (%)	Specimen Diameter (mm)	Quantity	
				h_t = 11.5 cm	h_t = 63 cm
M14	0.0	4	150	8	12
		4 & 7	100	0	6
	1.0	4, 7, & Field	150	9	9
		4, 7, & Field	100	0	9
	2.3	4, 7, & Field	150	9	9
		4, 7, & Field	100	0	9
	5.8	4, 7, & Field	150	9	9
		4, 7, & Field	100	0	7
	7.9	4, 7, & Field	150	9	9
		4, 7, & Field	100	0	9
M15	0.0	4	150	8	12
		4 & 7	100	0	6
	1.1	4, 7, & Field	150	9	9
		4, 7, & Field	100	0	9
	2.4	4, 7, & Field	150	9	9
		4, 7, & Field	100	0	9
	5.6	4, 7, & Field	150	9	9
		4, 7, & Field	100	0	7
	8.4	4, 7, & Field	150	9	9
		4, 7, & Field	100	0	9
M16	0.0	4	150	8	12
		4 & 7	100	0	6
	1.0	4, 7, & Field	150	9	9
		4, 7, & Field	100	0	9
	5.7	4, 7, & Field	150	9	9
		4, 7, & Field	100	0	9
	8.1	4, 7, & Field	150	9	9
		4, 7, & Field	100	0	9
	10.5	4, 7, & Field	150	9	9
		4, 7, & Field	100	0	9

395 Specimens Total; Specimen height (h_t)

a) Buckets of Mix Sampled During Paving *b) Pine AFGC 125X*

Figure 3.3. Laboratory Compaction of Plant Mixed Materials

3.3.2 Cores Taken Prior to Aging

A total of 1,375 field compacted specimens were collected from the parking lot before December 2, 2011 (described hereafter by as-constructed cores) and made available for this study. There were 738 cores with 15 cm diameters taken directly from the test section between November 9 and 19, 2011 and 637 cores (322 with 10 cm diameters and 315 with 15 cm diameters) that were cut from slabs collected between November 21 and December 2, 2011. Some of the specimens remaining from the original emergency paving study were discarded prior to testing performed herein, and the quantity of specimens remaining from the initial study was a controlling factor for the experimental program of this report (Table 3.8). Note that all Table 3.8 cores were stored in climate controlled laboratory conditions once they left the test section.

Table 3.8. As-Constructed Cores Available for Study

	Zone 1 Cores		Zone 2 Cores
Strip	15 cm diameter	10 cm diameter	15 cm diameter
1	63	32	29
2	48	21	32
3	57	27	30
4	58	27	30
5	62	30	31
6	54	26	30
7	43	19	31
8	55	26	31
9	62	30	30
10	58	25	30
11	60	29	32
12	62	30	35
Total	682	322	371

3.3.3 Cores Taken After Aging

A total of 1,659 field aged cores were collected on six occasions (Table 3.9) and used for experimental data in this report. Cores were collected in larger quantities in earlier years, with quantities reducing over time as more information became available. In addition to the Table 3.9 cores, 131 extra cores were taken whose test results are not reported herein.

Table 3.9. Field Aged Coring Summary

	2 Years		3 Years		4 Years		4.5 Years	5 Years		6 Years
Strip	**15 cm**	**10 cm**	**15 cm**	**10 cm**	**15 cm**	**10 cm**	**15 cm**	**15 cm**	**10 cm**	**15 cm**
1	40	20	40	20	24	12	4	18	10	19
2	---	---	---	---	---	---	4	10	10	---
3	55	25	55	25	24	12	4	18	10	19
4	---	---	---	---	---	---	4	10	10	---
5	40	20	40	20	25	10	4	18	10	19
6	---	---	---	---	---	---	4	10	10	---
7	45	20	45	20	24	10	4	18	10	19
8	---	---	---	---	---	---	4	10	10	---
9	80	35	80	35	24	12	4	18	10	19
10	60	30	60	30	40	20	4	29	16	34
11	---	---	---	---	---	---	4	10	10	---
12	---	---	---	---	---	---	4	10	10	---
Total	320	150	320	150	161	76	48	179	126	129

3.3.3.1 Coring After 2 and 3 Years of Aging

Initial plans envisioned sampling a variety of cores within the density range of full-pay and remove and replace within Mississippi Department of Transportation (MDOT) paving practices for the six test strips evaluated over multiple points of field aging. That range considers 7.0 to 10.0% air voids (V_a) based on pre-haul maximum specific gravity (G_{mm}) and bulk specific gravity (G_{mb}) measured with AASHTO T166. Thus, V_a distributions from Howard et al. (2012) were used to estimate the number of specimens to sample from each strip to achieve reasonable replication between 8.0 and 11.0% V_a based on AASHTO T331 measurements and G_{mm} measured on post-haul materials. The 1.0% V_a offset between AASHTO T166 and T331 measurements was chosen based on work from Howard and Doyle (2014), and post-haul G_{mm} measurements were used to account for variations between test strips. The Figure 3.4 layout planned sampling areas for 2, 3, 4, and 5 year samples, and areas with noticeable longitudinal cracking in strip 9 and strip 10 were marked and avoided throughout the investigation. The Figure 3.4 layout for years 4 and 5 was later abandoned. Year 2 coring occurred from October 30 to November 01 of 2013, and year 3 coring occurred from October 30 to October 31 of 2014.

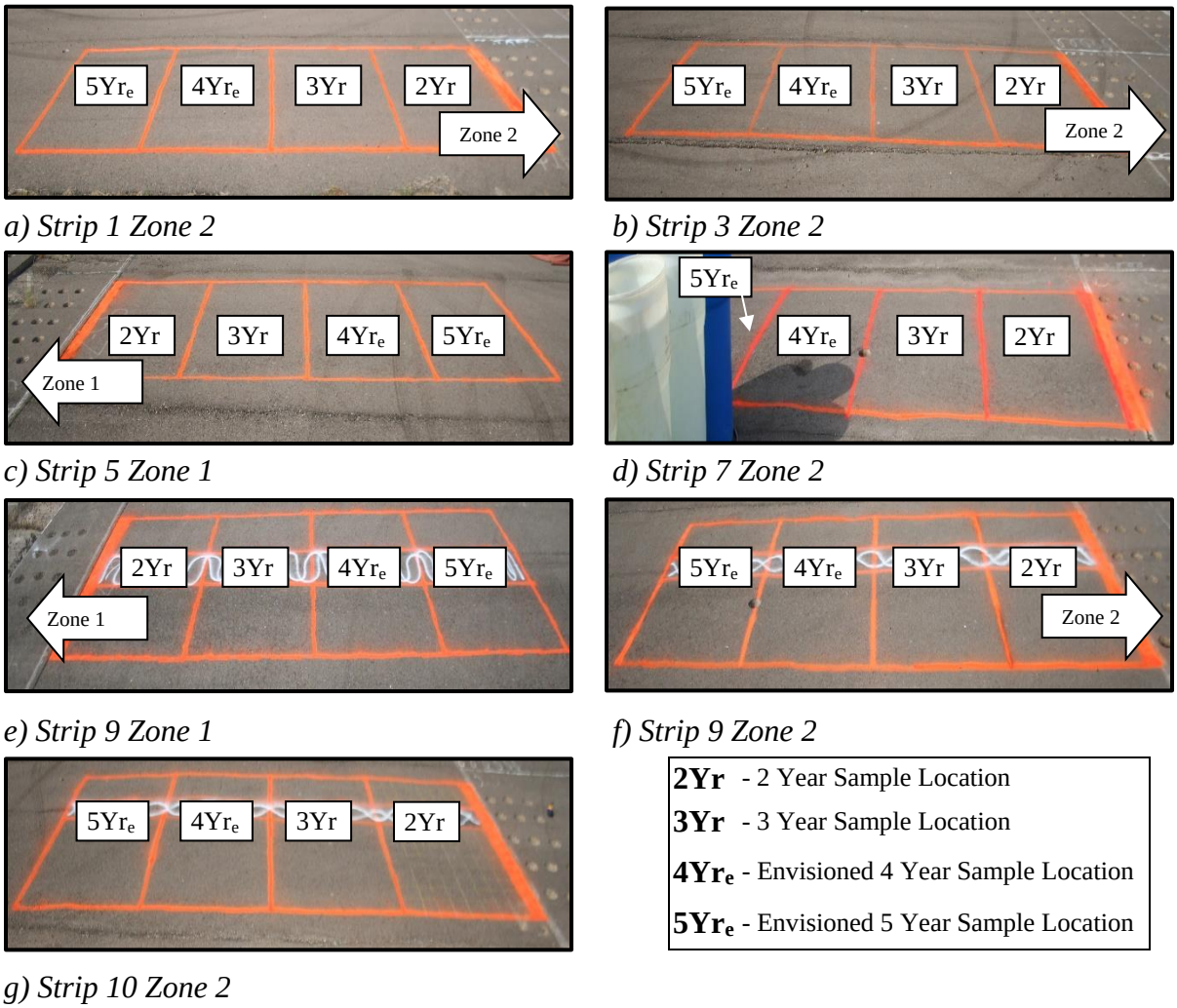

Figure 3.4. Years 2 and 3 Specimen Collection Layout

3.3.3.2 Coring After 4 Years of Aging

Coring performed after 4 years of field aging sought to investigate density variations in the longitudinal direction while decreasing the number of cores collected. Thus, coring performed during year 4 abandoned previously used zone designations (i.e. 4 yr and 5 yr markings from Figure 3.4 did not occur as originally planned) and elected to use eight coring locations per strip (Table 3.10). Three 15 cm diameter cores were removed from the Figure 3.1 baseline side of core locations 1 through 8 for each of the six test strips considered, and two 10 cm diameter cores were removed from some of the coring locations. The three 15 cm diameter cores from each coring location spanned the coring location width, and 10 cm diameter cores were sampled from spaces between 15 cm diameter cores. A photograph demonstrating how the test section was marked for sampling after 4 years of aging is provided in Figure 3.5 with strip and location or zone labels for visible sample locations. Year 4 coring occurred on October 30, 2015.

Table 3.10. Four Year Aging Coring Plan

	Coring Location Distance from Figure 3.1 Baseline (m)								
Strip	**L1**	**L2**	**L3**	**L4**	**L5**	**L6**	**L7**	**L8**	**Other**
1	5.3[a]	9.6	12.0[a]	14.5	16.9[a]	19.4[a]	26.1[a]	28.7[a]	---
3	5.3[a]	9.4	12.0[a]	14.5	16.9[a]	19.4[a]	26.1[a]	28.5[a]	
5	5.3[a]	10.5	14.5[a]	16.6	18.7[a]	20.9	23.0[a]	28.7[a]	Zone 1[b]
7	5.3[a]	9.9	12.3[a]	14.8	17.2[a]	19.7[a]	23.3	28.7[a]	
9	5.3[a]	12.5	15.2	18.0[a]	20.7[a]	23.2[a]	26.4[a]	28.7[a]	
10	5.3[a]	9.6	12.3[a]	15.1	17.8[a]	19.5	21.2[a]	28.5[a]	Zone 2[c]

[a] Three 15 cm cores and two 10 cm cores were removed.
[b] One 15 cm core was removed from the section originally intended for 3 year cores.
[c] Sixteen 15 cm and ten 10 cm cores were removed from the section originally intended for 3 year cores.

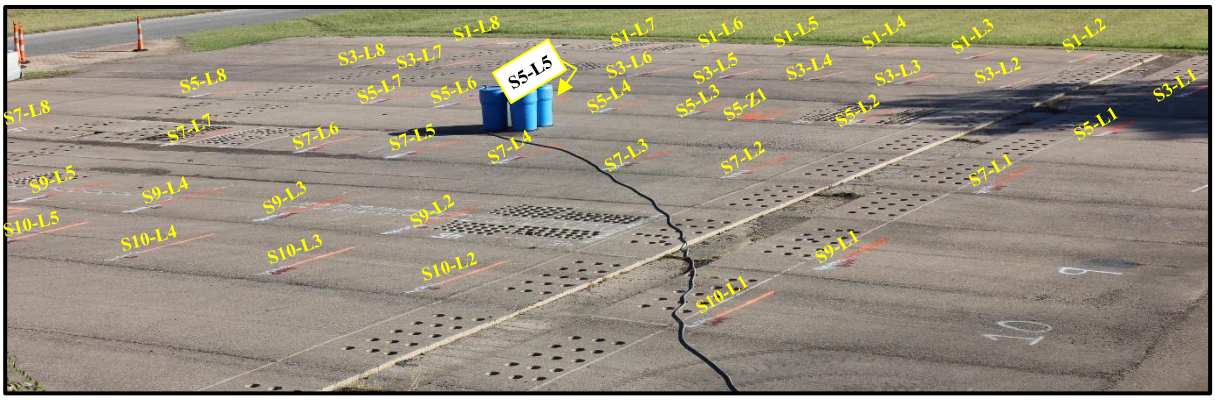

Figure 3.5. Year 4 Specimen Collection Layout

3.3.3.3 Coring After 4.5 Years of Aging

A density investigation discussed in Chapter 4 utilized four cores from each of the twelve test strips (48 total cores) that were taken on April 1, 2016. These cores were not used for mechanical property testing. Cores from individual test strips were removed simultaneously from 1,600 cm^2 areas approximately 4.6 m west of the Figure 3.1 baseline. These cores were ultimately monitored for moisture loss over time in three phases: after coring, after T166 evaluation, and after slicing to 63 mm.

3.3.3.4 Coring After 5 Years of Aging

Coring patters after 5 years of aging included samples collected from each of the twelve test strips. Strips 1, 3, 5, 7, 9, and 10 were given higher replication for analysis in field aging where multiple points in time were considered. Fewer cores were taken from strips 2, 4, 6, 8, 11, and 12 to evaluate short term aging effects during construction when coupled with 5 years of aging. Core locations were chosen based on V_a trends identified from coring performed after 4 years of aging where possible, but cores were collected from areas close to the zone with V_a most consistent with 0 year cores in strips not sampled after 4 years of aging. Core locations after 5 years are identified in the Figure 3.6 photograph after all 5 year samples were collected. All 5 year cores were taken on October 31, 2016.

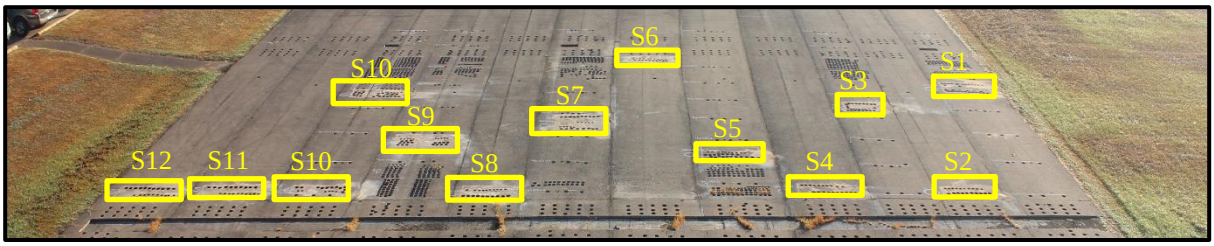

Figure 3.6. Year 5 Specimen Collection Layout

3.3.3.5 Coring After 6 Years of Aging

Coring at 6 years occurred ± 3 days of November 2, 2017. These cores were taken from any location in a given test strip so long as there was at least one core diameter between an existing core or slab hole and the current core. Note that 36 of the cores taken after 6 years were extras discussed in the next section

3.3.3.6 Extra Cores

There were 131 cores collected after 4.9, 5.3, or 6 years of aging that were not used in this report. These cores were taken for possible use in this report, but ultimately it was decided that their inclusion in this report was not optimal. These cores were used to provide additional clarity to density measurements, for exploratory efforts with other types of mechanical testing besides those relied upon herein, or stored for future testing (e.g. 6 year binder properties).

3.4 Handling and Property Determination of Field Cores

3.4.1 Specimen Handling and Storage

Cores were drilled using 15 cm and 10 cm inner diameter bits with water (Figure 3.7). A core removal tool fabricated from an exhausted coring bit was used to facilitate separation of the surface layer from tack coat without applying damaging forces to cores. After cores were removed, they were rinsed and allowed to dry adjacent to where they had been cored.

a) Field Coring

b) Core Removal Tools

Figure 3.7. Removal of Cores from Test Section

After specimen surfaces had dried enough to be labeled with markers, they were labeled and returned to the laboratory. Cores removed from slabs taken soon after construction or from initial core locations described in section 3.3.3.1 were only differentiated by sample condition (i.e. core age, test strip, and zone) prior to slicing and density measurement in the laboratory. Cores removed directly from the test section soon after construction were sampled more systematically (Howard et al. 2012), but for purposes of this study both were equivalent.

Specimen transportation was generally performed on a flat surface with a single layer of cores resting on towels or blankets (e.g. Figure 3.8a). Specimens were loaded so they were in-contact with one another during transportation to minimize the likelihood of shifting and subsequent specimen damage. Upon return to the laboratory, specimens were stored in laboratory temperature environments prior to testing without direct exposure to sunlight (Figure 3.8b).

a) Specimen Transportation

b) Specimen Storage

Figure 3.8. Specimen Handling and Storage

3.4.2 Specimen Trimming

Cores tested herein were initially trimmed to a nominal thickness of 63 mm by removing lower portions of the pavement. Cores from sections of pavement which were thinner than 63 mm were tested without trimming. All air void measurements were performed on cores with a thickness of 63 mm (or less), and mechanical tests requiring additional slicing considered air voids measured on the 63 mm thick portion of specimens. The same saw was used to slice all cores throughout this study, and collars were used mark cores and facilitate even slicing of core faces (i.e. tops or bottoms) when appropriate. Figure 3.9 demonstrates the saw used throughout the project and collar used to mark cores for trimming to 63 mm.

a) Core Saw

b) 63 mm Tall Core and Collar

Figure 3.9. Core Trimming

3.4.3 Density Measurement

Bulk specific gravity (G_{mb}), unless otherwise noted, was determined per AASHTO T331 throughout this report. The only exceptions were AASHTO T166 measurements performed as part of Chapter 4 and as a requirement for specimen saturation prior to conditioning. Maximum specific gravity (G_{mm}) was determined using AASHTO T209, and G_{mm} was measured on loose plant mixed materials as appropriate (i.e. after the same amount of haul time as specimens for mechanical testing). Air voids (V_a) were defined using T331 measurements and post haul G_{mm} values throughout this report unless specifically denoted otherwise. Note that standard MDOT practice would use pre-haul G_{mm}, but post-haul G_{mm} values were often used to account for variation between test strips.

a) AASHTO T331

b) AASHTO T166

c) AASHTO T209

Figure 3.10. Density Measurement

3.4.4 Core Drying Investigations

The density investigation mentioned in section 3.3.3.3 and discussed in Chapter 4 utilized four laboratory drying protocols: A) ambient drying in laboratory conditions B) fan drying at ambient temperature C) ASTM D7227 followed by ambient drying D) oven drying at 110°C. One core from each test strip was allocated to each of the four Figure 3.11 drying protocols. All cores from an individual strip were removed simultaneously, rinsed, and surface dried before returning to the laboratory. Cores allocated to protocols A, B, and C were dried three times: 1) for ten weeks after coring, 2) for two weeks after T166, 3) for two weeks after slicing cores to 63 mm thick. V_a measurements were performed using T166 after the first 10 weeks of drying for non-oven dried cores; oven dried cores were T166 tested the day of coring and oven dried for 1 week. Moisture loss was monitored over time for each of these 48 cores, and specimen masses in air were used to back calculate V_a.

a) Ambient

b) Fan

c) ASTM D7227

d) 110°C Forced Draft Oven

Figure 3.11. Core Drying Protocols

3.5 Laboratory Conditioning Protocols

There were seven conditioning protocols (CPs) used throughout this report (Table 3.11). These protocols consisted of three conditioning modes (oven, hot water, and freeze-thaw (FT)) that were applied in the order presented in the following three sub-sections.

Table 3.11. Laboratory Conditioning Protocols

Conditioning Protocol	Conditioning Mode		
	Oven	**64 °C Water**	**Freeze-Thaw (FT)**
CP1	5 Days at 85°C	---	---
CP2	28 Days at 60°C	---	---
CP3	---	14 Days	---
CP4	---	14 Days	1 Cycle
CP5	---	14 Days	2 Cycles
CP6	---	28 Days	---
CP7	5 Days at 85°C	14 Days	1 Cycle

3.5.1 Oven Conditioning

Oven conditioning was performed in forced-draft ovens without sleeves surrounding specimens. Conditioning was performed for 120 ± 0.5 hr at 85°C or for 672 ± 3 hr at 60°C. In all cases, room temperature specimens were transferred to pre-heated ovens when conditioning was started. After conditioning, specimens were allowed to cool to room temperature without being moved with ovens turned off and doors slightly opened.

3.5.2 Hot Water Conditioning

Specimens that were hot water conditioned were vacuum saturated, placed in room temperature water for varying amounts of time, and transferred to water pre-heated to 64°C. Vacuum saturation filled 70 to 80% of T166 measured V_a volumes with the Figure 3.10 T209 vacuum setup. Hot water conditioning used an approximately 1,136 liter tank capable of

conditioning approximately 100 specimens with 15 cm diameters in single layers on two levels of shelving. Tank fabrication is described in the next paragraph and Figure 3.12.

The water bath was fabricated using a tank with zinc-coated galvanized steel walls. The tank was contained in a plywood box, and spaces between the tank and box were filled with "Great Stuff" expanding foam insulation (insulation R-value of 2). The tank was covered with a zippered plastic sheet (18 mil vinyl and 14 oz fabric) and a 2.5 cm honeycombed-wall aluminum insulation panel (Plascore) to retain moisture and heat. Specimens were supported by stainless steel shelves supported with 15 cm sections of 7.5 cm inner diameter pipe. Two Gilson HM-651 water heating elements were used, and water was circulated with a Taco Model 006-ST4-1 pump. Two K-type thermocouples were placed approximately 30 cm from one of the heating elements to monitor water temperature during curing.

There were ten trials where the Figure 3.12 conditioning tank was used to complete the Table 3.11 conditioning protocols involving water. Summaries for each of the ten conditioning trials are provided in Table 3.12 where $t_{warm\text{-}up}$ indicates the amount of time to re-heat water to 64°C after transferring room temperature specimens to pre-heated water; conditioning time indicates the amount of time after water returned to 64°C until conditioning was completed. The final column in Table 3.12 indicates whether FT conditioning was conducted for specimens within each conditioning trial, and the following paragraph describes how specimens subjected to FT conditioning were treated slightly different with respect to hot water conditioning.

Table 3.12. Water Bath Conditioning Trials

Trial	Start Date	$t_{warm\text{-}up}$ (hours)	Conditioning Time (hours)	Conditioning Time (days)	Conditioning Temp		Followed by FT?
					Avg (°C)	St. Dev. (°C)	
1	11/25/2014	16.3	672.2	28.0	63.9	0.8	No
2	8/21/2015	4.3	335.2	14.0	64.1	0.8	No
3	9/25/2015	6.6	336.4	14.0	63.8	0.6	No
4	10/12/2015	8.4	335.4	14.0	64.2	0.4	Yes
5	10/28/2015	6.3	336.0	14.0	64.0	0.3	Yes
6	12/1/2015	6.3	336.2	14.0	64.2	0.3	Yes
7	1/4/2016	6.5	335.7	14.0	63.8	0.3	Yes
8	1/25/2016	10.0	335.9	14.0	63.5	0.4	Yes
9	2/15/2016	5.5	673.2	28.1	64.1	0.4	No
10	4/15/2016	3.5	335.3	14.0	64.2	0.6	Yes

There were two methods used to end hot water conditioning. All cases where hot water conditioning was conducted ended with a six week drying period in laboratory air and room temperature before testing. Specimens subjected to FT conditioning were slowly cooled to near-room temperature while submerged in water and transferred directly to FT conditioning while at their submerged saturation level. Hot water was drained away from specimens which were not FT conditioned as soon as conditioning ended. All specimens within a single run of the water bath were either FT or not-FT conditioned after water conditioning. Fans circulated room temperature air over the water surface to facilitate cooling hot water to near-room temperature.

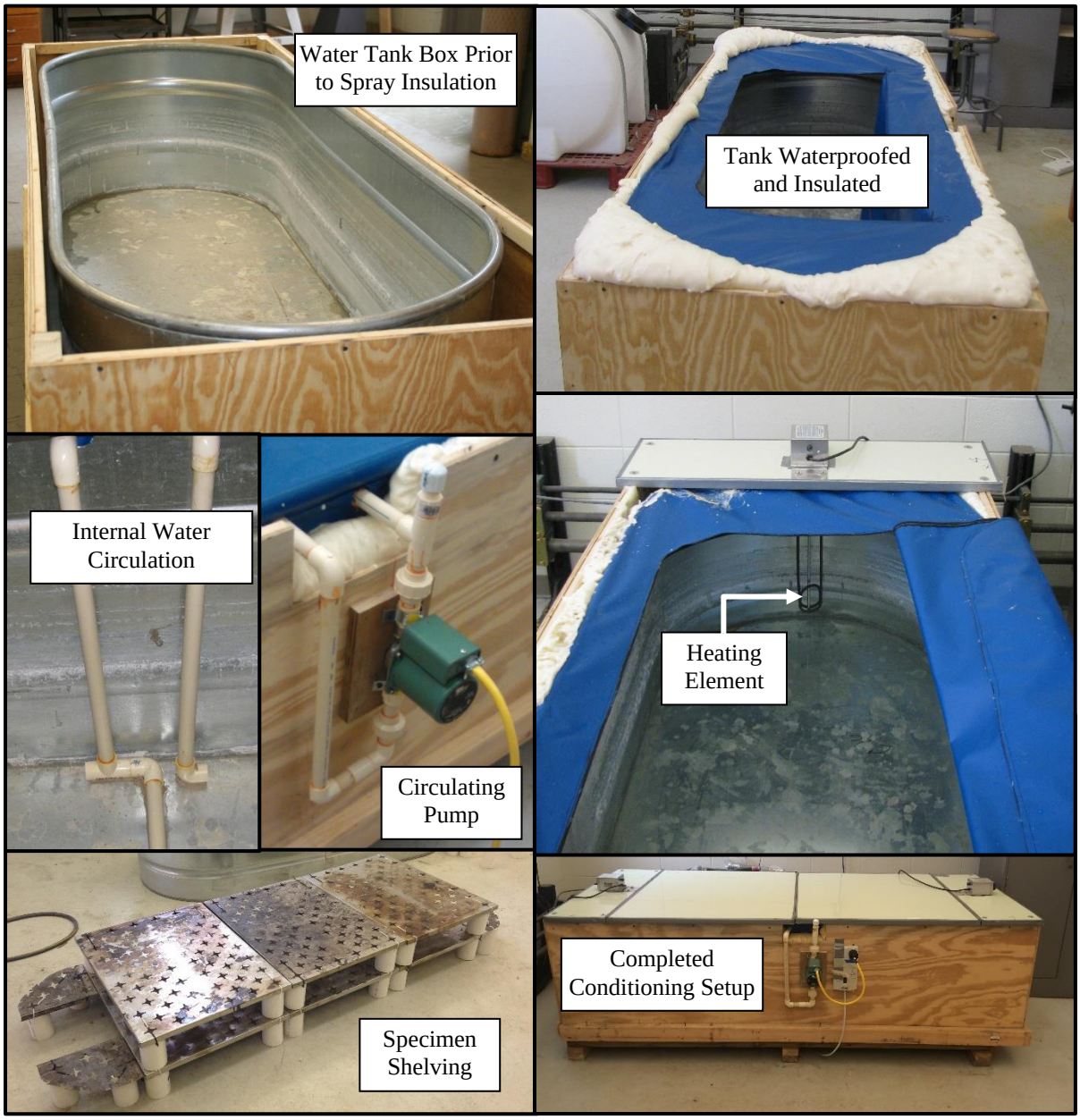

Figure 3.12. Water Conditioning Tank

3.5.3 Freeze-Thaw Conditioning Equipment

Freeze-Thaw (FT) conditioning was performed in two Frigidare 0.58m^3 upright freezers (Model: FFFU21M1QWA). The model of freezer was chosen to produce a uniform cooling pattern due to cooling coils running through each of the freezer shelves. Freezer shelves were fitted with plywood for support (Figure 3.13), and preliminary evaluations to measure temperature gradients with shelf height and relationships between freezer setting (1 to 7) and temperature are described in the remainder of this subsection.

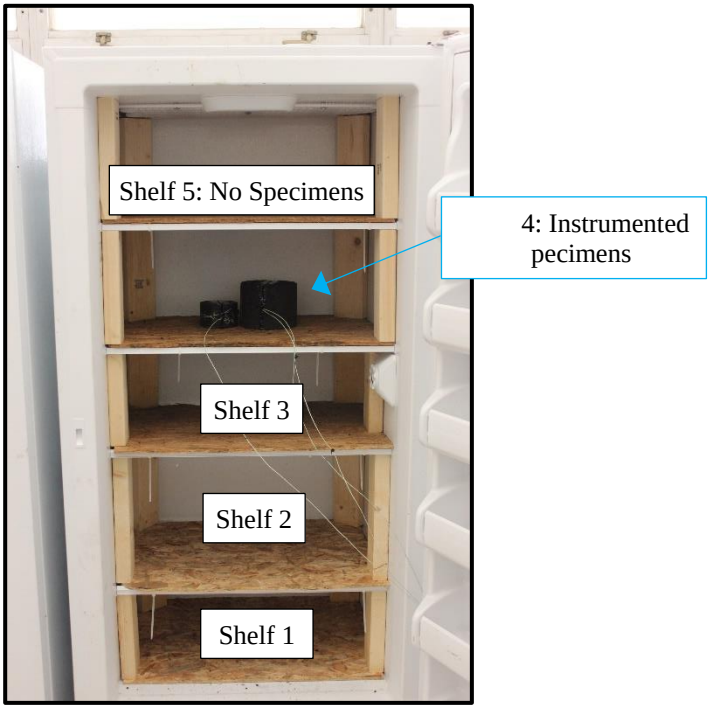

Figure 3.13. Conditioning Freezer

Temperatures were monitored using compacted specimens (10 cm diameter by 6.3 cm tall and 15 cm diameter by 11.5 cm tall) instrumented with K-type thermocouples. Specimens with 10 cm diameters were instrumented with one thermocouple at the center of the circular face, and specimens with 15 cm diameters were instrumented with one thermocouple at the center of the circular face and one thermocouple approximately ¼ diameter from the edge of the circular face. All thermocouples were placed mid-thickness within the instrumented specimens.

The first gradient evaluation considered three instrumented specimens placed on shelf 1 (10 cm diameter), shelf 3 (15 cm diameter), and shelf 5 (10 cm diameter) of freezer 1 with the freezer on setting 4. Specimens were placed on their respective shelves with the freezer off, and then the freezer was turned on. Specimen temperatures were monitored once every 5 minutes until a consistent temperature was reached, and temperatures were monitored for 2 hr thereafter. Shelf 5 was deemed inappropriate for conditioning after analyzing Trial 1 observations based on the noticeable difference in temperature measurement of shelf 5 when compared to shelves 1 and 3 (Table 3.13). A second trial considered 10 cm diameter specimens placed on shelves 1 and 4 with 15 cm specimens placed on shelves 2 and 3 of freezers 1 and 2. Trial 2 indicated that temperature differences measured between shelves were apparent, but reasonable.

Table 3.13. Temperature Gradients Within Freezers

Shelf	Trial 1		Trial 2			
	Freezer 1 Avg Temp (°C)	Stdev (°C)	Freezer 1 Avg Temp (°C)	Stdev (°C)	Freezer 2 Avg Temp (°C)	Stdev (°C)
1[a]	-18.4	0.2	-18.4	0.2	-17.5	0.1
2[b]	---	---	-19.7	0.1	-18.8	0.1
2[c]	---	---	-19.8	0.1	-19.0	0.1
3[b]	-20.4	0.2	-20.3	0.1	-19.6	0.1
3[c]	-20.5	0.1	-20.2	0.1	-19.7	0.2
4[a]	---	---	-19.4	0.2	-18.3	0.2

[a] Observations from center of a 10 cm diameter and 6.3 cm tall instrumented specimen.
[b] Observations form center of a 15 cm diameter and 11.5 cm tall instrumented specimen.
[c] Observations ¼ diameter from outside edge of a 15 cm diameter and 11.5 cm tall specimen.

After determining which shelves were appropriate for specimen conditioning, relationships between freezer setting and temperature were developed for both freezers. Instrumented specimens were placed on shelves 1 to 4 for both freezers as indicated in Trial 2 of the temperature gradient investigation. All temperature settings were monitored for freezer 1, and freezer 2 was monitored for settings 1, 4, and 7. Temperature was measured every 5 minutes over a 2 hour period after reaching equilibrium temperature (i.e. 144 measurements per freezer per setting) and Figure 3.14 presents relationships between individual temperature measurements and freezer setting for both freezers.

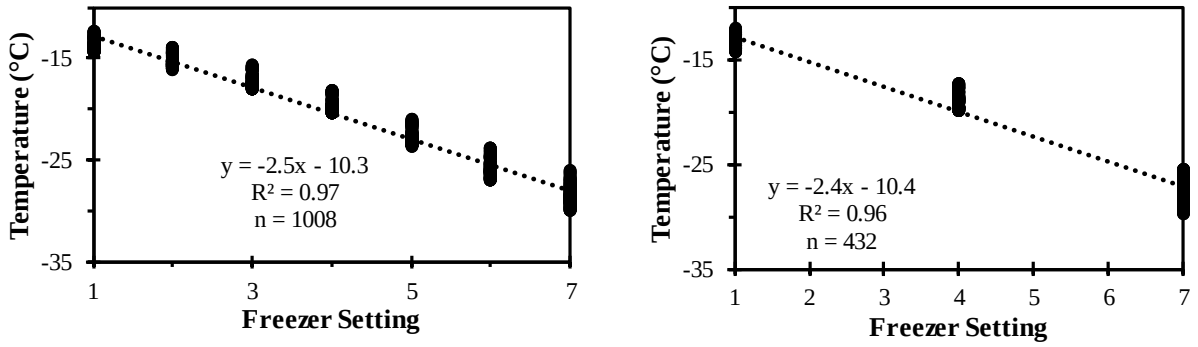

a) Freezer 1 *b) Freezer 2*

Figure 3.14. Freezer Calibration

3.5.4 Freeze Thaw Specimen Conditioning

During conditioning, near-room temperature specimens which had been hot water conditioned and slowly cooled were transferred to pre-chilled freezers and allowed to freeze to -22°C (nominal temperature) for 24 hours. Both freezers achieved this temperature when set to setting 5 of 7. Instrumented specimens containing K-type thermocouples were placed as shown in Figure 3.13 to verify that specimens were frozen to the correct temperature. After 24 hours, freezers were turned off and specimens were thawed with the doors closed.

For conditioning protocols where specimens were subjected to two FT protocols, specimens were frozen as described in the previous paragraph for the first cycle. The second FT cycle was modified slightly. After specimens had thawed to approximately 2°C from the

first FT cycle, freezer doors were opened for 30 min to ensure that specimens had thawed. Freezer doors were then shut and the freezers were turned back on for 24 hours before turning freezers off and allowing specimens to thaw to near-room temperature with the doors closed. After specimens were returned to room temperature, they were removed from the freezers and air dried for six weeks in laboratory conditions prior to testing.

3.6 Mixture Tests

Five types of mixture tests were utilized throughout this report. Intermediate temperature testing consisted of non-instrumented indirect tensile (IDT), instrumented IDT (referred to as SIDT for Superpave IDT), and Cantabro mass loss (CML) testing. Low temperature testing consisted only of SIDT. High temperature testing consisted only of Hamburg Loaded Wheel Testing (HLWT). Mixture infiltration testing was also conducted in field environments for test strips. Specific details of mixture testing are provided in the following sub-sections.

3.6.1 Indirect Tensile Testing (Non-Instrumented)

Non-instrumented indirect tensile (IDT) testing was performed on 10 cm diameter specimens after conditioning to 25°C in air (Figure 3.15). Loading conditions conformed to AASHTO T283, and IDT loading heads were used. Specimens were loaded diametrically at a rate of 50 mm/min until failure, and the IDT strength (S_t) was determined using Equation 3.3.

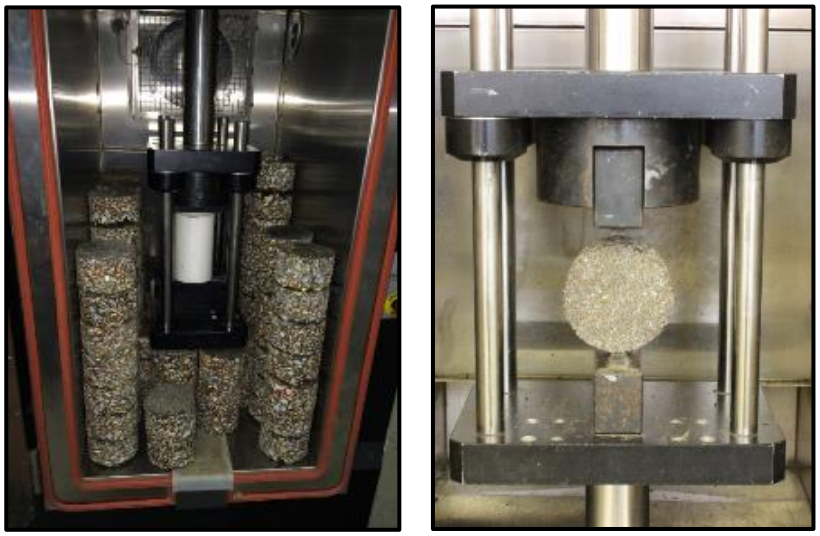

a) Conditioning to 25°C *b) Non-Instrumented IDT Test*

Figure 3.15. Non-Instrumented IDT Testing

$$S_t = \frac{2000 \times P_{max}}{\pi \times t \times D} \quad (3.3)$$

Where,

S_t = Indirect Tensile Strength (kPa)
π = 3.14159
P_{max} = Maximum Load (N)
t = Specimen Thickness (mm)
D = Specimen Diameter (mm)

3.6.2 Indirect Tensile Testing (Instrumented)

Instrumented IDT tests (referred to as SIDT tests) were conducted at 20°C and -10°C to determine fracture energy (FE) of approximately 31 mm thick specimens. For intermediate and low temperatures, a higher fracture energy is desired to withstand cracking. FE specimens were produced by removing an approximately 12.5 mm thick slice from the top and bottom of 63 mm cores (Figure 3.16a to 3.16c), and these slices were used for binder testing (or discarded in a few isolated cases). Steel gage points with nominal dimensions of 6 mm thickness and 8 mm diameter were affixed to specimen faces with 38 mm gage lengths using Devcon 5 Minute Epoxy Gel. Specimens were allowed 15 minutes in the Figure 3.16d gluing jig to allow sufficient strength gain prior to handling.

After gage points were affixed to FE specimens, specimens were conditioned in an environmentally controlled chamber set to 20°C or -10°C before testing. Specimens tested at 20°C were conditioned for a minimum of 2 hr before testing, and specimens tested at -10°C were conditioned for a minimum of 3 hr but not more than 24 hr before testing. For simplicity, FE_{+20C} and FE_{-10C} are used to indicated FE measured at 20°C and -10°C, respectively. Specimen deformation responses were measured using four Epsilon 3910 extensometers (LVDTs) that were magnetically attached to the previously discussed steel gage points (Figure 3.16e). Loading rates of 50 mm/min and 12.5 mm/min were targeted for FE_{+20C} and FE_{-10C}, respectively. FE was determined as the area under the stress-strain curve between initial loading that the peak point on the displacement differential curve (DDC) as discussed in section 2.6.4. Data analysis considered four cases for asphalt concrete specimens as described in section 4.5.11.4 of Cox et al. (2015a). Case 1 considered the test to be correctly conducted and performed no correction. Case 2 included cases where the point of fracture occurred after the peak load which resulted in excessive FE values, and analysis only considered the area under the stress-strain curve up to the point of max load in case 2 situations. Case 3 was described as situations where LVDTs seemed to have shifted during testing, and regressions of data prior to the point of shifting was used to estimate FE. Case 4 circumstances included tests where the DDC curve was never positive, and the test was considered invalid. Case 4 is also described in AASHTO T322.

a) 63 mm core

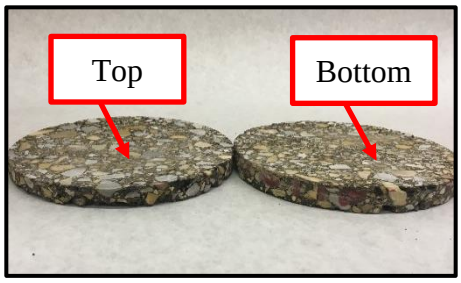

b) 12.5 mm slices

c) FE specimen interior (≈31 mm)

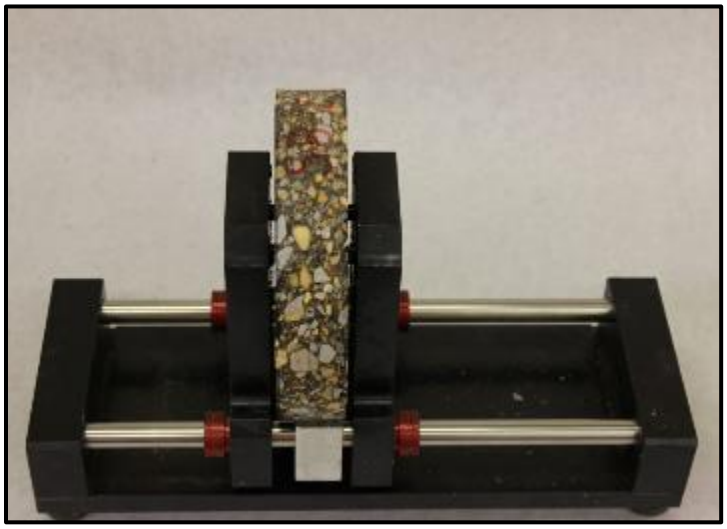

d) gluing gage points

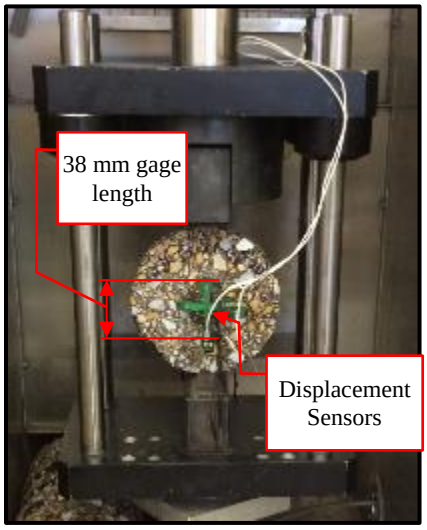

e) Instrumented IDT Test

Figure 3.16. Fracture Energy Test Process

3.6.3 Cantabro Mass Loss

Cantabro Mass Loss (CML) testing was performed on 15 cm diameter cores and 15 cm diameter lab compacted specimens after conditioning to 25°C in the environmental chamber shown in Figure 3.15. Specimens were weighed to determine an initial mass, subjected to 300 revolutions in a Las Angeles abrasion drum without steel spheres charge, brushed lightly, and weighed a second time to determine the mass lost during testing (Figure 3.17). Specimens were tested within 30 minutes of removal from the environmental chamber (they were in laboratory conditioned air during this time), and the abrasion drum internal temperature was maintained at 25±2°C. Specimen mass loss (*ML*) was calculated using Equation 3.4. Temperature conditions and the number of revolutions applied during CML testing were consistent regardless of specimen geometry or compaction method.

Figure 3.17. Cantabro Mass Loss Testing

$$ML = \frac{M_1 - M_2}{M_1} \times 100 \quad (3.4)$$

Where,
ML = Mass Loss (%)
M_1 = Initial Specimen Mass
M_2 = Final Specimen Mass

3.6.4 Hamburg Loaded Wheel Tracking

Hamburg Loaded Wheel Tracking (HLWT) was performed as per AASHTO T324-14. Testing was conducted using pairs of 15 cm diameter cores which were sliced using the saw shown in Figure 3.9. Temperature was maintained at 50°C for all HLWT tests conducted, and load was maintained at 0.7 kN for 20,000 passes. Test outputs of rut depth (RD_{HLWT}) at 20,000 passes unless otherwise noted and stripping inflection point (SIP) provide a measure of mixture stability and moisture induced damage. The HLWT setup and a set of specimens before and after testing are shown in Figure 3.18.

a) HLWT Equipment *b) Specimens Pre-Test* *c)Tested Specimens*

Figure 3.18. Hamburg Loaded Wheel Tracking Test

3.6.5 Mixture Infiltration

In-place infiltration was measured on test strips 1, 3, 5, 7, 9, and 10 in June of 2015 using the Mississippi permeameter (MSP) described in Cox et al. (2015b). The MSP consists of an acrylic standpipe with a 50.8 mm (2 in) inner diameter with marks indicative of 12.7 and 25.4 cm (5 and 10 in) of water head. A 6.3 mm thick neoprene foam rubber gasket conforming to ASTM D1056 provides a watertight seal with the pavement when a surcharge load is

applied. There were ten permeability locations (PLs) approximately 30 cm apart for each of the aforementioned strips with PLs increasing from south to north. All test locations were approximately equidistant from the Figure 3.1 baseline. The test standpipe and strip 1 test locations are shown in Figure 3.19. Infiltration rate (*Inf*) as defined in Equation 3.5 was the primary variable of interest for this test.

$$Inf = \frac{a}{At}(h_1 - h_2) \tag{3.5}$$

Where,
Inf = infiltration rate (cm/min)
a = inside cross-sectional area of permeameter standpipe (cm^2)
A = cross-sectional contact area (cm^2)
t = elapsed time between h_1 and h_2 (min)
h_1 = initial head across the test specimen (cm)
h_2 = final head across the test specimen (cm)

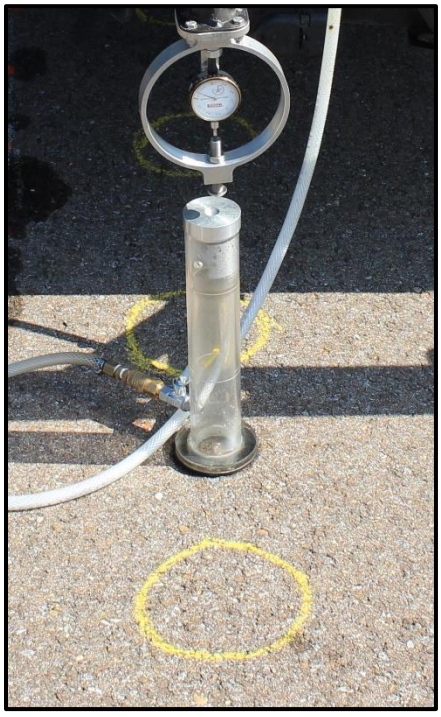

a) MSP Stand Pipe

b) MSP Field Testing Vehicle Support Frame

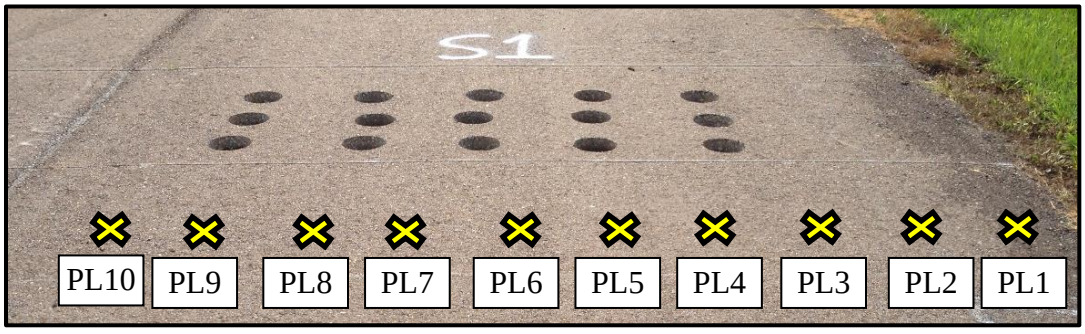

b) Strip 1 Permeability Test Locations

Figure 3.19. Field Permeability Testing

3.7 Binder Testing

Binder properties were measured on two types of samples: field core binder (FCB) that was extracted and recovered after varying levels of laboratory conditioning or field aging and 2) as-received binder (ARB) samples that were collected the morning of test section construction. The binder recovery process is described in Section 3.7.1 whereas ARB sample handling is described in Section 3.7.2. All binder samples were evaluated following the procedures described in Section 3.7.3.

3.7.1 Binder Extraction and Recovery

FCB samples recovered from groups of slices from specimen tops (i.e. 0 to 1.3 cm below the pavement surface) are referred to as FCB_0, and binders recovered from slices from specimen bottoms (i.e. 5.0 to 6.3 cm below the pavement surface) are referred to as FCB_5. Six slices were combined to produce approximately 2 kg of loose mix to provide enough binder for the range of tests described in Section 3.7.3 while also allowing all binder needed for a combination of conditions in a single extraction. In most cases, the material trimmed from SIDT specimens in Section 3.6.2 was used for FCB evaluations. However, FCB was not recovered from SIDT specimens that were not used for longer term aging considerations.

The binder recovery process consisted of two phases: extracting binder from aggregates and binder recovery. No more than one extraction was conducted per day, and mix from tops and bottoms of cores were recovered without blending top and bottom material since they have experienced different amounts of aging. Slices were initially heated in a 149°C forced draft oven in 5 minute intervals until loose enough to be separated (Figure 3.20a) before cooling to room temperature. The amount of time between producing loose mix and extraction was not monitored, but mix was stored in sealed bags between separation and extraction.

Primary extraction was performed using a Humboldt H-1471 centrifuge (Figure 3.20b) and a series of three solvents: 1) toluene which had been recovered from prior extractions, 2) virgin toluene, and 3) a blend of 85% virgin toluene and 15% ethanol. Mixes were initially submerged in recovered toluene and allowed to soak for 45 ± 5 mins. After initial soaking, the centrifuge was slowly accelerated to 3,600 rpm, and rotation was applied until extract drainage ceased. Secondary washes used 250 mL of virgin toluene with 5 minute soaks until extract was no longer black, and the extraction process finished with a minimum of 3 washes using the toluene/ethanol blend to produce an amber color. Two containers were used to keep extract containing ethanol separate from other extract.

A filterless centrifuge conforming to ASTM D1856 (Figure 3.20c) was used to remove material smaller than 0.075 mm from the extract produced during the process described in the previous paragraph to produce filtrate. The secondary centrifuge was initially primed with 350 mL of recovered toluene before processing extract, and extract containing no ethanol was processed first. Extract containing ethanol was processed second, and filtrate streams were separated by ethanol or no-ethanol.

The binder recovery process was performed using a BUCHI Rotavapor R-114 (Figure 3.20d). Ice-chilled water was circulated through condensation coils, and the recovery flask was heated in Paratherm heat transfer fluid during recovery. The heat transfer fluid was initially heated to 60°C, and an absolute pressure vacuum of approximately 600 mmHg was applied to the recovery system. Filtrate containing ethanol was transferred to the recovery flask first, and

the binder recovery (i.e., removal of toluene and ethanol) was allowed for approximately 15 minutes before increasing heat transfer fluid to 110°C and transferring additional filtrate to the recovery flask. Throughout the recovery process, additional filtrate was transferred to the recovery flask and the condensate flask was emptied as appropriate. The first flask of condensate was disposed of through proper handling protocols to minimize the potential for ethanol contamination in recovered toluene, and additional flasks were kept for re-use as recovered toluene.

Vacuum pressure was changed to 525 mm Hg after the recovery flask filtrate was stable enough to avoid boiling and heat transfer fluid was maintained at 110°C. Once all filtrate had been transferred to the recovery flask, the recovery flask pressure was decreased by approximately 25 mm Hg each time the condensate flask was emptied until the filtrate thickened noticeably and the system pressure was decreased to 200 mm Hg. Once condensation slowed to 1 or 2 drops every 30 seconds, the recovery flask was heated to 163 °C, and the system pressure was changed to 150 mm Hg. The recovery process continued for 30 minutes at these conditions.

Ultimately, the recovery process was ended by removing the system vacuum and transferring recovered binder samples to a 6 oz tin. To facilitate the transfer of recovered binder to sample tins, recovery flasks were inverted and held over sample tins in a 163°C oven for 15 minutes (Figure 3.20e). During that period, binder was allowed to drip into sample tins. A complete recovered binder sample is shown in Figure 3.20f. Recovered samples were sealed and stored in ambient conditions (i.e. approximately 21°C out of sunlight and sealed to minimize oxygen access) until transportation to Paragon Technical Services, Inc. (PTSi) for testing.

a) loose mix

b) Humboldt H-1471

c) ASTM D1856 centrifuge

d) Büchi Rotavapor R-114

e) inverted flask setup

f) recovered binder sample

Figure 3.20. Binder Extraction and Recovery Process

3.7.2 As-Received Binder Sample Handling

During construction, binder was collected as-received at the asphalt mix plant (i.e. a representative sample of what was in the delivery tanker) and stored for consideration after conditioning. ARB samples were conditioned at PTSi and tested after 8 levels of binder conditioning as described in Table 3.14. Both binders were tested as-received. Then, there were seven conditions considered following standard short term conditioning per AASHTO T240. All long term conditioning was conducted at standard pressure and temperatures per AASHTO R28 with pressure aging vessel (PAV) times of 0 hr, 10 hr, 20 hr, 30 hr, 40 hr, 60 hr, and 80 hr (a range of times outside current R28 protocols). Rolling Thin Film Oven (RTFO) was performed for 85 minutes at 163 ^{o}C as per T240, and PAV conditioning was at 2.1 MPa and 100 ^{o}C.

Table 3.14. As-Received Binder Test Matrix

Binder	Short Term Conditioning	Long Term Conditioning
Neat PG 67-22	None	None
	AASHTO T240	0, 10, 20, 30, 40, 60, and 80 hours
PG 67-22 with Evotherm 3G™	None	None
	AASHTO T240	0, 10, 20, 30, 40, 60, and 80 hours

3.7.3 Binder Test Methods

All binder testing was conducted by PTSi. FCB samples were tested without further conditioning by PTSi (i.e. PAV and RTFO were not used for FCB samples). ARB samples were conditioned as described in Section 3.7.2. Three rheology tests were performed to evaluate binder properties over a wide range of temperatures, and Fourier Transform Infrared Spectroscopy (FTIR) was also performed.

During testing, samples were exposed to the minimum amount of heat as reasonably possible. For example, when shipping specimens via third party carriers, specimens were shipped overnight to minimize the amount of time in non-climate controlled conditions. The minimum amount of oven heating to produce appropriate binder samples was also applied by PTSi during testing, and binder samples were heated only one time prior to testing for most cases.

3.7.3.1 Penetration at 25°C

Binder samples were tested for penetration (*Pen*) per ASTM D5. After transferring samples to 3 oz testing containers, samples were cooled in air, conditioned to 25°C in water for a minimum of 1 hour, and penetration tests were performed in triplicate while submerged. The conditioning bath and penetration equipment are shown in Figure 3.21.

a) Penetration Water Bath

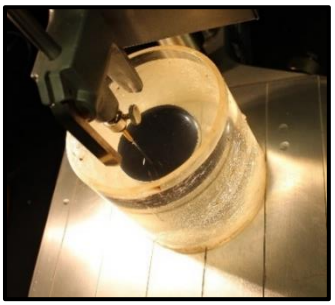

b) Penetration Setup

Figure 3.21. Asphalt Binder Penetration

3.7.3.2 Dynamic Shear Rheometer

Dynamic shear rheometer (DSR) testing was performed at intermediate and high temperatures to determine the complex shear modulus (G^*) and phase angle (δ) for each binder. Intermediate temperature DSR testing was performed using 8.0 mm plates (DSR_8) with a 2.0 mm gap, and high temperature DSR testing was performed using 25.0 mm plates (DSR_{25}) and a 1.0 mm gap. Testing was performed according to AASHTO T315 to determine critical temperatures (T_c) for intermediate and high temperature behaviors. Critical temperatures were defined as the temperature where $G^*/\sin\delta$ was 2.20 kPa for $T_c(DSR_{25})$ or $G^*\sin\delta$ was 5,000 kPa for $T_c(DSR_8)$. DSR tests were conducted with an Anton Paar SmartPave Plus 301 (Figure 3.22).

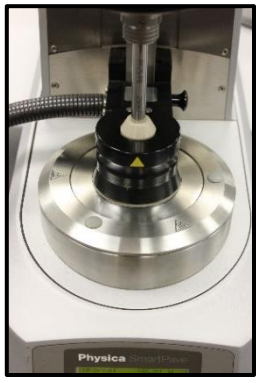

a) Heating Chamber

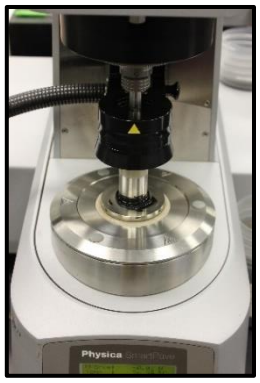

b) 25 mm Test

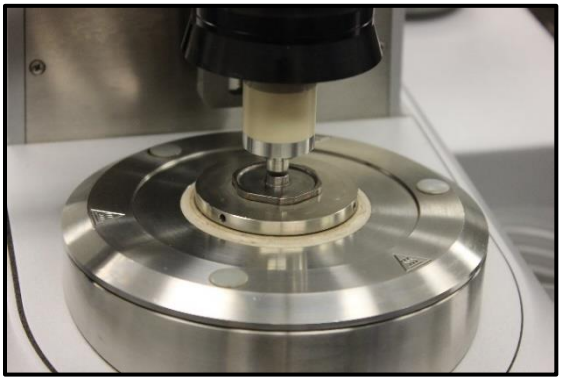

c) 8 mm Plates

Figure 3.22. Anton Paar SmartPave Plus 301 DSR

3.7.3.3 Bending Beam Rheometer

Bending beam rheometer (BBR) testing assessed low temperature properties throughout this study. Tests were conducted to determine critical temperatures based on AASHTO T313. Critical temperature was defined as the temperature where stiffness (S) reached 300 MPa $T_c(BBR_S)$ or *m-value* reached 0.300 $T_c(BBR_m)$. The BBR equipment used throughout this study is was a Cannon TE-BBR Thermoelectric Bending Beam Rheometer shown in Figure 3.23. The difference between $T_c(BBR_S)$ and $T_c(BBR_m)$ where $T_c(BBR_m)$ is subtracted from $T_c(BBR_S)$, referred to here as ΔT_c, was suggested as a durability parameter of

virgin binders by Anderson et al. (2011). Rowe (2011) suggested a minimum limit for ΔT_c of -5°C before taking immediate action.

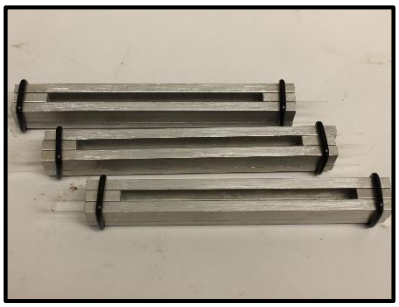

a) BBR Beam Molds

b) BBR Beam Molding

c) Cannon TE-BBR

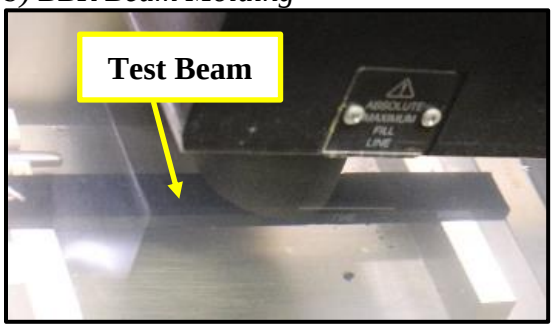

d) BBR Testing

Figure 3.23. BBR Testing and Equipment

3.7.3.4 Fourier Transform Infrared Spectroscopy

Fourier Transform Infrared Spectroscopy (FTIR) was performed to observe chemical characteristics of binder samples. FTIR analysis was conducted using the Nicolet 380 FTIR analyzer shown in Figure 3.24 and FTIR samples were prepared at the same time as rheology samples by pouring material onto wax paper, cooling, and trimming smaller pieces of the binder sample away using a heated spatula. Sliced areas were not placed over the FTIR spectrometer detector, and there was no control on film thickness in this investigation. Absorbance peak (Abs_P) spectra were used to determine the carbonyl index (CI) and sulfoxide index (SI) relative to asphalt aging. In analysis, the Abs_P peak heights at wave counts of 1700 cm^{-1} and 1031 cm^{-1} were divided by the Abs_P level at 1375 cm^{-1} to produce CI and SI indices, respectively.

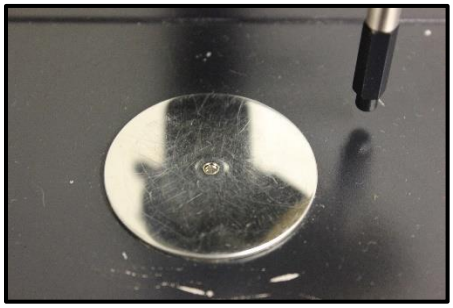

Figure 3.24. FTIR Testing Equipment

CHAPTER 4 - DENSITY OBSERVATIONS

4.1 Overview of Density Observations

Reasonable measurement of in-place density is imperative to properly consider performance of field aged cores. In-place density has been long understood as a primary contributor to multiple pavement performance behaviors (e.g. Epps and Monismith, 1969; Santucci et al., 1985; Epps et al., 2002; Monismith et al., 2004). As such, air voids (V_a) are a primary consideration for analysis performed throughout this report, and this chapter discusses a series of density observations from the first 4.5 years of this study relative to fundamental density properties.

The two phase investigation presented in this chapter has direct implications to chapters 5 to 8 of this report and is identical to the two phase investigation presented in Smith et al. (2017), which was written to address the paving industry on a broader scale. Phase I briefly describes five density measurement observations that occurred during the construction, sampling, and evaluation of materials for the test section. Phase II presents a controlled investigation of specimen drying to provide more clarity on a specific observation from Phase I. Much of the discussion in Smith et al. (2017) is not provided here for brevity, but the technical content leads to the same conclusions.

4.2 Phase I Density Observations

There were five density observations that occurred during investigation for Chapters 5 to 8. The first four observations are relative to understanding the pavement test section considered, but the fifth observation ultimately led to the Phase II density evaluation. The key observations were: accuracy of on-site density measurement techniques, pavement density gradients with depth, pavement density distribution in the longitudinal direction, maximum specific gravity (G_{mm}) variations, and moisture retention after CoreDry®(ASTM D7227).

4.2.1 On-Site Density Measurement

On-site density was measured using two devices (Figure 3.1b and 3.1c) during test section construction: a PQI Model 301 and a Troxler Model 3440 nuclear density gauge (NDG) Density was measured with both gauges at a single location in Zone 2 during construction and one month after construction. Following the second in-place density measurement, the locations were cored and tested using T166. Howard et al. (2012) developed linear relationships through the origin to relate V_a measurements for each of the strip locations. NDG measurements were more consistent over time than PQI measurements. NDG measured V_a had a 1:1.00 (X:Y) relationship when comparing measurements during construction to the measurements taken one month later, and PQI V_a measurements had a 1:1.15 relationship when comparing construction measurements to measurements taken one month later. Similar relationships between gauge measurements during construction and T166 measurements provided ratios of 1:1.06 for NDG to T166 and 1:1.50 for PQI to T166. The NDG provided greater reliability for this pavement. This observation is consistent with Williams et al. (2011) where the authors claimed that NDG measurements trended well with core density measurements.

4.2.2 Density Gradients with Depth

There were 324 cores collected soon after construction which were tested with AASHTO T331 including the full layer (FL) thickness and re-tested after trimming to nominal heights of 63 mm. The Figure 4.1 equality plot compares V_a of cores considering the FL to V_a of cores considering the 63 mm closest to the surface. As shown, V_a for sliced cores was lower then FL cores, which is consistent with results in Al-Omari et al. (2002)

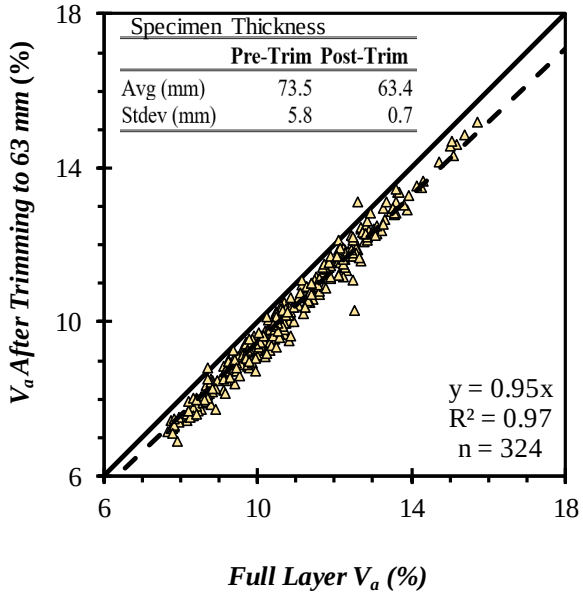

Figure 4.1. Density Gradient with Depth

4.2.3 Spatial Density Variations

Compaction patterns varied between Zone 1 and Zone 2 with one vibratory compactor used during construction, and this created an opportunity to assess compaction effects on in-place V_a, and high replication samples collected prior to 4 years of field aging indicated that pavement density varied longitudinally. Figure 4.2 provides density observations for varying locations with high replicate samples indicated by 95% confidence interval boxes and the quantity of specimens for bulk samples indicated; V_a measurements from 150 mm cores collected after 4 years of aging are indicated by points. The high V_a variability in the longitudinal direction indicates that modifying compaction patterns can meaningfully alter in-place V_a. This is not surprising, but the test section considered herein provided an opportunity to quantify vibratory roller effects on pavement density.

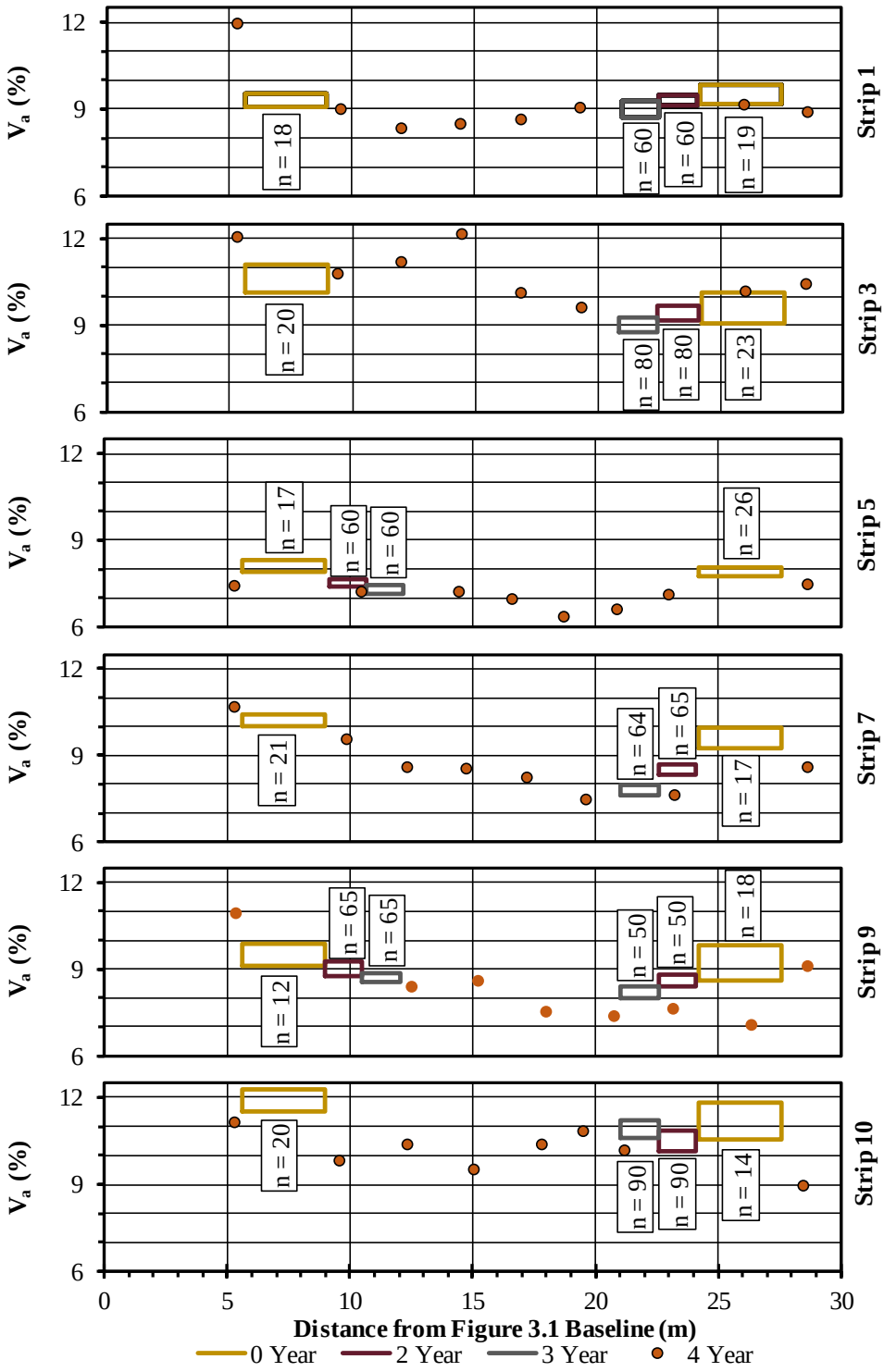

Figure 4.2. Longitudinal Direction Air Voids Variation

4.2.4 G_{mm} Measurements Over Time

Maximum specific gravity (G_{mm}) tests were performed on loose mix sampled from the paver during construction and aged cores to determine if aggregate pores were absorbing binder during field aging (Figure 4.3). Although West et al. (2014) documented G_{mm} changes after field aging, there were no meaningful changes to G_{mm} after field aging in this study (e.g. highest change in core measured G_{mm} over time was 0.012 g/cm^3). In fact, G_{mm} from loose mixtures sampled during paving was the highest density measurement for each strip considered. The difference between loose mix G_{mm} and core measured G_{mm} from unaged materials was likely caused by trapped air pockets in broken up cores when compared to loose mixtures which had never been compacted.

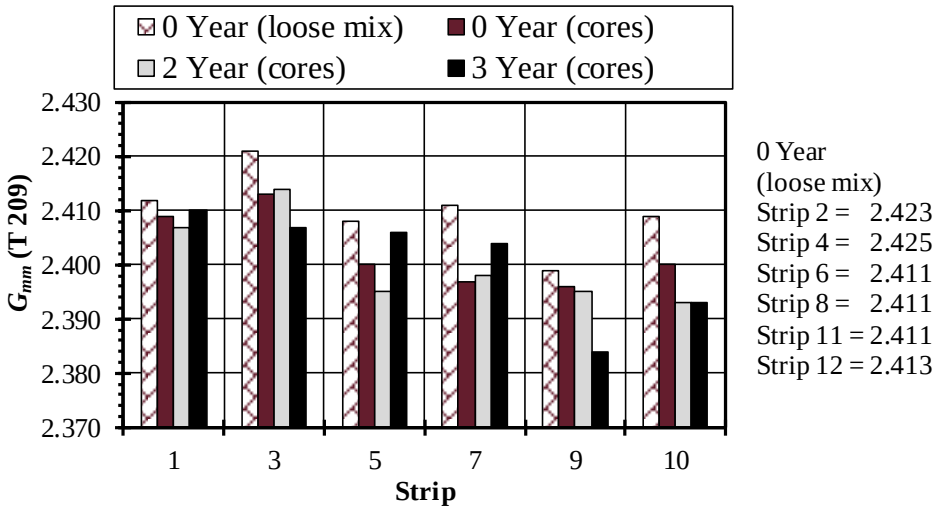

Figure 4.3. G_{mm} Results

4.2.5 Initial Drying Observations

The fifth observation from Phase I of this chapter was based on 470 cores that were sampled after two years of field aging, sliced to 63 mm, dried with ASTM D7227, and measured for V_a with AASHTO T331. Cores were then stored in laboratory conditions and re-weighed five months later; several cores had dried by 5 g or more (some as much as 29 g). All cores that had dried by 5 g or more were re-evaluated using AASHTO T331, and Figure 4.4 provides an equality plot comparing V_a after air drying to V_a after ASTM D7227. The average change in V_a was 0.44% for the specimens that were re-tested. After this observation, all field aged cores were dried at room temperature for a minimum of six weeks and monitored to ensure that there was not an appreciable amount of moisture drying from cores to affect V_a measurements.

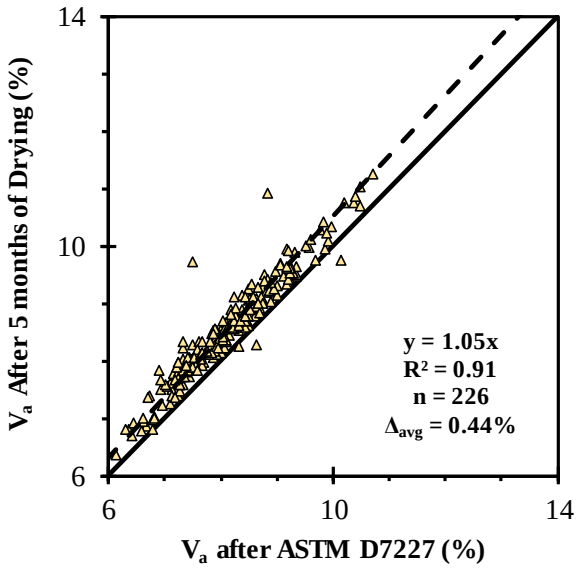

Figure 4.4. Long Term Drying vs. ASTM D7227

The accidental nature leading to Figure 4.4 also prevented key points of investigation from being captured, which led to Phase II. The Phase II experimental program was developed to observe moisture drying in a controlled environment that allowed comparisons between ASTM D7227 and traditional drying approaches over several points in time. The next section presents the Phase II drying investigation of 48 cores sampled from the test section on April 1st, 2016.

4.3 Secondary Drying Investigation

4.3.1 Results of Secondary Drying Investigation

Drying behaviors after field sampling are shown in Figure 4.5 and Table 4.1, which were collected as per Section 3.4.4. Note that the observed error in V_a measurement ($V_{a-\Delta o}$) after varying points in time indicates the difference between V_a measured after 10 weeks of drying and V_a measured after the amount of drying time indicated.

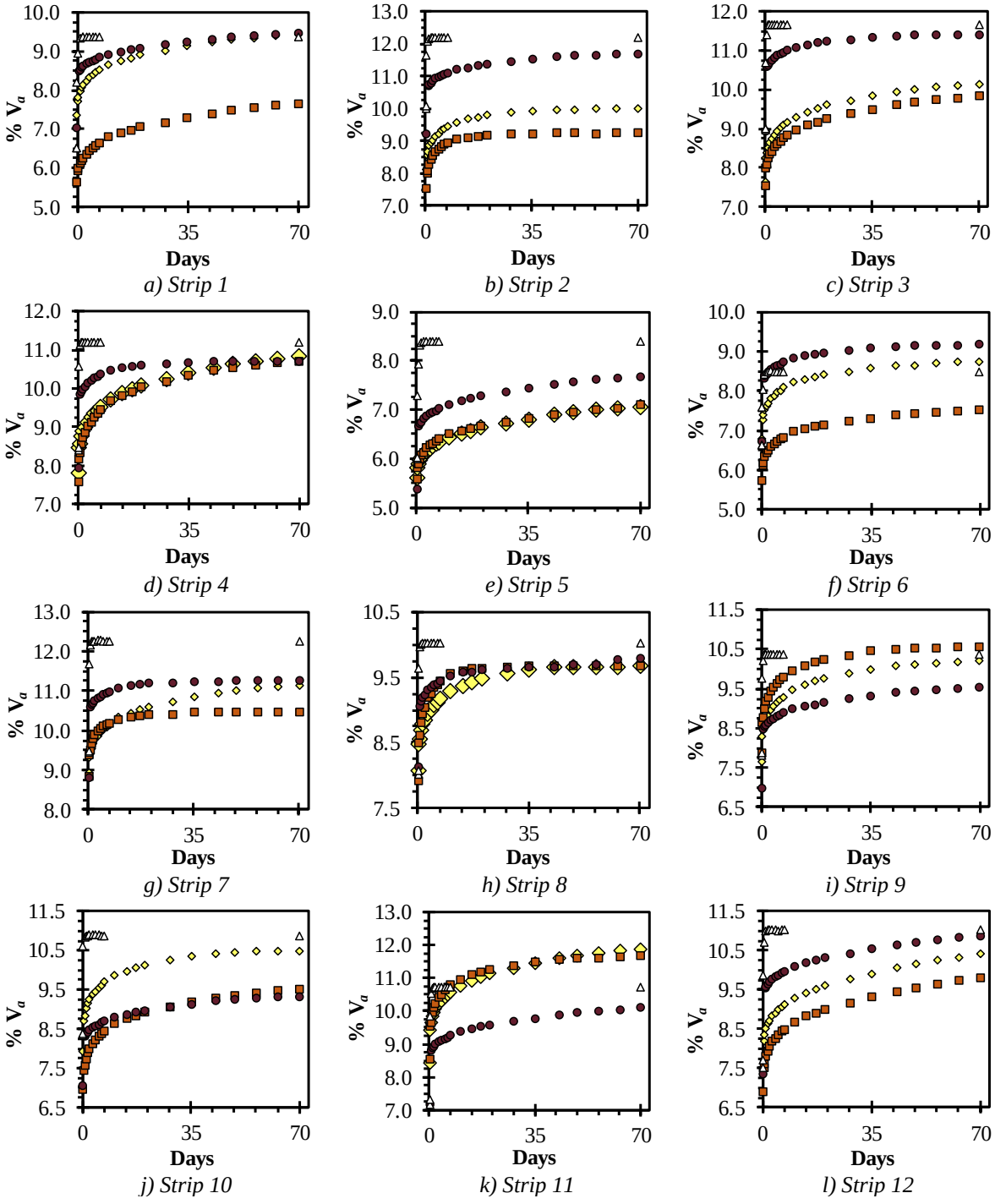

Figure 4.5. Air Voids Measured Over Drying Time after Coring

TABLE 4.1. Calculated V_a as a Function of Drying Time

Strip		1 day				2 days				1 week				4 weeks			
		Drying Protocol				Drying Protocol				Drying Protocol				Drying Protocol			
		A	B	C	D	A	B	C	D	A	B	C	D	A	B	C	D
1	V_a (%)[1]	7.96	6.11	8.53	9.33	8.14	6.26	8.63	9.38	8.52	6.62	8.83	9.37	9.01	7.17	9.15	9.37
	$V_{a-\Delta o}$ (%)	1.48	1.54	0.95	0.04	1.30	1.39	0.85	-0.01	0.92	1.03	0.65	0.00	0.43	0.48	0.33	0.00
2	V_a (%)[1]	8.88	8.30	10.78	12.18	9.05	8.55	10.87	12.21	9.46	8.95	11.11	12.20	9.88	9.22	11.47	12.20
	$V_{a-\Delta o}$ (%)	1.13	0.95	0.91	0.02	0.96	0.70	0.82	-0.01	0.55	0.30	0.58	0.00	0.13	0.03	0.22	0.00
3	V_a (%)[1]	8.53	8.25	10.63	11.65	8.74	8.42	10.74	11.68	9.16	8.83	11.00	11.68	9.73	9.38	11.29	11.68
	$V_{a-\Delta o}$ (%)	1.62	1.59	0.77	0.03	1.41	1.42	0.66	0.00	0.99	1.01	0.40	0.00	0.42	0.46	0.11	0.00
4	V_a (%)[1]	8.77	8.57	9.93	11.19	9.00	8.85	10.06	11.20	9.52	9.45	10.36	11.20	10.25	10.20	10.64	11.20
	$V_{a-\Delta o}$ (%)	2.05	2.13	0.79	0.01	1.82	1.85	0.66	0.00	1.30	1.25	0.36	0.00	0.57	0.50	0.08	0.00
5	V_a (%)	5.96	5.99	6.70	8.32	6.07	6.12	6.80	8.38	6.33	6.38	7.02	8.39	6.71	6.73	7.35	8.39
	$V_{a-\Delta o}$ (%)	1.09	1.10	0.97	0.07	0.98	0.97	0.87	0.01	0.72	0.71	0.65	0.00	0.34	0.36	0.32	0.00
6	V_a (%)[1]	7.51	6.33	8.37	8.40	7.68	6.48	8.48	8.48	8.08	6.82	8.72	8.48	8.48	7.22	9.01	8.48
	$V_{a-\Delta o}$ (%)	1.22	1.18	0.80	0.08	1.05	1.03	0.70	0.00	0.65	0.69	0.46	0.00	0.25	0.29	0.17	0.00
7	V_a (%)[1]	9.54	9.67	10.63	12.24	9.74	9.87	10.73	12.25	10.16	10.16	10.97	12.24	10.71	10.40	11.20	12.24
	$V_{a-\Delta o}$ (%)	1.58	0.78	0.61	0.00	1.38	0.58	0.51	-0.01	0.96	0.29	0.27	0.00	0.41	0.05	0.04	0.00
8	V_a (%)[1]	8.68	8.80	9.14	10.01	8.84	9.04	9.23	10.03	9.18	9.45	9.45	10.02	9.56	9.66	9.64	10.02
	$V_{a-\Delta o}$ (%)	0.99	0.88	0.65	0.01	0.83	0.64	0.56	-0.01	0.49	0.23	0.34	0.00	0.22	0.02	0.15	0.00
9	V_a (%)[1]	8.61	9.01	8.53	10.36	8.82	9.28	8.64	10.38	9.30	9.78	8.88	10.38	9.89	10.35	9.25	10.38
	$V_{a-\Delta o}$ (%)	1.59	1.56	1.02	0.02	1.38	1.29	0.91	0.00	0.90	0.79	0.67	0.00	0.31	0.22	0.30	0.00
10	V_a (%)[1]	9.04	7.75	8.38	10.88	9.25	7.99	8.49	10.90	9.72	8.46	8.70	10.89	10.26	9.07	9.06	10.89
	$V_{a-\Delta o}$ (%)	1.46	1.78	0.96	0.01	1.25	1.54	0.85	-0.01	0.78	1.07	0.64	0.00	0.24	0.46	0.28	0.00
11	V_a (%)[1]	9.84	9.94	8.88	10.69	10.06	10.24	9.00	10.72	10.59	10.78	9.26	10.72	11.29	11.36	9.69	10.72
	$V_{a-\Delta o}$ (%)	2.03	1.73	1.23	0.03	1.81	1.43	1.11	0.00	1.28	0.89	0.85	0.00	0.58	0.31	0.42	0.00
12	V_a (%)[1]	8.54	7.82	9.61	11.01	8.73	8.07	9.73	11.04	9.15	8.51	9.99	11.04	9.78	9.17	10.45	11.04
	$V_{a-\Delta o}$ (%)	1.18	2.00	1.29	0.03	1.69	1.75	1.17	0.00	1.27	1.31	0.91	0.00	0.64	0.65	0.45	0.00
Average	$V_{a-\Delta o}$ (%)	1.51	1.44	0.91	0.03	1.32	1.22	0.81	0.00	0.90	0.80	0.57	0.00	0.37	0.32	0.24	0.00

[1] V_a back-calculated using mass over time and T166 bulk volume; $V_{a-\Delta o}$ (%) = V_a at end of experiment – Calculated V_a

4.3.2 Analysis of Results from Secondary Drying Investigation

Results from Figure 4.5 indicate noticeable changes in back calculated V_a over time for protocols A to C; this suggests that all non-oven dried specimens dried gradually after coring. This observation was not surprising based on the initial drying observation of Phase I, but it does not agree with other references which claim that D7227 enables users to accurately measure V_a of field cores within 1 day of coring (Bae et al. 2012). However, the gradual trends of V_a measurements over time appear to reach relatively constant values after 6 weeks of drying in Figure 4.5, which supports that the six week drying period in laboratory conditions used for all field aged specimens used in Chapters 5 to 8 was appropriate.

The Table 4.2 analysis of variance (ANOVA) and subsequent Table 4.3 ranking of drying protocols over time was used to evaluate differences in the Phase II drying protocols. The Table 4.2 ANOVA considers a block statistical evaluation using drying protocol and time as treatments and strips as blocks. Note that all V_a errors discussed in this chapter are absolute values and not ratios to be applied to V_a values (e.g., an incorrect V_a observation of 9.0% for a core with actual 10% V_a corresponds to $V_{a\text{-}\Delta o}$ of 1.0%).

Table 4.2. Phase II ANOVA

Source	d.f.	Sig?
Total (corr)	191	---
Strip	11	Yes
Protocol	3	Yes
Drying Time	3	Yes
Protocol * Drying Time	9	Yes
Error	165	---

Table 4.2 reports that test strip, drying protocol, and drying time produced significant effects on $V_{a\text{-}\Delta o}$, and there was significant interaction between drying protocol and drying time. Thus Table 4.3 ranks drying protocol and drying time combinations simultaneously based on $V_{a\text{-}\Delta o}$ where lower values are desired.

Table 4.3. Ranking of Drying Protocols

Protocol	Drying Time (days)	Mean $V_{a\text{-}\Delta o}$ (%)	t Grouping
A	1	1.51	A
B	1	1.44	A B
A	2	1.32	B C
B	2	1.22	C
C	1	0.91	D
A	7	0.90	D
C	2	0.81	D
B	7	0.80	D
C	7	0.57	E
A	28	0.37	F
B	28	0.32	F
C	28	0.24	F
D	1	0.03	G
D	28	0.00	G
D	7	0.00	G
D	2	0.00	G

When considering the Table 4.3 ranking, Protocol D (oven) was the only protocol to sufficiently dry cores within 1 day. There was no significant difference between $V_{a\text{-}\Delta o}$ of Protocol A and B, and Protocol C seemed to accelerate the drying process by approximately 1 week. Further, there were no non-oven drying protocols to have non-significant $V_{a\text{-}\Delta o}$ within 4 weeks of drying. However, $V_{a\text{-}\Delta o}$ had decreased to a much more manageable level after 4 weeks of drying. It is possible that the highly absorbent aggregates used in M14 to M16 affected the drying potential of field cores as discussed in the following subsection.

4.3.3 Mixture Volumetric Considerations

Figure 4.6 identifies three volumes which have potential to contain moisture in field aged cores: inter-connected air void volumes (V_{aic}), non-connected air void volumes (V_{anc}), and the volume in aggregate pores that did not fill with asphalt binder ($V_{Gsa\text{-}Gse}$). The first two volumes in the previous list are frequently considered in V_a, but the third volume is rarely considered past measuring effective specific gravity (G_{se}). $V_{Gsa\text{-}Gse}$ can be quantified provided that traditional mixture volumetric properties are known.

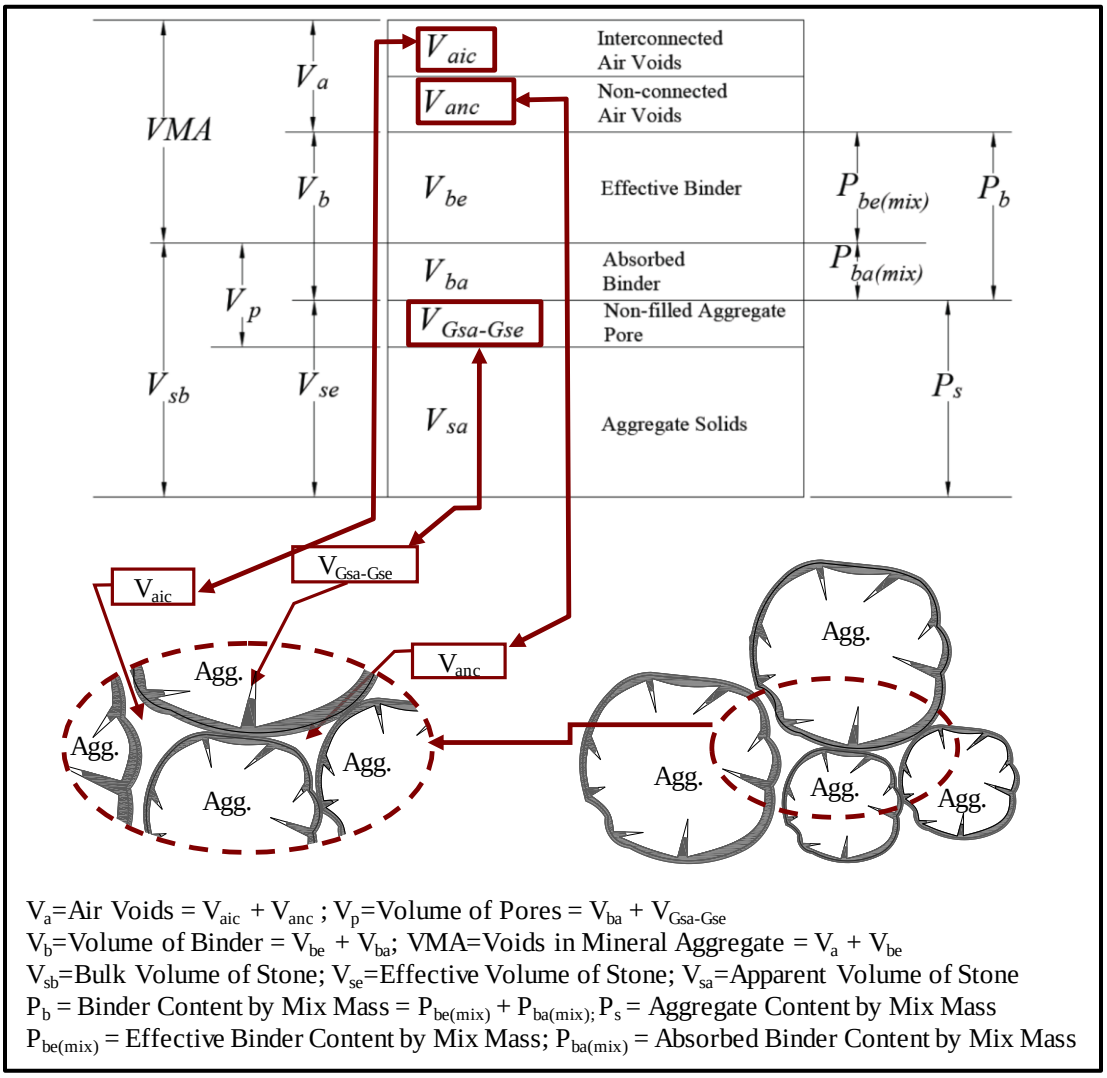

V_a=Air Voids = V_{aic} + V_{anc} ; V_p=Volume of Pores = V_{ba} + $V_{Gsa\text{-}Gse}$
V_b=Volume of Binder = V_{be} + V_{ba}; VMA=Voids in Mineral Aggregate = V_a + V_{be}
V_{sb}=Bulk Volume of Stone; V_{se}=Effective Volume of Stone; V_{sa}=Apparent Volume of Stone
P_b = Binder Content by Mix Mass = $P_{be(mix)}$ + $P_{ba(mix)}$; P_s = Aggregate Content by Mix Mass
$P_{be(mix)}$ = Effective Binder Content by Mix Mass; $P_{ba(mix)}$ = Absorbed Binder Content by Mix Mass

Figure 4.6. Asphalt Mixture Volumetrics

To consider the likelihood of the moisture retained in field cores after D7227 being contained in $V_{Gsa\text{-}Gse}$, a matched pair *t*-test was conducted to compare $V_{a\text{-}\Delta o}$ to the approximate change in V_a measurement if $V_{Gsa\text{-}Gse}$ was the only volume to contain water and $V_{Gsa\text{-}Gse}$ was completely filled with water. This approximated change in V_a measurement was described as $V_{a\text{-}\Delta a}$ and calculated with Equation 4.1. These values were matched with $V_{a\text{-}\Delta o}$ calculated based on the V_a measured on the 12 protocol C cores after 10 weeks of laboratory drying to the specimen mass in air immediately after D7227.

$$V_{a-\Delta a} = (100\% - V_a)\left(\frac{M_{core} + V_{Gsa-Gse}\gamma_{water}}{M_{core}} - 1\right)100\% = (100\% - V_a)\left(P_s(Abs) - \frac{P_{ba(mix)}}{G_b}\right) \qquad (4.1)$$

Where,
γ_{water} = specific gravity of water
M_{core} = core mass
P_s = percent of stone
Abs = aggregate moisture absorption
$P_{ba(mix)}$ = percent of binder absorbed into aggregate pores based on mix mass
G_b = specific gravity of binder

In the matched pairs *t*-test, the $V_{a\text{-}\Delta a}$ was 1.22% on average and $V_{a\text{-}\Delta o}$ was 1.02% on average. The difference between $V_{a\text{-}\Delta a}$ and $V_{a\text{-}\Delta o}$ was 0.06% to 0.30% based on a 95% confidence interval, which suggests that $V_{a\text{-}\Delta a}$ and $V_{a\text{-}\Delta o}$ are related. Stated another way, the amount of error in V_a measurement immediately after D7227 was within 0.3% V_a of the amount of error that would occur if $V_{Gsa\text{-}Gse}$ was completely filled with moisture and D7227 removed all moisture contained in the interconnected and non-interconnected air void volumes. Further, there were only 2 cases (strips 11 and 12) where $V_{a\text{-}\Delta o}$ was greater than $V_{a\text{-}\Delta a}$.

4.3.4 Drying Observations of Previously Dried Cores

To evaluate the differences between moisture which had longer periods (i.e. years) to absorb into aggregate pores to moisture absorbed into cores during laboratory activities (e.g. T166 density measurement), specimen weights for the non-oven protocols in Phase II were monitored for two weeks after T166 measurement. As shown in Figure 4.7, there is no meaningful change in V_a after the first day of drying after T166 for each of the D7227 dried specimens. This suggests that D7227 was sufficient in removing moisture absorbed during a short period. The amount of time required to achieve constant Va measurements for Protocols A and B was also much lower for moisture induced from T166 testing than moisture retained from field aging.

A third drying trial was conducted for 24 of the 36 non-oven dried cores which were trimmed to nominal thicknesses of 63 mm. There were eight strips with specimens requiring slicing, and there were no cases where only some of the cores from a respective strip were trimmed. While density of cores after slicing is not reported in this chapter, core masses were monitored over a two week period after slicing. There was evidence that D7227 was adequate in removing all meaningful moisture from cores that were sliced after being fully dried (i.e. D7227 cores dried by no more than 0.1% over a two week period after D7227), and cores dried in Protocols A and B after slicing achieved constant mass within two week. Thus, moisture

retained after slicing with a wet-saw also dried from field cores more readily than moisture retained from field aging.

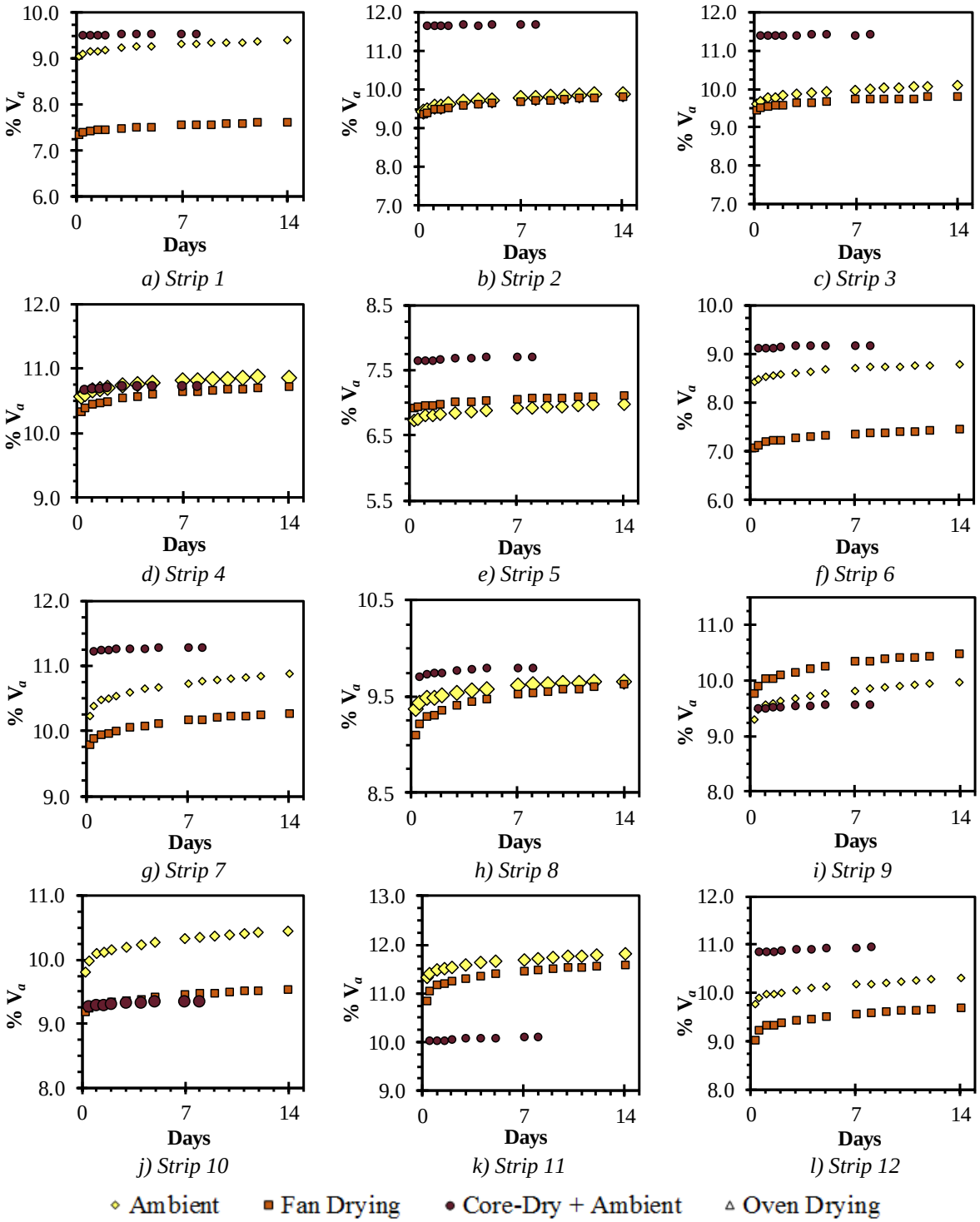

Figure 4.7. Air Voids Measured over Drying Time after AASHTO T166

4.4 Summary and Conclusions of Density Observations

The work of this chapter was performed to ensure that density measurements throughout this report were reasonable. Phase one provides five initial observations that occurred while verifying accurate density of field cores sampled after 0 to 4 years of field aging, and Phase II evaluated the effects of moisture retained in field cores in a controlled experiment. While there were multiple points of investigation presented, the information ultimately leads to one conclusion relative to this report. There was substantial moisture retained in field aged cores, and ASTM D7227 did not sufficiently remove this moisture that had absorbed into field cores over long periods of field aging. It is likely that this moisture is contained within aggregate pores, and the type of error documented in the Phase II investigation will always result in a higher G_{mb} or lower V_a measurement than what is accurate. This conclusion had two impacts on practices in Chapters 5 to 8 of this report:

- All field aged cores were dried in ambient laboratory conditions for six weeks prior to density measurement to allow sufficient drying time.

- ASTM D7227 was only relied on for the removal of moisture introduced during short periods such as sawing or density measurement.

CHAPTER 5 – TEST RESULTS

5.1 Overview of Material Test Results

The nature of this report where multiple factors are investigated using a single test section lends itself to the repeated use of some data for multiple purposes. All test data collected through five years of aging is presented in this chapter, including specimens taken immediately after construction and either tested in that state or after being laboratory conditioned. Chapters 6 to 8 utilize the data reported in this chapter for analysis. Data collected after six years of aging was used herein in a standalone manner, and as such it is reported in Chapter 9 alongside pertinent assessment of that data.

5.2 Hamburg Loaded Wheel Test Results

Table 5.1 summarizes HLWT test results from PMLC specimens first reported in Howard et al. (2012) and PMFC specimens collected soon after construction and annually after 2 to 5 years of field aging. Of the 24 tests conducted on PMLC specimens, specimens had an average V_a of 5.8% when measured with T166. There were 173 HLWT tests (346 specimens) conducted on PMFC specimens. Each column represents the rut depth (RD_{HLWT}) after 20k cycles. There were a few cases where RD_{HLWT} reached the test limit of 14 mm for 0 year tests (high air voids); subscripted numbers after the number of tests indicate the number of tests where RD_{HLWT} reached 14 mm. However, there were no cases where a stripping inflection point (SIP) was observed.

Table 5.1. Summary of HLWT Test Results Over Time

Strip	0 Year – PMLC	0 Year – PMFC	2 Year – PMFC	3 Year – PMFC	4 Year – PMFC	5 Year – PMFC
1	5.8 (2) [0]	8.2 (6) [0]	4.2 (4) [0]	3.9 (7) [0]	4.0 (2) [0]	3.4 (2) [0]
2	6.1 (2) [0]	8.1 (6) [0]	---	---	---	---
3	5.4 (2) [0]	7.9 (6) [0]	2.8 (5) [0]	3.3 (9) [0]	4.4 (2) [0]	1.9 (2) [0]
4	4.7 (2) [0]	8.9 (6) [0]	---	---	---	---
5	6.5 (2) [0]	8.4 (6) [0]	2.9 (4) [0]	2.8 (5) [0]	2.1 (6) [0]	2.3 (2) [0]
6	4.7 (2) [0]	8.7 (6) [0]	---	---	---	---
7	5.1 (2) [0]	10.2 (6) [0]	4.2 (2) [0]	3.5 (7) [0]	---	2.0 (2) [0]
8	6.5 (2) [0]	9.6 (6) [0]	---	---	---	---
9	5.2 (2) [0]	10.7 (6) [0]	4.0 (8) [0]	3.8 (13) [0]	5.6 (2) [0]	2.4 (2) [0]
10	4.1 (2) [0]	9.3 (6_1) [0]	3.8 (2) [0]	3.6 (8) [0]	3.5 (3) [0]	2.3 (2) [0]
11	6.3 (2) [0]	11.8 (6_2) [0]	---	---	---	---
12	6.5 (2) [0]	11.9 (6_3) [0]	---	---	---	---

Columns indicate average RD_{HLWT} (mm) after 20k cycles (no. of tests) and [no. of SIPs].

5.3 Plant Mixed and Lab Compacted Cantabro and Indirect Tensile Test Results

Table 5.2 summarizes all results collected from PMLC specimens. Of the 395 PMLC specimens, there were 144 CML tests with specimen height (h_t) of 6.3 cm, 132 CML tests with a 11.5 cm h_t, and 119 IDT tests. Three target V_a levels of 4%, 7%, and field (respective of each strip) were used.

Table 5.2. Short Term Aged Tensile Strength and Mass Loss of PMLC Specimens

Mix	HT (hr)	Target V_a (%)	*ML* (h_t = 6.3 cm) Avg (%)	COV (%)	n	V_a (%)	*ML* (h_t = 11.5 cm) Avg (%)	COV (%)	n	V_a (%)	S_t (h_t = 6.3 cm) Avg (kPa)	COV (%)	n	V_a (%)
M14	0	4	14.4	7	12	4.3	10.4	10	8	3.9	2,047	5	3	4.8
		7	---	---	---	---	---	---	---	---	1,652	1	3	8.0
	1.0	4	13.1	3	3	4.4	13.3	4	3	4.5	1,986	2	3	4.7
		7	19.0	9	3	7.7	18.1	5	3	7.8	1,617	6	3	7.7
		Field	18.4	11	3	9.1	17.3	11	3	9.3	1,407	2	3	9.4
	2.3	4	14.0	17	3	4.2	13.8	5	3	4.1	2,040	5	3	5.0
		7	20.4	5	3	7.6	18.2	7	3	7.8	1,635	5	3	7.9
		Field	23.0	11	3	10.3	19.2	6	3	10.3	1,225	11	3	10.9
	5.8	4	15.9	4	3	4.2	15.6	11	3	4.6	2,124	7	2	5.1
		7	18.7	11	3	7.6	20.0	4	3	7.7	1,524	6	3	8.0
		Field	25.6	10	3	10.6	21.0	8	3	11.0	1,251	11	2	11.4
	7.9	4	18.9	7	3	4.6	15.3	9	3	4.6	2,275	5	3	4.7
		7	22.0	11	3	7.8	21.7	13	3	8.0	1,688	2	3	7.8
		Field	34.3	7	3	13.4	28.0	10	3	13.1	1,056	6	3	13.2
M15	0	4	14.9	11	12	4.3	9.1	9	8	3.3	1,994	4	3	4.9
		7	---	---	---	---	---	---	---	---	1,518	3	3	7.6
	1.1	4	13.7	11	3	4.1	12.0	3	3	4.3	1,945	6	3	5.0
		7	17.8	15	3	7.7	16.8	7	3	7.9	1,638	3	3	7.7
		Field	18.1	10	3	8.3	17.7	14	3	8.5	1,491	3	3	8.9
	2.4	4	13.8	17	3	4.2	13.5	9	3	4.4	2,204	2	3	4.8
		7	17.7	6	3	7.6	18.0	14	3	7.9	1,759	4	3	7.6
		Field	19.9	4	3	8.4	18.1	4	3	8.6	1,606	3	3	9.1
	5.6	4	15.7	8	3	4.1	13.3	4	3	4.4	2,151	2	2	4.9
		7	18.9	8	3	7.5	18.9	9	3	7.7	1,562	10	3	7.7
		Field	23.9	11	3	10.2	21.9	9	3	10.7	1,316	7	2	10.8
	8.4	4	14.7	3	3	4.4	13.3	6	3	4.5	2,027	4	3	4.7
		7	16.8	2	3	7.9	16.5	4	3	7.9	1,564	6	3	8.1
		Field	23.3	6	3	10.8	21.9	9	3	10.8	1,223	3	3	10.8
M16	0	4	13.6	7	12	4.6	8.6	24	8	3.8	2,086	6	3	4.9
		7	---	---	---	---	---	---	---	---	1,620	7	3	8.0
	1.0	4	13.5	6	3	4.3	11.0	3	3	4.6	2,023	3	3	4.7
		7	18.3	7	3	7.9	17.2	8	3	7.8	1,625	11	3	8.0
		Field	19.5	6	3	10.6	22.1	8	3	10.7	1,236	5	3	11.2
	5.7	4	15.7	7	3	4.3	14.1	9	3	4.4	2,207	4	3	5.0
		7	21.0	11	3	7.6	18.8	3	3	7.7	1,773	3	3	7.5
		Field	28.5	12	3	12.3	23.9	4	3	12.2	1,198	3	3	12.3
	8.1	4	15.8	3	3	4.2	13.7	3	3	4.3	2,293	---	1	5.3
		7	21.2	9	3	7.7	17.6	5	3	7.9	1,652	3	3	7.8
		Field	30.1	5	3	11.8	25.0	3	3	12.1	1,266	5	2	12.1
	10.5	4	15.9	8	3	4.2	13.9	6	3	4.4	2,196	1	3	4.9
		7	19.0	7	3	7.6	17.1	6	3	7.9	1,723	3	3	7.9
		Field	24.0	3	3	11.3	18.0	8	3	11.6	1,287	6	3	11.8

--- All specimens Lab-SGC compacted; CML specimens diameter (D) = 15 cm; V_a reported as average; S_t specimen D = 10 cm

5.4 Plant Mixed and Field Compacted Cantabro, IDT, and SIDT Test Results

There were 2,253 PMFC specimens tested using CML, IDT, or SIDT for investigations in Chapters 6 to 8. In all, there were 1,264 CML tests, 797 IDT tests, and 192 SIDT tests conducted as presented in Tables 5.3 to 5.5. Table 5.3 summarizes the results of all PMFC specimens collected after varying levels of field aging and CML or IDT tested

without laboratory conditioning. Table 5.4 summarizes the results of all PMFC specimens collected soon after construction that were subjected to varying conditioning protocols (CPs). Later chapters divide M16 into M16a and M16b based on haul distance effects, thus strip 12 that was hauled for 10.5 hours is considered separately in Table 5.4. Table 5.5 summarizes SIDT test results considered for short term and longer term characterization.

Table 5.3. *ML* and S_t of Non-Conditioned and Field Aged PMFC Cores

			ML					S_t				
Age (Yr)	**Mix**	**HT (hr)**	**n**	**Avg *ML* (%)**	**COV *ML* (%)**	**Avg V_a (%)**	**COV V_a (%)**	**n**	**Avg S_t (kPa)**	**COV S_t (%)**	**Avg V_a (%)**	**COV V_a (%)**
0	M14	**1.0**	15	24.6	43	9.5	12	19	992	10	9.3	10
		2.3	15	32.1	60	10.9	10	8	1,034	9	10.6	9
		5.8	20	29.4	35	10.5	13	12	1,057	13	10.6	11
		7.9	19	48.6	37	13.2	12	14	748	17	13.2	13
	M15	**1.1**	16	19.2	30	8.2	8	14	1,175	8	8.5	11
		2.4	13	19.4	21	8.8	14	11	1,206	10	8.4	16
		5.6	16	19.4	17	9.9	14	9	1,022	12	9.7	8
		8.4	12	27.9	26	11.0	15	11	926	12	10.6	8
	M16	**1.0**	21	22.1	27	10.7	18	15	1,063	15	10.6	16
		5.7	27	31.6	47	11.9	22	15	956	22	12.2	20
		8.1	19	36.7	49	12.3	16	11	1,083	11	11.9	16
		10.5	21	35.4	55	12.9	19	10	1,081	5	11.7	11
2	M14	**1.0**	21	34.8	36	9.2	9	20	1,272	11	9.2	9
		5.8	34	36.8	37	9.3	15	21	1,258	14	9.6	11
	M15	**1.1**	26	21.4	16	7.6	7	5	1,622	8	7.4	7
		5.6	31	23.9	18	8.6	9	7	1,355	16	8.6	6
	M16	**1.0**	54	26.5	26	9.0	10	35	1,503	8	8.7	12
		5.7	44	40.3	30	11.5	12	25	1,490	11	9.1	13
3	M14	**1.0**	24	31.1	34	9.1	15	19	1,330	11	8.6	10
		5.8	35	34.4	22	9.1	11	25	1,392	13	9.2	15
	M15	**1.1**	28	22.2	15	7.3	8	20	1,666	5	7.3	8
		5.6	28	23.4	26	7.9	10	20	1,435	13	7.8	11
	M16	**1.0**	52	25.2	28	8.5	9	35	1,511	7	8.5	9
		5.7	42	41.4	37	11.2	16	30	1,430	13	11.2	9
4	M14	**1.0**	11	42.9	55	9.7	18	12	1,462	20	9.3	14
		5.8	14	55.5	33	11.3	16	12	1,468	15	9.6	10
	M15	**1.1**	13	28.5	29	6.9	11	10	1,764	11	7.6	11
		5.6	13	35.4	18	8.6	19	10	1,489	11	9	18
	M16	**1.0**	14	36.1	36	8.3	25	12	1,624	13	8.3	20
		5.7	25	41.8	49	9.9	13	19	1,462	12	9.9	13
5	M14	**1.0**	14	53.0	20	9.3	7	10	1,541	7	9.2	14
		2.3	10	32.0	18	9.7	9	10	1,491	8	9.7	8
		5.8	14	44.5	42	9.5	14	10	1,275	16	9.7	19
		7.9	10	48.2	26	11.2	8	10	1,392	14	11.1	7
	M15	**1.1**	14	35.9	33	7.2	5	10	1,762	9	7.4	7
		2.4	10	25.2	22	6.5	9	10	1,775	9	6.6	11
		5.6	14	35.2	26	8.8	13	10	1,711	9	8.2	8
		8.4	10	45.5	16	11.1	4	10	1,421	9	9.7	7
	M16	**1.0**	14	33.0	27	8.0	8	10	1,503	10	8.4	9
		5.7	25	57.1	35	10.8	13	16	1,479	13	10.4	10
		8.1	10	45.9	33	11.6	15	10	1,490	7	12.7	9
		10.5	10	56.2	15	13.4	7	10	1,341	9	11.9	6

Note: all data is included in this table, which includes potential outliers removed for select types of analysis in Chapters 6 to 8.

Table 5.4. Mass Loss and Tensile Strength of Lab Conditioned PMFC Cores

CP	Mix	*ML*					S_t				
		n	Avg *ML* (%)	COV *ML* (%)	Avg V_a (%)	COV V_a (%)	n	Avg S_t (kPa)	COV S_t (%)	Avg V_a (%)	COV V_a (%)
CP1	M14	20	33.0	44	11.1	18	10	1063	25	10.7	18
	M15	19	26.2	28	9.0	17	12	1323	14	9.3	13
	M16a	12	32.0	18	12.2	10	11	1130	13	11.9	17
	M16b	5	35.6	27	12.1	5	5	1202	10	11.4	7
CP2	M14	20	35.4	54	10.8	17	--	---	---	---	---
	M15	21	23.0	23	9.2	17	--	---	---	---	---
	M16a	10	32.4	50	12.1	11	--	---	---	---	---
	M16b	4	25.5	33	12.6	15	--	---	---	---	---
CP3	M14	18	73.5	35	11.3	17	--	---	---	---	---
	M15	18	25.9	26	8.9	15	--	---	---	---	---
	M16a	13	40.9	32	11.8	11	--	---	---	---	---
	M16b	7	37.1	27	12.5	7	--	---	---	---	---
CP4	M14	16	44.8	44	11.2	16	12	827	17	11.4	18
	M15	17	31.0	40	9.1	17	12	1041	9	8.6	11
	M16a	15	41.4	29	11.5	13	10	872	17	12.0	10
	M16b	7	45.5	25	12.4	8	5	963	11	11.3	10
CP5	M14	20	49.0	39	11.1	17	--	---	---	---	---
	M15	18	35.1	38	9.2	16	--	---	---	---	---
	M16a	11	44.1	16	12.2	10	--	---	---	---	---
	M16b	6	46.3	48	12.2	5	--	---	---	---	---
CP6	M14	18	52.5	38	11.1	17	12	777	24	10.9	17
	M15	18	32.0	35	8.9	16	14	862	26	8.9	15
	M16a	12	46.6	43	12.3	10	8	794	13	12.3	10
	M16b	7	44.7	27	12.5	10	6	914	13	11.8	12
CP7	M14	16	53.5	26	11.6	17	14	872	22	10.9	18
	M15	18	35.7	30	9.3	16	13	1105	12	9.2	15
	M16a	13	48.5	44	11.1	19	9	927	22	11.9	14
	M16b	7	45.6	25	12.7	10	4	961	10	11.6	5

Note: all data is included in this table, which includes potential outliers removed for select types of analysis in Chapters 6 to 8.

Table 5.5. Fracture Properties of PMFC Cores

Investigation	Age or CP	Test Temp (°C)	M14						M15						M16					
			HT (hr)	n*	FE Avg (kJ/m³)	FE COV (%)	V_a Avg (%)	V_a COV (%)	HT (hr)	n*	FE Avg (kJ/m³)	FE COV (%)	V_a Avg (%)	V_a COV (%)	HT (hr)	n*	FE Avg (kJ/m³)	FE COV (%)	V_a Avg (%)	V_a COV (%)
Short Term	0 Yr	20	**1.0**	3(3)	2.4	9	9.2	4	**1.1**	3(4)	3.1	22	8.5	3	**1.0**	3(3)	3.5	4	10.7	4
			2.3	3(4)	2.4	12	9.5	4	**2.4**	3(4)	2.2	32	9.0	6	**5.7**	3(4)	3.2	26	11.2	3
			5.8	3(4)	3.0	32	9.2	3	**5.6**	3(4)	2.6	33	9.4	2	**8.1**	3(4)	1.7	5	10.9	6
			7.9	3(4)	2.0	16	11.0	8	**8.4**	3(4)	1.5	17	9.2	8	**10.5**	3(3)	3.0	9	10.7	3
		-10	**1.0**	3(4)	0.6	21	9.2	4	**1.1**	3(4)	0.6	6	8.6	2	**1.0**	3(4)	0.3	34	10.5	2
			2.3	3(3)	0.4	22	9.4	4	**2.4**	3(4)	0.6	18	9.0	6	**5.7**	3(4)	0.5	17	11.3	2
			5.8	3(4)	0.3	20	9.1	3	**5.6**	3(3)	0.4	26	9.5	3	**8.1**	3(4)	0.4	9	11.2	5
			7.9	3(4)	0.3	7	11.2	7	**8.4**	3(3)	0.3	54	9.4	7	**10.5**	3(4)	0.4	31	11.0	6
Longer Term	0 Yr	20	**1.0**	3(3)	2.4	9	9.2	4	**1.1**	3(4)	2.9	23	8.0	3	**1.0**	3(4)	2.7	27	8.6	5
			5.8	3(4)	3.0	32	9.2	3	**5.6**	3(4)	2.6	33	9.4	2	**5.7**	3(4)	3.2	26	10.8	3
		-10	**1.0**	3(4)	0.6	21	9.2	4	**1.1**	3(4)	0.5	15	8.0	3	**1.0**	3(4)	0.4	17	8.9	6
			5.8	3(4)	0.3	20	9.1	3	**5.6**	3(3)	0.4	26	9.5	3	**5.7**	3(4)	0.5	17	11.3	2
	2 Yr	20	**1.0**	3(3)	1.5	5	9.2	4	**1.1**	3(4)	1.2	22	8.0	3	**1.0**	3(4)	1.4	14	8.2	3
			5.8	3(3)	0.8	42	9.3	5	**5.6**	3(3)	1.2	4	8.9	2	**5.7**	3(3)	1.3	10	11.1	2
		-10	**1.0**	3(4)	0.2	40	9.3	4	**1.1**	3(4)	0.5	14	7.9	3	**1.0**	3(4)	0.4	25	8.7	4
			5.8	3(4)	0.3	9	9.3	3	**5.6**	3(3)	0.4	10	9.1	4	**5.7**	3(4)	0.3	40	11.0	1
	4 Yr	20	**1.0**	3(4)	0.8	33	9.0	5	**1.1**	3(3)	0.9	8	7.6	5	**1.0**	3(4)	1.0	24	8.8	5
			5.8	3(4)	1.1	24	9.4	6	**5.6**	3(4)	0.9	29	9.2	6	**5.7**	3(4)	0.7	21	11.0	2
		-10	**1.0**	3(4)	0.4	12	8.8	4	**1.1**	3(3)	0.3	22	7.5	3	**1.0**	3(4)	0.4	27	8.3	4
			5.8	3(4)	0.3	27	9.2	7	**5.6**	3(4)	0.4	54	8.8	7	**5.7**	3(4)	0.3	71	10.9	3
	CP4	20	**1.0**	3(4)	0.9	45	9.1	4	**1.1**	3(4)	1.9	5	8.0	4	**1.0**	3(4)	2.0	29	8.4	6
			5.8	3(4)	1.6	20	9.3	2	**5.6**	3(4)	1.9	21	9.5	3	**5.7**	3(4)	1.0	47	11.4	2
		-10	**1.0**	3(4)	0.1	96	9.0	4	**1.1**	3(3)	0.3	35	8.0	4	**1.0**	3(3)	0.3	18	8.9	7
			5.8	3(3)	0.3	24	9.2	1	**5.6**	3(3)	0.2	20	9.4	4	**5.7**	3(3)	0.1	28	11.2	3

*Number of specimens tested (n) with number of fracture faces considered within parenthesis.

5.5 Binder Test Results

There were 48 samples of field core binder (FCB) extracted and recovered from PMFC specimens used to assess aging, and as-received binders (ARB) were considered after eight conditions. All FTIR data from FCB is presented in Table 5.6, and FTIR data from ARB samples is provided in Table 5.7. Physical properties of FCB samples recovered from the pavement surface (i.e. FCB_0) are presented in Table 5.8, and physical properties of FCB samples recovered from 5.0 to 6.3 cm below the pavement surface (i.e. FCB_5) are presented in Table 5.9. Table 5.10 presents physical property measurements of ARB samples.

Table 5.6. FTIR Results from Field Core Binders

			FCB_0					**FCB_5**				
			Absorbance Peak Heights					**Absorbance Peak Heights**				
Mix	**HT (hr)**	**Age or CP**	**1700 cm^{-1}**	**1031 cm^{-1}**	**1375 cm^{-1}**	**CI**	**SI**	**1700 cm^{-1}**	**1031 cm^{-1}**	**1375 cm^{-1}**	**CI**	**SI**
M14	1.0	0 Yr	0.008	0.026	0.059	0.14	0.43	0.007	0.027	0.060	0.11	0.45
		2 Yr	0.006	0.027	0.066	0.09	0.40	0.010	0.024	0.060	0.17	0.39
		4 Yr	0.008	0.023	0.040	0.21	0.59	0.009	0.028	0.053	0.16	0.53
		CP4	0.007	0.024	0.051	0.14	0.46	0.009	0.026	0.059	0.15	0.45
	5.8	0 Yr	0.006	0.025	0.065	0.09	0.38	0.009	0.026	0.060	0.14	0.43
		2 Yr	0.011	0.028	0.056	0.19	0.50	0.012[a]	0.029[a]	0.053[a]	0.23	0.57
		4 Yr	0.012	0.030	0.055	0.22	0.54	0.010	0.027	0.059	0.16	0.45
		CP4	0.010	0.027	0.061	0.17	0.45	0.008	0.027	0.061	0.12	0.44
M15	1.1	0 Yr	0.006	0.025	0.057	0.11	0.45	0.010	0.027	0.060	0.16	0.45
		2 Yr	0.012	0.029	0.060	0.20	0.48	0.008	0.025	0.060	0.12	0.41
		4 Yr	0.012	0.022	0.039	0.31	0.57	0.008	0.028	0.064	0.13	0.43
		CP4	0.008	0.022	0.046	0.18	0.46	0.010	0.029	0.060	0.16	0.48
	5.6	0 Yr	0.008	0.025	0.060	0.13	0.43	0.010	0.026	0.059	0.16	0.44
		2 Yr	0.014	0.030	0.058	0.24	0.53	0.008	0.025	0.055	0.15	0.45
		4 Yr	0.009	0.026	0.035	0.28	0.75	0.010	0.031	0.055	0.18	0.57
		CP4	0.007	0.032	0.057	0.12	0.57	0.008	0.031	0.060	0.13	0.52
M16	1.0	0 Yr	0.009	0.025	0.058	0.15	0.42	0.006	0.027	0.055	0.11	0.49
		2 Yr	0.009	0.030	0.058	0.16	0.51	0.007	0.025	0.059	0.12	0.43
		4 Yr	0.008	0.030	0.054	0.15	0.56	0.008	0.022	0.050	0.15	0.44
		CP4	0.009	0.026	0.057	0.16	0.45	0.007	0.030	0.058	0.12	0.52
	5.7	0 Yr	0.008	0.026	0.060	0.13	0.43	0.008	0.026	0.059	0.14	0.44
		2 Yr	0.012	0.029	0.059	0.20	0.49	0.008	0.027	0.061	0.13	0.44
		4 Yr	0.010	0.027	0.044	0.23	0.61	0.007	0.019	0.044	0.16	0.44
		CP4	0.007	0.024	0.049	0.13	0.49	0.005	0.024	0.051	0.10	0.47

[a] Measured values believed to be erroneous.

Table 5.7. FTIR Results from As-Received Binder

		Neat PG 67-22 Used in M14 and M15					PG 67-22 Used in M16				
	PAV	Absp Heights					Absp Heights				
Short Term	Time (hr)	1700 cm^{-1}	1031 cm^{-1}	1375 cm^{-1}	CI	SI	1700 cm^{-1}	1031 cm^{-1}	1375 cm^{-1}	CI	SI
None	None	0.002	0.008	0.059	0.02	0.14	0.001[a]	0.028[a]	0.053[a]	0.02	0.52
T240	0	0.000	0.013	0.063	0.00	0.21	0.000	0.012	0.064	0.00	0.18
T240	10	0.000	0.020	0.061	0.00	0.32	0.000	0.018	0.063	0.00	0.28
T240	20	0.001	0.020	0.059	0.02	0.34	0.000	0.020	0.059	0.00	0.35
T240	30	0.003	0.023	0.062	0.05	0.37	0.003	0.021	0.063	0.05	0.32
T240	40	0.006	0.023	0.062	0.10	0.36	0.004	0.023	0.059	0.07	0.39
T240	60	0.008	0.025	0.061	0.13	0.41	0.007	0.026	0.062	0.11	0.42
T240	80	0.009	0.025	0.058	0.16	0.43	0.008	0.028	0.058	0.14	0.49

PAV conditioning conducted at 100°C and 2.1 MPa

[a] Measured values believed to be erroneous.

Table 5.8. Physical Properties of FCB_0 Binders

			Pen	DSR_{25}			DSR_8			BBR					
				G*/sinδ = 2.20 kPa[a]			G*sinδ = 5.0 MPa[a]			Stiffness = 300 MPa[a]			*m*-value = 0.300[a]		
Mix	HT (hr)	Age/CP	Pen_{avg} (dmm)	T_1 [b] kPa (°C)	T_2 [b] kPa (°C)	T_c (°C)	T_1 [b] MPa (°C)	T_2 [b] MPa (°C)	T_c (°C)	T_1 [b] MPa (°C)	T_2 [b] MPa (°C)	T_c (°C)	T_1 [b] --- (°C)	T_2 [b] --- (°C)	T_c (°C)
M14	1.0	0 Yr	23	3.3 (76)	1.6 (82)	79.3	4.3 (22)	6.2 (19)	20.8	182 (-18)	385 (-24)	-22.0	0.315 (-18)	0.269 (-24)	-19.9
		2 Yr	15	4.2 (82)	2.1(88)	87.5	3.8 (28)	5.2 (25)	25.4	120 (-12)	244 (-18)	-19.7	0.321 (-12)	0.269 (-18)	-14.4
		4 Yr	10	2.2 (94)	1.2 (100)	94.1	3.8 (31)	5.0 (28)	28.0	98 (-6)	182 (-12)	-16.8	0.324 (-6)	0.282 (-12)	-9.5
		CP4	23	3.4 (76)	1.7 (82)	79.6	4.0 (22)	5.4 (19)	19.8	193 (-18)	373 (-24)	-22.0	0.302(-18)	0.266 (-24)	-18.4
	5.8	0 Yr	27	3.6 (76)	1.7 (82)	80.1	3.7 (22)	5.3 (19)	19.5	163 (-18)	332 (-24)	-23.1	0.319 (-18)	0.271 (-24)	-20.4
		2 Yr	16	2.7 (88)	1.4 (94)	90.0	3.8 (28)	5.2 (25)	25.4	121(-12)	246 (-18)	-19.7	0.323 (-12)	0.273 (-18)	-14.7
		4 Yr	10	2.9 (94)	1.5 (100)	96.4	3.8 (31)	5.2 (28)	28.3	106 (-6)	203 (-12)	-15.6	0.318 (-6)	0.268 (-12)	-8.1
		CP4	22	4.6 (76)	2.2 (82)	82.0	4.0 (22)	5.4 (19)	19.8	196 (-18)	382 (-24)	-21.8	0.303 (-18)	0.265 (-24)	-18.4
M15	1.1	0 Yr	28	3.4 (70)	1.5 (76)	73.3	3.5 (19)	5.0 (16)	16.0	252 (-24)	493 (-30)	-25.6	0.303 (-24)	0.250 (-30)	-24.3
		2 Yr	25	4.6 (76)	2.1 (82)	81.6	4.1 (22)	5.7 (19)	20.1	164 (-18)	320 (-24)	-23.4	0302 (-18)	0.269 (-24)	-18.4
		4 Yr	11	3.9 (88)	1.8 (94)	92.6	3.9 (31)	5.2 (28)	28.4	97 (-6)	184 (-12)	-16.6	0.325 (-6)	0.283 (-12)	-9.6
		CP4	24	3.1 (76)	1.5 (82)	78.9	3.8 (22)	5.4 (19)	19.7	184 (-18)	371 (-24)	-22.2	0.308 (-18)	0.267 (-24)	-19.1
	5.6	0 Yr	49	2.8 (70)	1.3 (76)	71.9	4.1 (16)	5.8 (13)	14.5	187 (-24)	383 (-30)	-28.0	0.322 (-24)	0.258 (-30)	-26.0
		2 Yr	17	4.2 (82)	2.0 (88)	87.1	4.5 (25)	6.0 (22)	23.9	124 (-12)	246 (-18)	-19.8	0.321 (-12)	0.272 (-18)	-14.5
		4 Yr	11	2.5 (94)	1.3 (100)	95.0	4.4 (31)	5.8 (28)	29.6	120 (-6)	209 (-12)	-15.9	0.313 (-6)	0.261 (-12)	-7.5
		CP4	22	3.8 (76)	1.9 (82)	80.6	4.2 (22)	5.9 (19)	20.5	204 (-18)	396 (-24)	-21.5	0.300 (-18)	0.261 (-24)	-18.0
M16	1.0	0 Yr	48	2.3 (70)	1.2 (760	70.2	4.8 (13)	6.3 (10)	12.5	204 (-24)	403 (-30)	-27.4	0.324 (-24)	0.262 (-30)	-26.3
		2 Yr	16	3.5 (82)	1.7 (88)	85.8	4.4 (25)	6.1 (22)	23.8	120 (-12)	242 (-18)	-19.9	0.326 (-12)	0.271 (-18)	-14.8
		4 Yr	10	4.2 (88)	2.1 (94)	93.7	4.4 (31)	5.8 (28)	29.6	116 (-6)	211 (-12)	-15.5	0.313 (-6)	0.272 (-12)	-7.9
		CP4	20	3.3 (76)	1.6 (82)	79.3	4.4 (22)	6.3 (19)	20.9	102 (-12)	205 (-18)	-21.3	0.354 (-12)	0.296 (-18)	-17.6
	5.7	0 Yr	26	2.3 (76)	1.2 (82)	76.5	4.9 (19)	7.0 (16)	18.9	174 (-18)	342 (-24)	-22.9	0.313 (-18)	0.276 (-24)	-20.2
		2 Yr	15	2.4 (88)	1.2 (94)	88.9	4.1 (28)	5.6 (25)	26.1	151 (-12)	282 (-18)	-18.6	0.309 (-12)	0.252 (-18)	-12.9
		4 Yr	10	2.8 (94)	1.4 (100)	96.0	4.9 (31)	6.6 (28)	30.8	141 (-6)	249 (-12)	-14.0	0.301 (-6)	0.257 (-12)	-6.1
		CP4	18	4.2 (76)	2.1 (82)	81.4	4.9 (22)	6.9 (19)	21.9	113 (-12)	233 (-18)	-20.1	0.347 (-12)	0.293 (-18)	-17.2

First Test Temperature (T_1); Second Test Temperature (T_2)

[a]Critical property; [b]Measured property with test temperature in parenthesis.

Table 5.9. Physical Properties of FCB_5

			Pen	DSR_{25}			DSR_8			BBR					
				G*/sinδ = 2.20 kPa[a]			G*sinδ = 5.0 MPa[a]			Stiffness = 300 MPa[a]			*m*-value = 0.300[a]		
Mix	HT (hr)	Age/CP	Pen (dmm)	T_1 [b] kPa (°C)	T_2 [b] kPa (°C)	T_c (°C)	T_1 [b] MPa (°C)	T_2 [b] MPa (°C)	T_c (°C)	T_1 [b] MPa (°C)	T_2 [b] MPa (°C)	T_c (°C)	T_1 [b] --- (°C)	T_2 [b] --- (°C)	T_c (°C)
M14	1.0	0 Yr	29	4.6 (70)	2.1 (76)	75.7	4.4 (19)	6.2 (16)	17.8	151 (-18)	331 (-24)	-23.2	0.322 (-18)	0.287 (-24)	-21.7
		2 Yr	41	4.0 (70)	1.9 (76)	74.7	4.9 (16)	7.0 (13)	15.9	217 (-24)	442 (-30)	-26.7	0.316 (-24)	0.260 (-30)	-25.7
		4 Yr	17	3.1 (82)	1.5 (88)	84.7	4.2 (25)	5.7 (22)	23.3	142 (-12)	255 (-18)	-19.6	0.320 (-12)	0.276 (-18)	-14.7
		CP4	27	2.5 (76)	1.2 (82)	77.0	4.4 (19)	6.2 (16)	17.9	151 (-18)	357 (-24)	-22.8	0.320 (-18)	0.269 (-24)	-20.3
	5.8	0 Yr	25	3.3 (76)	1.7 (82)	79.6	5.3 (19)	3.7 (22)	19.5	100 (-12)	205 (-18)	-21.2	0.343 (-12)	0.297 (-18)	-17.6
		2 Yr	21	2.5 (82)	1.3 (88)	83.2	4.1 (25)	5.6 (22)	23.1	95 (-12)	207 (-18)	-20.9	0.358 (-12)	0.293 (-18)	-17.3
		4 Yr	19	2.7 (82)	1.4 (88)	83.8	4.8 (22)	6.7 (19)	21.6	109 (-12)	214 (-18)	-21.0	0.340 (-12)	0.297 (-18)	-17.6
		CP4	21	2.3 (82)	1.2 (88)	82.5	4.5 (22)	6.2 (19)	21.0	208 (-18)	449 (-24)	-20.9	0.300 (-18)	0.247 (-24)	-18.0
M15	1.1	0 Yr	50	2.4 (70)	1.1 (76)	70.8	3.7 (19)	5.4 (16)	16.7	217 (-24)	413 (-30)	-27.0	0.316 (-24)	0.262 (-30)	-25.7
		2 Yr	45	2.9 (70)	1.4 (76)	72.2	3.5 (19)	5.1 (16)	16.1	241 (-24)	456 (-30)	-26.0	0.307 (-24)	0.254 (-30)	-24.7
		4 Yr	18	2.4 (82)	1.2 (88)	82.6	4.1 (25)	5.7 (22)	23.2	143 (-12)	281 (-18)	-18.6	0.329 (-12)	0.285 (-18)	-15.9
		CP4	21	2.8 (76)	1.4 (82)	78.0	3.9 (22)	5.5 (19)	19.8	190 (-18)	407 (-24)	-21.6	0.307 (-18)	0.257 (-24)	-18.8
	5.6	0 Yr	29	2.6 (76)	1.3 (82)	77.3	4.9 (19)	7.0 (16)	18.9	172 (-18)	349 (-24)	-22.7	0.319 (-18)	0.270 (-24)	-20.3
		2 Yr	30	2.3 (76)	1.1 (82)	76.2	4.4 (19)	6.3 (16)	17.9	163 (-18)	327 (-24)	-23.2	0.325 (-18)	0.287 (-24)	-21.9
		4 Yr	16	3.4 (82)	1.6 (88)	85.6	4.5 (25)	6.0 (22)	23.8	138 (-12)	254 (-18)	-19.6	0.310 (-12)	0.273 (-18)	-13.6
		CP4	21	3.6 (76)	1.7 (82)	80.0	4.6 (22)	6.3 (19)	21.2	105 (-12)	218 (-18)	-20.6	0.358 (-12)	0.298 (-18)	-17.8
M16	1.0	0 Yr	36	3.9 (70)	1.8 (76)	74.4	4.1 (19)	6.0 (16)	17.4	148 (-18)	297 (-24)	-24.1	0.331 (-18)	0.288 (-24)	-22.3
		2 Yr	25	4.6 (70)	2.1 (76)	75.7	4.3 (19)	6.1 (16)	17.7	166 (-18)	331 (-24)	-23.1	0.319 (-18)	0.281 (-24)	-21.0
		4 Yr	22	3.1 (76)	1.5 (82)	78.8	4.1 (22)	5.8 (19)	20.3	204 (-18)	417 (-24)	-21.2	0.311 (-18)	0.256 (-24)	-19.2
		CP4	23	2.7 (76)	1.3 (82)	77.6	4.1 (22)	5.6 (19)	20.1	198 (-18)	399 (-24)	-21.5	0.307 (-18)	0.266 (-24)	-19.0
	5.7	0 Yr	28	2.5 (76)	1.3 (82)	77.2	4.9 (19)	6.9 (16)	18.9	196 (-18)	383 (-24)	-21.8	0.306 (-18)	0.268 (-24)	-18.9
		2 Yr	22	4.4 (76)	2.0 (82)	81.4	4.4 (25)	6.1 (22)	23.8	128 (-12)	251 (-18)	-19.6	0.339 (-12)	0.288 (-18)	-16.6
		4 Yr	20	4.0 (76)	1.9 (82)	81.0	4.9 (22)	6.9 (19)	21.8	232 (-18)	510 (-24)	-20.0	0.302 (-18)	0.244 (-24)	-18.2
		CP4	20	3.3 (76)	1.6 (82)	79.5	4.2 (22)	6.0 (19)	20.5	205 (-18)	399 (-24)	-21.4	0.303 (-18)	0.262 (-24)	-18.4

First Test Temperature (T_1); Second Test Temperature (T_2)

[a]Critical property; [b]Measured property with test temperature in parenthesis.

Table 5.10. Physical Properties of ARB

Binder	Short Term Condition	PAV Time (hr)	Pen Pen_{avg} (dmm)	DSR_{25} G*/sinδ = 2.20 kPa[a] T_1 [b] kPa (°C)	DSR_{25} G*/sinδ = 2.20 kPa[a] T_2 [b] kPa (°C)	DSR_{25} G*/sinδ = 2.20 kPa[a] T_c (°C)	DSR_8 G*sinδ = 5.0 MPa[a] T_1 [b] MPa (°C)	DSR_8 G*sinδ = 5.0 MPa[a] T_2 [b] MPa (°C)	DSR_8 G*sinδ = 5.0 MPa[a] T_c (°C)	BBR Stiffness = 300 MPa[a] T_1 [b] MPa (°C)	BBR Stiffness = 300 MPa[a] T_2 [b] MPa (°C)	BBR Stiffness = 300 MPa[a] T_c (°C)	BBR *m*-value = 0.300[a] T_1 [b] --- (°C)	BBR *m*-value = 0.300[a] T_2 [b] --- (°C)	BBR *m*-value = 0.300[a] T_c (°C)
B1	None	0	63	1.5 (64)	3.3 (58)	61.1	3.5 (16)	5.8 (13)	13.8	189 (-18)	432 (-24)	-21.4	0.375 (-18)	0.282 (-24)	-22.8
	T240	0	37	1.1 (76)	2.3 (70)	70.4	4.1 (19)	6.3 (16)	17.6	246 (-18)	497 (-24)	-19.7	0.323 (-18)	0.256 (-24)	-20.1
	T240	10	25	1.3 (82)	2.7 (76)	77.6	4.2 (22)	6.1 (19)	20.6	134 (-12)	286 (-18)	-18.4	0.331 (-12)	0.285 (-18)	-16
	T240	20	21	1.3 (88)	2.6 (82)	83.3	3.9 (25)	5.5 (22)	22.8	159 (-12)	318 (-18)	-17.5	0.302 (-12)	0.265 (-18)	-12.3
	T240	30	18	1.2 (94)	2.3 (88)	88.5	4.8 (25)	6.5 (22)	24.6	88 (-6)	175 (-12)	-16.7	0.321 (-6)	0.277 (-12)	-8.9
	T240	40	16	2.0 (94)	4.1 (88)	93.2	4.2 (28)	5.6 (25)	26.2	52 (0)	97 (-6)	-16.8	0.335 (0)	0.299 (-6)	-5.8
	T240	60	11	1.3 (106)	2.5 (100)	101.2	4.0 (31)	5.2 (28)	28.5	61 (0)	108 (-6)	-16.8	0.302 (0)	0.266 (-6)	-0.3
	T240	80	10	2.2 (112)	4.3 (106)	112.0	4.3 (34)	5.4 (31)	32.1	24 (12)	44 (6)	-13.5	0.328 (12)	0.290 (6)	7.2
B2	None	0	57	1.8 (64)	4.0 (58)	62.6	4.1 (16)	6.6 (13)	14.7	212 (-18)	465 (-24)	-20.7	0.366 (-18)	0.275 (-24)	-22.4
	T240	0	35	1.1 (76)	2.4 (70)	70.7	4.2 (19)	6.4 (16)	17.7	252 (-18)	518 (-24)	-19.5	0.324 (-18)	0.257 (-24)	-20.1
	T240	10	24	1.3 (82)	2.7 (76)	77.7	4.5 (22)	6.5 (19)	21.1	138 (-12)	298 (-18)	-18.1	0.333 (-12)	0.284 (-18)	-16
	T240	20	20	1.2 (88)	2.4 (82)	82.6	4.1 (25)	5.9 (22)	23.4	164 (-12)	323 (-18)	-17.3	0.304 (-12)	0.266 (-18)	-12.6
	T240	30	17	2.1 (88)	4.3 (82)	87.4	4.9 (25)	6.8 (22)	24.9	84 (-6)	182 (-12)	-15.9	0.328 (-6)	0.281 (-12)	-9.6
	T240	40	15	1.5 (94)	3.1 (88)	90.9	4.1 (28)	5.6 (25)	26.1	99 (-6)	193 (-12)	-16	0.308 (-6)	0.265 (-12)	-7.1
	T240	60	12	1.7 (100)	3.5 (94)	98.0	4.0 (31)	5.3 (28)	28.6	58 (0)	112 (-6)	-14.9	0.315 (0)	0.280 (-6)	-2.6
	T240	80	11	2.2 (106)	4.3 (100)	105.8	4.1 (34)	5.2 (31)	31.5	42 (6)	75 (0)	-14.4	0.314 (6)	0.282 (0)	3.4

First Test Temperature (T_1); Second Test Temperature (T_2)

[a]Critical property; [b]Measured property with test temperature in parenthesis.

Neat PG 67-22 used in Strips 1 to 8 (B1); Neat PG 67-22 with 0.5% M1 Evotherm 3G^{TM} (B2); PAV conditioning conducted at 100°C and 2.1 MPa

CHAPTER 6 – EFFECTS OF SHORT TERM AGING

6.1 Overview of Short Term Aging

The construction approach used for the Figure 3.1 test section provided an opportunity to consider the effects of short term aging with respect to early age and longer term mixture performance. However, it presents a challenge when considering the Figure 3.1 test section for longer term field aging. Details of short term aging, the period where loose asphalt mixtures are exposed to high temperature and oxygen (to varying degrees) prior to compaction, is not always monitored, documented, or controlled, and there is limited information with respect to the effects of short term aging on mixture performance over time. There have been investigations to consider effects of silo storage (e.g. Kari, 1982; Jacques et al. 2016) and haul time (e.g. Wright and Paquette, 1966). Few have considered the effects of increased short term aging on mixture performance and there is even less documentation of short term effects on mixture performance after longer term aging. This chapter considers the effects of short term aging time on mixture performance in two phases: 1) materials collected soon after construction and 2) materials collected after longer term field aging.

This chapter's primary objective is to characterize the effects of short term aging time during construction on short term and longer term mixture behaviors. Secondary emphasis is placed on factors to be considered in later chapters. To complete these objectives, the chapter uses binder properties from 24 extracted and recovered binder samples, and results from 2,379 compacted mix specimen tests summarized in Chapter 5.

6.2 Volumetrics and Stability of Mixtures Over Time

High absorption aggregates, like those used in mixes M14 to M16, have increased potential for binder to absorb into aggregate pores and can be susceptible to moisture induced damage. This section discusses changes to G_{mm} and HLWT results over time. G_{mm} was chosen based on the fundamental principle that additional binder absorption in aggregate pores, all other factors being equal, increases G_{mm}. HLWT testing was chosen based on the ability of RD_{HLWT} and SIP to evaluate stability and moisture susceptibility of mixes.

Figure 6.1 plots the increase in G_{mm} (ΔG_{mm}) experienced during mixture hauling. Meaningful changes to G_{mm} due to increased HT were not observed when comparing the increase in G_{mm} due to binder absorption during hauling. The maximum and minimum increase in G_{mm} were both within T209 single operator limits for differences between two results (d2s) of the average increase observed, and the range of G_{mm} increase was less than the multiple laboratory d2s limit. Further, Section 4.2.4 demonstrates that binder did not continue absorbing into aggregate pores over longer term aging. In fact, the loose mixture G_{mm} values collected during construction were the highest G_{mm} values observed (Figure 4.3). This is expected to be the result of conglomerates in cores trapping small volumes of air when measuring G_{mm} on loose material collected from field cores.

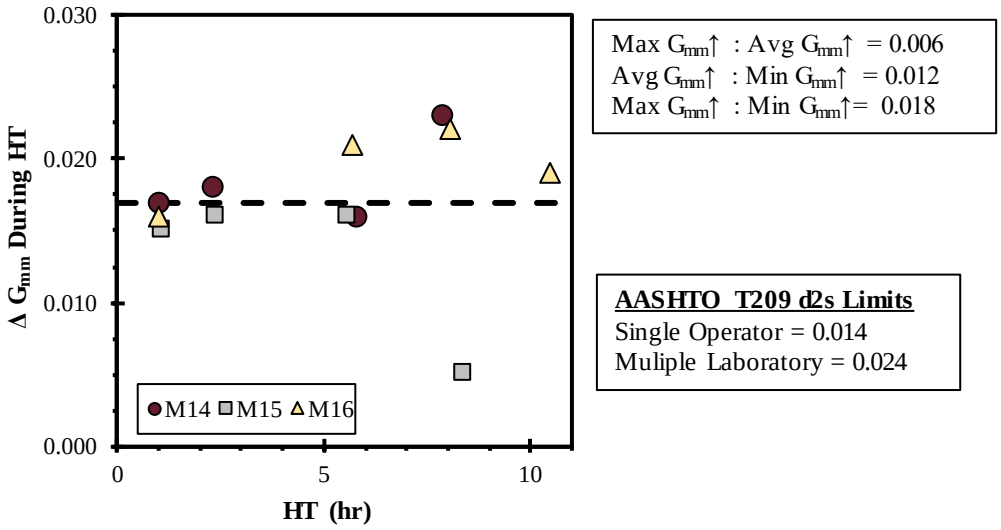

Figure 6.1. Short Term Aging Effects on G_{mm}

6.3 Cantabro Mass Loss Test Protocol Considerations

The primary mixture analysis in this chapter utilizes Cantabro data collected from cores with nominal heights of 6.3 cm and compares the effects of haul time (HT) to Cantabro factors identified in Cox et al. (2017). However, those results were for laboratory compacted SGC specimens with nominal heights of 11.5 cm. Thus, two Cantabro test protocol factors should be considered with respect to validating the use of 6.3 cm tall cores in this chapter: specimen geometry and compaction method.

6.3.1 Cantabro Test Specimen Geometry

A matched pairs evaluation between SGC specimens with 11.5 cm heights and SGC specimens with 6.3 cm heights was used to consider specimen geometry effects. Three pairs of specimens were produced between comparable triplicate groups (i.e. the same mix, target V_a, and HT) by pairing specimens with the greatest, intermediate, and least V_a. Figure 6.2a provides an equality plot comparing *ML* of both specimen sizes. The observable trend indicates that *ML* for 6.3 cm tall specimens should be divided by a factor of 1.10 for reasonable comparisons to 11.5 cm tall specimens. This observation is acceptable as test dynamics with specimens being different sizes, and the differences caused by specimen height changes do not seem to be prohibitive for reasonable test results based on the coefficient of determination (R^2) of 0.70 and *p*-value of < 0.01.

6.3.2 Cantabro Test Specimen Compaction Method

A second evaluation considered matched pairs between 6.3 cm tall specimens that were either field cores or SGC specimens. Figures 6.2b and 6.2c present equality plots where matched pairs were formed between specimens that were not longer term aged, were of comparable height, and were of comparable V_a (i.e., less than 0.5% difference in V_a). The

relationship of Figure 6.2b (slope of 1.17 and R^2 of 0.47) indicates that *ML* is higher in cores than in SGC specimens. However variability is visually increased when *ML* is greater than 35%. Figure 6.2c compares the same specimen pairs when considering only results with *ML* less than 35%, which is also more representative of the Cox et al. (2017) database. The close relationship in Figure 6.2c (slope of 0.97 and R^2 of 0.69) when considering *ML* results within the range of those used in the Cox et al. (2017) database suggests that it is reasonable to directly compare *ML* results from Superpave Gyratory Compactor (SGC) specimens and cores that are Cantabro tested if specimen geometry is considered.

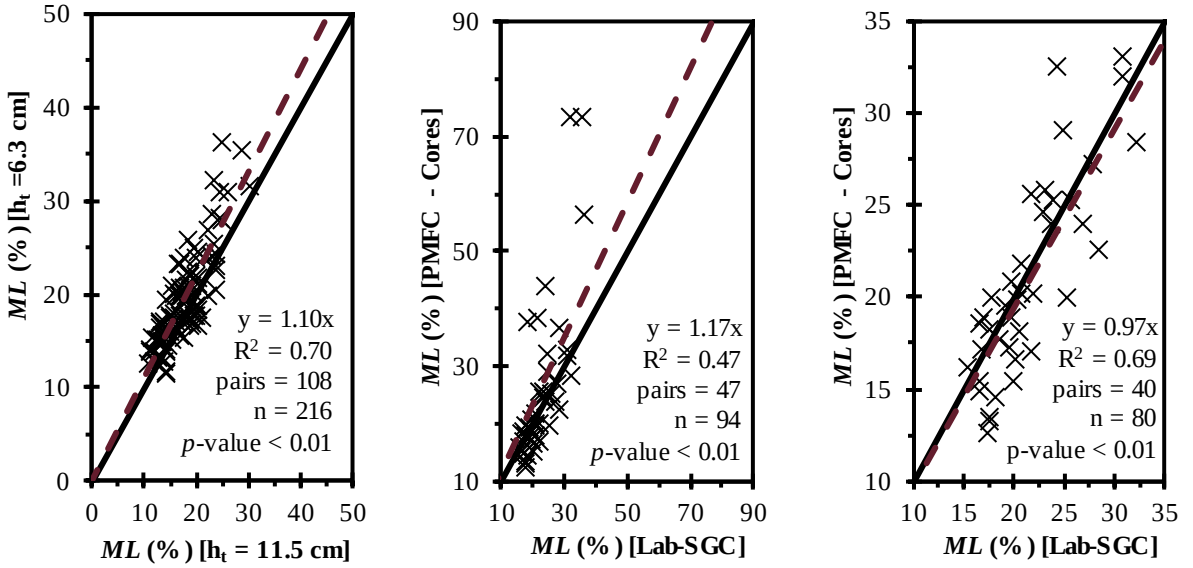

a) SGC Specimen Size *b) Compaction – All Data* *c) Compaction – Select Data*

Figure 6.2. Cantabro Test Protocol Considerations

6.4 Analysis of Short Term Aging Effects

The following four subsections present a four phase analysis of short term aging effects, including: 1) extracted binder property observations, 2) assessment of SIDT data, 3) assessment of *ML* and S_t results from plant mixed and laboratory compacted (PMLC) specimens, and 4) assessment of *ML* and S_t results from plant mixed and field compacted (PMFC) cores.

6.4.1 Phase I – Extracted Binder Property Observations

Figure 6.3 presents extracted binder property results provided in Chapter 5 alongside continuous binder grades per AASHTO M320 that were collected soon after the test section was constructed. AASHTO M320 grading included DSR_{25} testing of as-recovered samples and AASHTO R28 conditioning of recovered binders prior to DSR_8 or BBR testing.

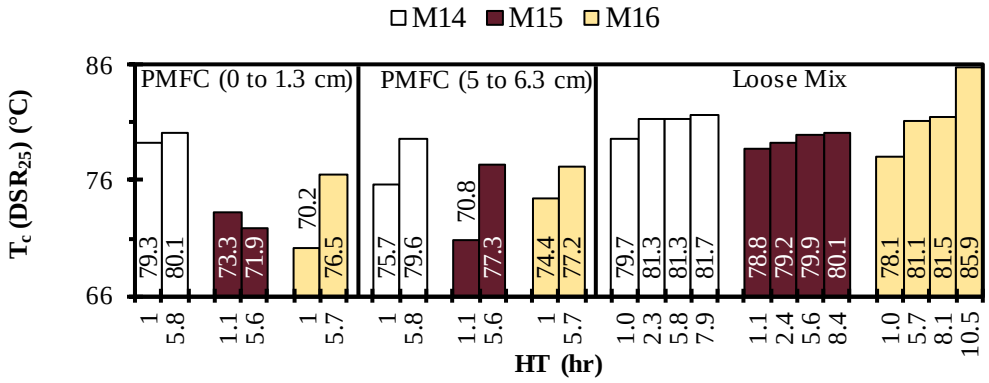

a) High Temperature

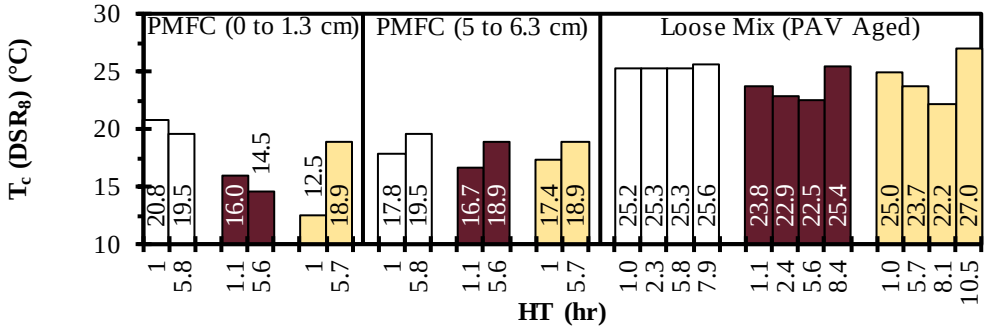

b) Intermediate Temperature

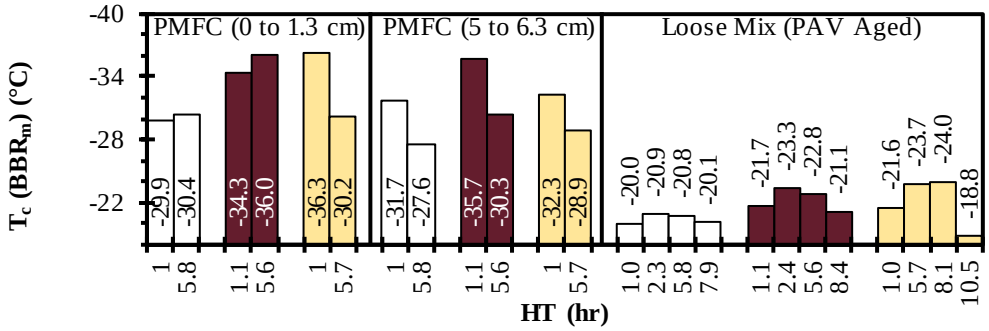

c) Low Temperature

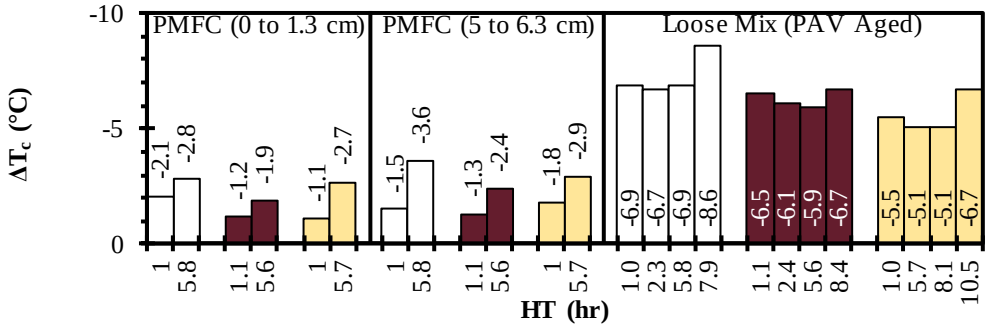

d) ΔT_c

Figure 6.3. Extracted Binder Properties

As shown in Figure 6.3a to 6.3c, most field core cases indicated modest binder stiffening as haul time increased based on increases in $T_c(DSR_{25})$, $T_c(DSR_8)$, and $T_c(BBR_m)$. However, haul time does not seem to produce prohibitive binder properties in field core extracted binders. ΔT_c did consistently decrease 0.7 to 2.1°C for all field core binder cases when increasing haul time from approximately 1 to approximately 6 hours, which indicates a increased potential for non-load associated distresses (Figure 6.3d). However no field core binder ΔT_c values were below the -5°C that was suggested by (Rowe, 2011).

Haul time effects were observable in $T_c(DSR_{25})$ properties of loose mix cases, but not in loose mix cases where binder were subjected to AASHTO R28 conditioning before binder testing (i.e. $T_c(DSR_8)$, $T_c(BBR_m)$, and ΔT_c). The only case where increased haul time led to concerning properties was when binders were hauled for 10.5 hours as was the case for strip 12. Further, the ΔT_c trend was not apparent with haul time for loose mix cases, which indicates that haul time effects were secondary to longer term aging, as would be simulated by AASHTO R28. While the ΔT_c values provided for loose mix in Figure 6.3d were below the -5°C suggested in Rowe (2011), there is no indication that haul time caused these values.

Though there were modest signs of increased susceptibility to non-load associated cracking as haul time increased based on binders stiffening and decreased ΔT_c, there were no haul times of 8.4 hours or less that indicated prohibitive effects of haul time. Thus, there were measurable, but modest, haul time effects on binder properties when hauled for 1 to 8.4 hours. This same general conclusion was reached by Howard et al. (2013) where the authors considered the loose mix data presented in Figure 6.3a to 6.3c alongside other measurements.

6.4.2 Phase II – Assessment of SIDT Results

Results of SIDT testing are provided in Figure 6.4a and 6.4b for FE_{+20C} and FE_{-10C} with notes to indicate the average V_a of all specimens tested. An outlier removal process which followed those of Moore and McCabe (2004) to identify potential outliers was completed (i.e. results more than 1.5 times the interquartile range away from the average). Ultimately, there were three to four FE measurements used in each Figure 6.4 bar. As shown, both FE_{+20C} and FE_{-10C} generally decrease with increased haul time, but with a large amount of variability. Regression assessments (Table 6.1) were used to evaluate the significance of FE vs HT and FE vs V_a relationships. As shown, there was only one regression where FE_{+20C} was 95% significant. Thus, this chapter does not attempt to assess the magnitude of FE_{+20C} reduction based on HT. however, slopes from the four FE_{-10C} regression with 95% significance (FE_{-10C} vs haul time and FE_{-10C} vs V_a for M14 and M15) indicate that a 1% increase in V_a was approximately 2.0 to 3.6 times more effective at changing FE_{-10C} as a 1 hour increase in haul time.

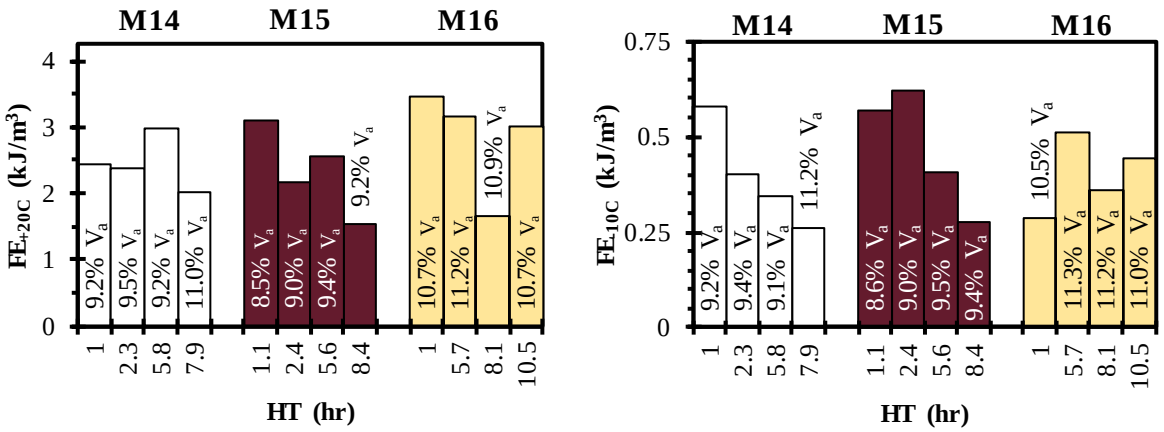

a) FE_{+20C} *b) FE_{-10C}*

Figure 6.4. Fracture Energy Results

Table 6.1. Fracture Energy Relationships

Mix	Behavior	Relationship	R^2	*p*-value	Significant?
M14	FE_{+20C}	$FE_{+20C} = 2.55 - 0.02\ HT$	<0.01	0.73	No
		$FE_{+20C} = 5.47 - 0.31\ V_a$	0.22	0.08	No
M15	FE_{+20C}	$FE_{+20C} = 3.09 - 0.14\ HT$	0.35	0.01	Yes
		$FE_{+20C} = 3.87 - 0.16\ V_a$	0.01	0.66	No
M16	FE_{+20C}	$FE_{+20C} = 3.48 - 0.12\ HT$	0.13	0.11	No
		$FE_{+20C} = 1.43 - 0.12\ V_a$	<0.01	0.83	No
M14	FE_{-10C}	$FE_{-10C} = 0.57 - 0.04\ HT$	0.65	<0.01	Yes
		$FE_{-10C} = 1.20 - 0.08\ V_a$	0.37	0.02	Yes
M15	FE_{-10C}	$FE_{-10C} = 0.67 - 0.05\ HT$	0.63	<0.01	Yes
		$FE_{-10C} = 2.14 - 0.18\ V_a$	0.33	0.03	Yes
M16	FE_{-10C}	$FE_{-10C} = 0.32 - 0.01\ HT$	0.15	0.14	No
		$FE_{-10C} = -0.14 + 0.04\ V_a$	0.04	0.48	No

6.4.3 Phase III – Assessment of *ML* and S_t Results in PMLC Specimens

Figure 6.5 plots the plant mixed and SGC compacted results at 4% and 7% V_a provided in Table 5.2. Figures 6.5a to 6.5c present trends for specimens compacted to 11.5 cm thick whereas Figures 6.5d to 6.5i provide results of specimens compacted to 6.3 cm thick. Relationships were evaluated generally in Figure 6.5 and statistical evaluations are provided in Tables 6.2 to 6.5. General assessments of trends analysis are provided in subsection 6.4.3.1 and statistical assessments are provided in subsection 6.4.3.2.

6.4.3.1 General Assessment of PMLC Results

ML or S_t relationships with haul time were best produced using linear regressions in most cases where effects of haul time were shown in Figure 6.5, but logarithmic relationships provided the best fit between *ML* of 11.5 cm tall specimens compacted to 4% V_a and haul time. First, haul time only had noticeable effects on *ML* or S_t in eight of the eighteen relationships (44%). Second, seven of the eight regressions (88%) that detected effects of haul time were for

specimens compacted to 4% V_a. The tendency of haul time to primarily be detected only in specimens compacted to 4% V_a suggests that haul time effects are secondary effects, which may not be noticed at densities of typical pavements. Third, the relationships with the highest R^2 were logarithmic, which indicates that haul time effects are more severe during the first two hours of haul time. Fourth, there were more significant regressions detected for M14 specimens than for M15 or M16 mixes, which could be due to the higher mix temperatures during production (T_{pre} of 164°C for M14 vs 153°C for M15 and 148°C for M16).

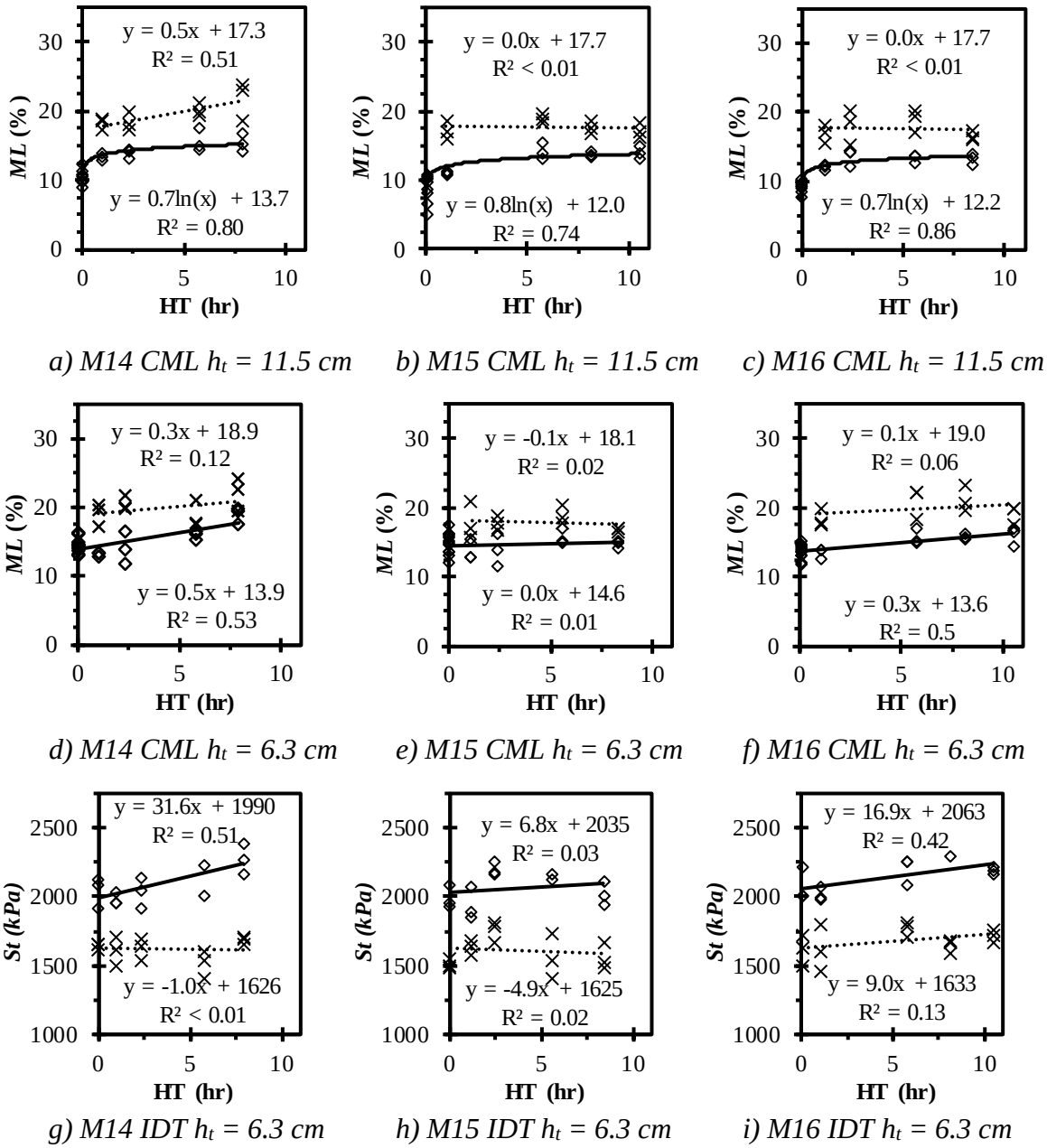

a) M14 CML h_t = 11.5 cm *b) M15 CML h_t = 11.5 cm* *c) M16 CML h_t = 11.5 cm*

d) M14 CML h_t = 6.3 cm *e) M15 CML h_t = 6.3 cm* *f) M16 CML h_t = 6.3 cm*

g) M14 IDT h_t = 6.3 cm *h) M15 IDT h_t = 6.3 cm* *i) M16 IDT h_t = 6.3 cm*

Figure 6.5. Cantabro and Indirect Tensile Analysis of PMLC Specimens

Table 6.2. Cantabro and Indirect Tensile Regressions of PMLC Data

CML (h_t = 11.5 cm)				CML (h_t = 6.3 cm)				IDT (h_t = 6.3 cm)			
Mix	**V_a (%)**	***p*-value**	**Significant?**	**Mix**	**V_a (%)**	***p*-value**	**Significant?**	**Mix**	**V_a (%)**	***p*-value**	**Significant?**
M14	4	<0.01	Yes	M14	4	<0.01	Yes	M14	4	<0.01	Yes
	7	<0.01	Yes		7	.26	No		7	0.90	No
M15	4	<0.01	Yes	M15	4	0.72	No	M15	4	0.54	No
	7	0.90	No		7	.70	No		7	0.64	No
M16	4	<0.01	Yes	M16	4	<0.01	Yes	M16	4	0.02	Yes
	7	0.90	No		7	.46	No		7	0.19	No

6.4.3.2 Statistical Assessment of PMLC Results

To further investigate the Figure 6.5 trends, four analysis of variance (ANOVA) assessments were conducted at the 95% confidence level to evaluate the effects of HT on *ML* and S_t in plant mixed and SGC compacted specimens (Table 6.3). *ML* evaluations were divided by target V_a and considered treatments of mix and haul time (HT) rounded to the nearest hour with specimen height (h_t) as a block factor. S_t evaluations considered the same treatments as *ML* evaluations, but had no block factors. As expected, the ANOVAs indicate significant effects of h_t, mix and HT on *ML* for both evaluations, but treatment interaction was evident in specimens compacted to 7% V_a. Thus, Table 6.4 *ML* rankings can consider treatment factors individually at 4% V_a but must consider treatments collectively when compacted to 7% V_a. Table 6.4 first presents rankings of all *ML* data and subsequently presents *ML* corresponding to separate specimen sizes. S_t ANOVA results indicate significant effects of HT on S_t at 4% with no evidence of interaction, but S_t at 7% V_a was only sensitive to treatment interaction and neither treatment individually. Thus, Table 6.4 S_t rankings consider HT independently at 4% V_a, but consider combinations of mix and HT at 7% V_a.

Table 6.3. PMLC ANOVAs

		4% V_a			7% V_a		
Response	**Source**	**d.f.**	**p-value**	**Significant?**	**d.f.**	**p-value**	**Significant?**
ML	Total (Corrected)	131	---	---	71	---	---
	h_t	1	<0.01	Yes	1	0.01	Yes
	Mix	2	<0.01	Yes	2	<0.01	Yes
	HT	5	<0.01	Yes	4	0.03	Yes
	Mix * HT	7	0.23	No	5	0.01	Yes
	Error	116	---	---	59	---	--
S_t	Total (Corrected)	40	---	---	44	---	
	Mix	2	0.08	No	2	0.09	No
	HT	5	<0.01	Yes	5	0.20	No
	Mix * HT	7	0.06	No	7	0.04	Yes
	Error	26	---	---	14	---	

For interpretation, Table 6.4 rankings present the average *ML* or S_t for the indicated number of specimens (n) meeting the criteria indicated by test type, mix, and HT. However, statistical differences are only indicated when two averages do not belong to the same *t*-group. For example, there is no significant difference in *ML* of specimens compacted to 4% V_a (all data) and hauled for 6 to 11 hr as all three combinations belong to *t*-group "A". However, there is a significant difference detected between *ML* of specimens from mix hauled for 1 hr or 11 h

as specimens hauled for 1 hr belong to *t*-groups “C” and “D” while specimens hauled for 11 hr belong to *t*-groups “A” and “B”.

Rankings for both mixture tests provide more conclusive results at 4% V_a than at 7% V_a, which agrees with the previous observation that most relationships with significance for *ML* or S_t to HT were in specimens compacted to 4% V_a. Rankings at 4% V_a suggest that most changes to *ML* and S_t occurred during the first 2 hr of HT with non-significant differences occurring after 2 hr. This observation also mimics the finding from Figure 6.3 where the strongest relationships were logarithmic and indicated little change after 2 hr. Further, the average increase in *ML* between 1 and 8 hr of HT was 2.5% in 4% V_a specimens without respect to specimen geometry (Table 6.4). The average *ML* increase over the same amount of time was 2.0% and 3.1% for 11.5 cm and 6.3 cm tall specimens, respectively. Test results at 7% V_a do not provide as much clarity. Substantial chaining across *t*-groups for both tests at 7% V_a limits the conclusions at 7% V_a.

Table 6.4. Rankings of PMLC Results

Ranking	*ML* (all data)					*ML* (h_t = 11.5 cm)					*ML* (h_t = 6.3 cm)					S_t				
	Mix	HT (hr)	n	Avg (%)	t-group	Mix	HT (hr)	n	Avg (%)	t-group	Mix	HT (hr)	n	Avg (%)	t-group	Mix	HT (hr)	n	Avg (kPa)	t-group
Mix (4% V_a)	M14	---	44	14.0	A	M14	---	20	12.9	A	M14	---	24	14.9	A	M16	---	13	2,142	---
	M15	---	44	13.2	B	M15	---	20	11.4	B	M15	---	24	14.7	A	M14	---	14	2,094	---
	M16	---	44	13.0	B	M16	---	20	11.3	B	M16	---	24	14.4	A	M15	---	14	2,059	---
HT (4% V_a)	---	8	18	15.3	A	---	6	9	14.3	A	---	8	9	16.5	A	---	11	3	2,197	A
	---	6	18	15.0	A	---	8	9	14.1	A	---	11	3	15.9	A	---	8	7	2,173	A
	---	11	6	14.9	AB	---	11	3	13.9	A	---	6	9	15.8	A	---	6	7	2,169	A
	---	2	12	13.8	BC	---	2	6	13.6	A	---	0	36	14.3	B	---	2	6	2,124	AB
	---	1	18	12.8	CD	---	1	9	12.1	B	---	2	6	13.9	B	---	0	9	2,044	BC
	---	0	60	12.3	D	---	0	24	9.4	C	---	1	9	13.4	B	---	1	9	1,986	C
Mix and HT (7% V_a)	M14	8	6	21.8	A	M14	8	3	21.7	A	M14	8	3	22.0	A	M16	6	3	1,774	A
	M16	6	6	19.9	B	M14	6	3	20.0	AB	M16	8	3	21.2	AB	M15	2	3	1,760	AB
	M16	8	6	19.4	BC	M15	6	3	18.9	BC	M16	6	3	21.0	AB	M16	11	3	1,724	AB
	M14	6	6	19.4	BC	M16	6	3	18.8	BC	M14	2	3	20.4	ABC	M14	8	3	1,689	ABC
	M14	2	6	19.3	BCD	M14	2	3	18.2	BC	M14	1	3	19.0	BCD	M16	8	3	1,653	ABCD
	M15	6	6	18.9	BCD	M14	1	3	18.1	BC	M16	11	3	19.0	BCD	M14	0	3	1,653	ABCD
	M14	1	6	18.5	BCDE	M15	2	3	18.0	BC	M15	6	3	18.9	BCD	M15	1	3	1,639	ABCD
	M16	11	6	18.0	BCDE	M16	8	3	17.6	BC	M14	6	3	18.7	BCD	M14	2	3	1,636	ABCD
	M15	2	6	17.8	CDE	M16	1	3	17.2	C	M16	1	3	18.3	BCD	M16	1	3	1,626	ABCD
	M16	1	6	17.7	CDE	M16	11	3	17.1	C	M15	1	3	17.8	CD	M16	0	3	1,621	BCD
	M15	1	6	17.3	DE	M15	1	3	16.8	C	M15	2	3	17.7	CD	M14	1	3	1,618	BCD
	M15	8	6	16.7	E	M15	8	3	16.5	C	M15	8	3	16.8	D	M15	8	3	1,565	CD
	---	---	---	---	---	---	---	---	---	---	---	---	---	---	---	M15	6	3	1,563	CD
	---	---	---	---	---	---	---	---	---	---	---	---	---	---	---	M14	6	3	1,525	D
	---	---	---	---	---	---	---	---	---	---	---	---	---	---	---	M15	0	3	1,519	D

Note HT values shown are rounded to the nearest hour

Both Section 6.4.3 assessments lead to the same observations: 1) HT effects are detectable in PMLC specimens compacted to 4% V_a, but HT effects were less detectable in PMLC specimens compacted to 7% V_a, 2) most *ML* or S_t increase during hauling occurred during the first 2 hr, and 3) less desirable and more pronounced behaviors were observed in M14 specimens than M15 or M16 specimens. Stated another way, haul time effects were detected in PMLC specimens compacted to 4% V_a, where there is inherently less variability, but PMLC specimens compacted to more realistic density levels for in-place pavements (i.e. 7% V_a) did not indicate the effects of haul time.

6.4.4 Phase IV – Assessment of *ML* and S_t Results in PMFC Cores

Phase IV assessments conducted a global assessment (Section 6.4.4.1) and a controlled assessment (Section 6.4.4.2) of 848 CML and 640 IDT tests conducted on PMFC cores that were sampled soon after construction or after up to five years of field aging. Figure 6.6 presents scatter plots between mixture test results and production variables of interest, including: haul time (HT), mix temperature before hauling (T_{pre}), presence of chemical warm mix technology, field age in years, and air voids (V_a). The Figure 6.6 trends suggest that there could be effects of each of the five factors considered, but these trends neglect the potential for factor interaction (e.g. generally increased V_a in strips with longer haul times). Thus, the following two sub-sections conduct more detailed analysis which consider the effects of factors independently of one another.

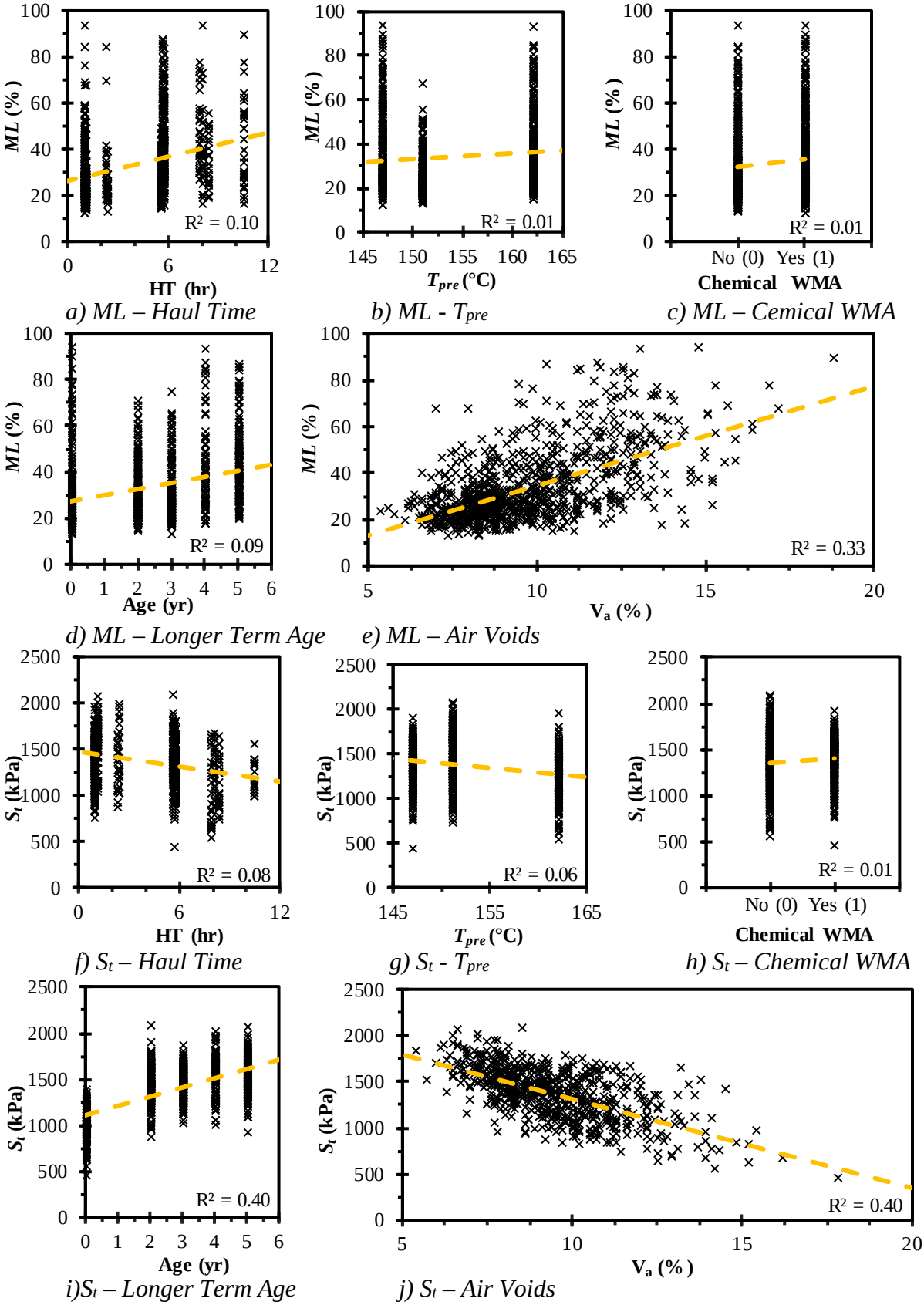

Figure 6.6. Global Assessment of CML and IDT Data from PMFC Cores

6.4.4.1 Global Assessment of PMFC Results

Multiple regression was used to individually assess the impact of the Figure 6.6 variables on *ML* and S_t. This analysis was conducted in SAS statistical software using PROC REG, which estimates linear coefficients for all variables considered. Table 6.5 presents two analysis approaches. The first approach considered all Figure 6.6 variables, and the second approach considered only the variables identified as having significant effects on *ML* or S_t during the first analysis. Variable transformations (i.e. logarithmic and quadratic relationships) were evaluated for each variable of interest, but the inability of variable transformations to meaningfully improve regression fit led to only considering linear regressions. The final regressions determined in Table 6.5 are provided as equations in Equation 6.1 and 6.2.

Table 6.5. Multiple Regression Analysis of CML and IDT Results from PMFC Cores

	CML (All Parameters)			**IDT (All Parameters)**			**CML (Sig Parameters)**			**IDT (Sig Parameters)**		
Parameter	**Value**	***p*-value**	**Sig?**	**Value**	***p*-value**	**Sig?**	**Value**	***p*-value**	**Sig?**	**Value**	***p*-value**	**Sig?**
β_0	-81.2	<0.01	Yes	2796.3	<0.01	Yes	-76.5	<0.01	Yes	2780.1	<0.01	Yes
β_{HT}	-0.17	0.26	No	-1.0	0.68	No	---	---	---	---	---	---
$\beta_{ChemWMA}$	0.49	0.70	No	57.7	<0.01	Yes	---	---	---	59.7	<0.01	Yes
β_{Tpre}	0.34	<0.01	Yes	-5.8	<0.01	Yes	0.32	<0.01	Yes	-5.4	<0.01	Yes
β_{Age}	4.27	<0.01	Yes	82.0	<0.01	Yes	4.26	<0.01	Yes	81.8	<0.01	Yes
β_{Va}	5.34	<0.01	Yes	-84.2	<0.01	Yes	5.25	<0.01	Yes	-85.3	<0.01	Yes
Model	---	<0.01	Yes	---	<0.01	Yes	---	<0.01	Yes	---	<0.01	Yes
R^2_{adj}	0.56	---	---	0.72	---	---	0.56	---	---	0.72	---	---

$$ML = -76.5 + 0.32\,(T_{pre}) + 4.26\,(Age) + 5.25\,(V_a) \quad (6.1)$$

$$S_t = 2780.1 + 59.7\,(ChemWMA) - 5.4\,(T_{pre}) + 81.8\,(Age) - 85.3\,(V_a) \quad (6.2)$$

Where,
ML = Cantabro Mass Loss (%)
S_t = Indirect Tensile Strength (kPa)
T_{pre} = Mix Temperature Before Hauling
ChemWMA = Presence of Chemically Based Warm Mix Additive (no = 0 ; yes = 1)
Age = Longer Term Aging Time (years)
V_a = Air Voids (%)

As shown in Table 6.5, the Equation 6.1 model had an adjusted coefficient of determination (R^2_{adj}) of 0.56 and was statistically significant with a *p*-value of < 0.01, which is acceptable based on the amount of scatter which is inherent with CML results when testing field cores. The Equation 6.2 model had R^2_{adj} of 0.72 and was also statistically significant with *p*-value of < 0.01. There were statistically significant coefficients determined for T_{pre}, *Age*, and V_a for both regressions, and there was a significant coefficient detected for *ChemWMA* in Equation 6.2. For both models, there was no significant effect of HT detected. This suggests that there were no significant effects of HT detected in field core tests for *ML* or S_t.

6.4.4.2 Controlled Assessment of PMFC Results

Two further controlled assessments were completed to consider the effects of HT and V_a on *ML* and S_t in cores. The first considered HT effects at single points in time between test strips, and the second considered HT effects on *ML* or S_t change over five years of environmental exposure. These assessments are described in the next two paragraphs in the order mentioned. Both assessments produced pairs of cores that were from the same mix, had within 0.2% V_a of one another, and differed by only one variable (i.e. haul time between strips of the same mix or field aging time within the same test strip). After pairs were produced, the effects of HT were evaluated by producing mass loss ratio (*MLR*) or tensile strength ratio (S_tR) between control specimen tests or specimens with increased HT or increased field aging.

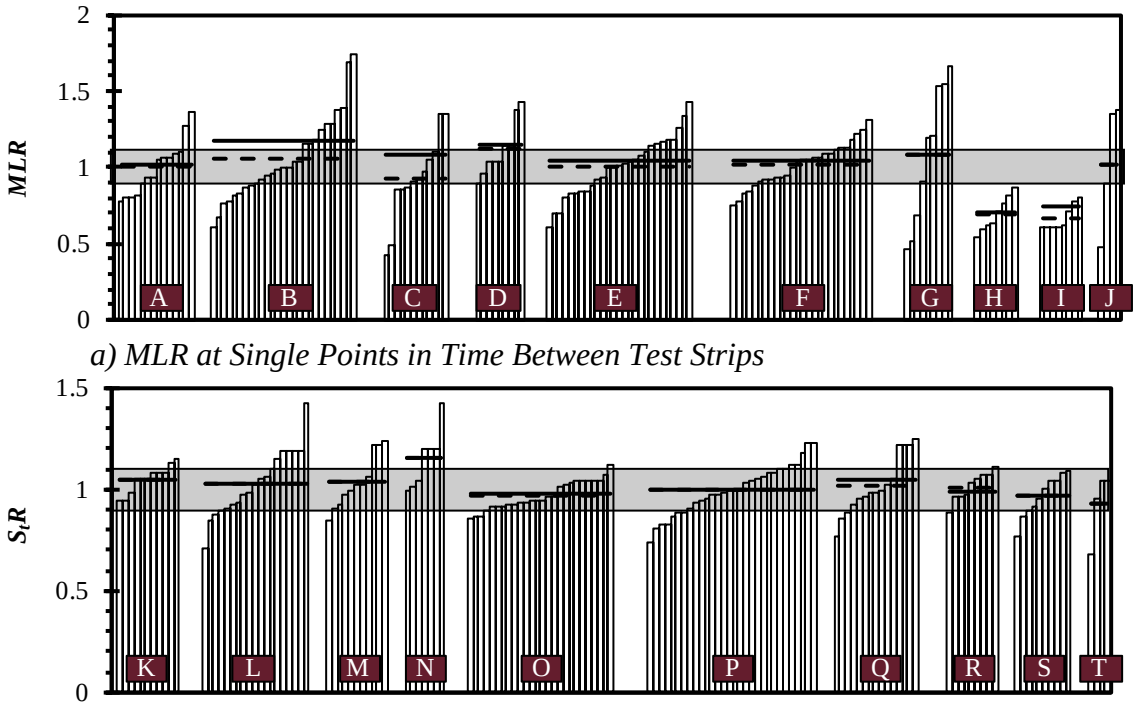

a) MLR at Single Points in Time Between Test Strips

b) S_tR at Single Points in Time Between Test Strips

			All Data		Outliers Removed					All Data		Outliers Removed	
Plot ID	ΔHT (hr)	Age (yr)	Avg *MLR*	n	Avg *MLR*	n	Plot ID	ΔHT (hr)	Age (yr)	Avg S_tR	n	Avg S_tR	n
A	1.3	0	1.02	32	1.00	28	**K**	1.3	0	1.05	26	1.05	22
B	4.5 to 4.8	0	1.18	60	1.06	54	**L**	4.5 to 4.8	0	1.03	38	1.03	38
C	6.9 to 7.3	0	1.09	28	0.93	24	**M**	6.9 to 7.3	0	1.04	22	1.04	22
D	9.5	0	1.15	22	1.12	18	**N**	9.5	0	1.15	14	1.15	14
E	4.5 to 4.8	2	1.04	60	1.00	54	**O**	4.5 to 4.8	2	0.98	60	0.97	52
F	4.5 to 4.8	3	1.04	66	1.02	52	**P**	4.5 to 4.8	3	1.00	60	1.00	60
G	4.5 to 4.8	4	1.08	18	1.08	18	**Q**	4.5 to 4.8	4	1.05	32	1.02	30
H	1.3	5	0.71	24	0.69	16	**R**	1.3	5	0.99	20	1.01	18
I	4.5 to 4.8	5	0.74	18	0.67	16	**S**	4.5 to 4.8	5	0.97	20	0.97	20
J	6.9 to 7.3	5	1.02	8	1.02	8	**T**	6.9 to 7.3	5	0.93	8	0.93	8

Figure 6.7. Controlled Assessment of PMFC Core Data at Single Points in Time

Figure 6.7 contains plots for the relative change in *ML* and S_t resulting from changes in HT. The ten cases describe the effects of HT increase (ΔHT) for a single age in time by using cores from strips hauled for approximately 1 hour as control tests. For example, a bar with ΔHT of 1.10 *MLR* indicates that *ML* of a specimen hauled for approximately 2 hours produced *ML* that was 1.10 times the *ML* of a paired specimen hauled for approximately 1 hour. Shaded areas indicate the ranges where the effects of ΔHT are not considered as meaningful differences (i.e. behavior ratios between 0.9 and 1.1). Potential outliers were identified by determining which ratios were more than 1.5 times the interquartile range away from the average ratio (Moore and McCabe, 2004). There were four cases where meaningful effects of ΔHT were detected (i.e. D, H, I, and N) when potential outliers were removed, and six cases detected when all ratios were considered (i.e. B, C, D, H, I, and N). This observation leads to the same conclusion as Section 6.4.4.1 where there was little to no effect of HT detected in field core tests.

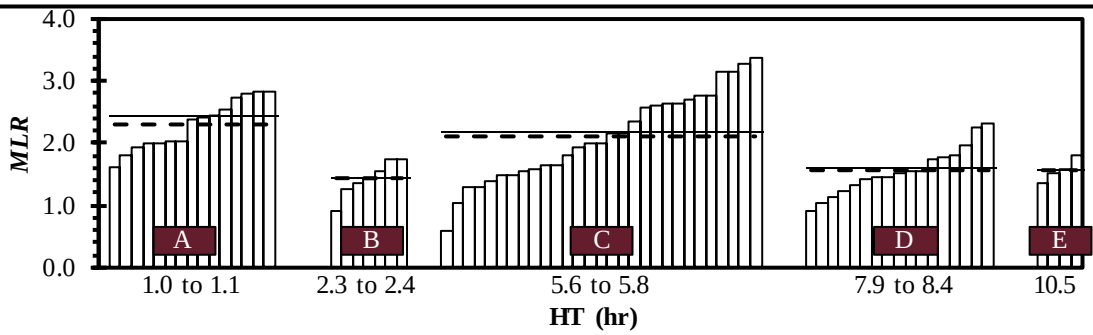

a) MLR Over 5 Years Within Test Strips

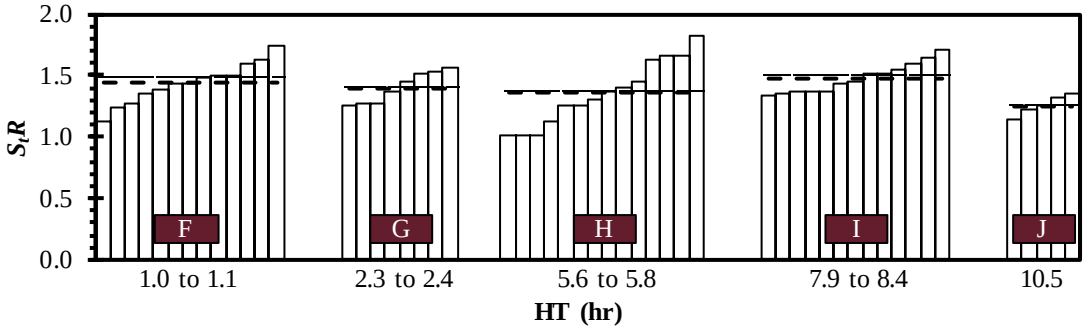

b) S_tR Over 5 Years Within Test Strips

		All Data		Outliers Removed				All Data		Outliers Removed	
Plot ID	**HT (hr)**	**Avg *MLR***	**n**	**Avg *MLR***	**n**	**Plot ID**	**HT (hr)**	**Avg S_tR**	**n**	**Avg S_tR**	**n**
A	1.0 to 1.1	2.41	18	2.29	15	**F**	1.0 to 1.1	1.47	14	1.44	13
B	2.3 to 2.4	1.42	7	1.42	7	**G**	2.3 to 2.4	1.40	8	1.40	8
C	5.6 to 5.8	2.17	30	2.10	29	**H**	5.6 to 5.8	1.36	14	1.36	14
D	7.9 to 8.4	1.60	18	1.55	17	**I**	7.9 to 8.4	1.49	15	1.48	13
E	10.5	1.56	4	1.56	4	**J**	10.5	1.25	5	1.25	5

Figure 6.8. Controlled Assessment of PMFC Core Data Over Five Years

Figure 6.8 considers the effects of HT on the increase in *ML* or S_t between 0 year and 5 year field cores of the same HT using 133 matched pairs. Unaged cores were considered as

the control and ratios present the test property after 5 years of aging compared to the test property of specimens from the same pair when tested without longer term aging. As shown, there were no signs of HT causing increased *ML* or S_t after 5 years of field aging. Observations from Figures 6.7 and 6.8 lead to the same conclusion from section 6.4.4.1 where there was little to no effect of haul time detected in field core tests.

6.5 Discussion of Short Term Aging Effects

Table 6.6 summarizes the four phase analysis conducted in Section 6.4. The four phase analysis detected haul time effects with binder and mixture tests in some cases, but most phases resulted in not detecting haul time effects. In fact, there were no cases where field cores from the full-scale test section detected negative effects from haul time. Thus, the effects of haul time were secondary for this test section. However, the magnitude of haul time effects where detected in mixture tests is worth further discussion.

Table 6.6. Summary of Short Term Aging Effects on Material Properties

Phase	Description	Haul Time Observations
I	Binder Data Analysis	- All data collected without longer term aging - There were no prohibitive binder properties measured where HT ≤ 8.4 hr - ↑HT ➔ ↑$T_c(DSR_{25})$ in binder samples extracted from cores (no binder conditioning) and binder samples extracted from loose mix samples (PAV conditioned) - ↑HT ➔ ↑$T_c(BBR_m)$ and ↓ΔT_c in in binder samples extracted from cores (no binder conditioning) but not binder samples extracted from loose mix samples (PAV conditioned)
II	Assessment of Fracture Energy Data	- All data collected without longer term aging - FE_{+20C} of sliced specimen was not sensitive to V_a measured on upper 6.3 cm - FE_{-10C} of sliced specimens was sensitive to V_a measured on upper 6.3 cm in M14 and M15, but not M16 - Based on FE_{-10C} reduction: 1% V_a↓ was 2.0 to 3.6 times as impactful as 1 hour ↑ in HT
III	Assessment of PMLC Specimen Data	- All data collected without longer term aging - HT effects are detectable at 4% V_a, but are less obvious at 7% V_a - Average *ML*↑ was 2.2% in 11.5 cm tall specimens at 4% V_a as HT increased from 1 to 8 hr - Average *ML*↑ was 3.1% (2.8% after Figure 6.2a* factor) in 6.3 cm tall specimens at 4% V_a as HT increased from 1 to 8 hr - HT effects are more pronounced in M14 than in M15 or M16 - Highest R^2 values observed in logarithmic relationships between *ML* and HT in specimens with 4% V_a and h_t = 11.5 cm - Significant effects of HT on *ML* and S_t occurred in first 2 hr of haul time
IV	Assessment of PMFC Specimen Data	- Data collected after 0, 2, 3, 4, and 5 years of field aging - HT effects were not significant in *ML* or S_t multiple regression models - *MLR* due to HT was 1.04 (0.99 without outliers) on average in the ten cases considered - S_tR due to HT was 1.01 (1.01 without outliers) on average in the ten cases considered - Average HT based *MLR* or *StR* was 0.9 to 1.1 in 16 of 20 groups - HT did not affect increase in *ML* or S_t due to longer term aging

*The Figure 6.2a factor indicated that *ML* results in 6.3 cm tall specimens should be divided by 1.1 for comparison to the Cox et al. (2017) database. This factor does not apply to *MLR*.

Sections 6.4.2 and 6.4.3 where the analysis phases where meaningful effects of haul time were detected, and there were minimal to no effects of haul time detected in Section 6.4.1 or Section 6.4.4. Section 6.4.2 determined that a 1% V_a increase was 2.0 to 3.6 times as impactful at decreasing FE_{-10C} through SIDT testing. Section 6.4.3 indicated that increasing haul time from 1 to 8 hours produced a 2.5% *ML* increase in all specimens tested (i.e. all data

ML column at 4% V_a from Table 6.4). This effect on *ML* can be used to compare with the effects of mixture property changes from Cox et al. (2017) as summarized in Table 6.7. Based on Figure 6.2a, it is inappropriate to made direct comparisons between *ML* of specimens with different dimensions, and the following paragraph relies on the *ML* increase in 11.5 cm specimens (2.0% *ML* or *MLR* of 1.17) to make comparisons to Table 6.7 where the database relied completely on 11.5 cm Cantabro tests.

Table 6.7. Effects of Mixture Changes on *ML* after Cox et al. (2017)

Mixture Change	General Effect on *ML*
High PG Grade	6°C↑ ➔ ↑*ML* 6.9%
Inclusion of SBS Polymer	PG 67-22 (neat) to PG 76-22 (SBS) ➔ ↓*ML* 2.3% PG 64-22 (neat) similar to PG 76-22 (SBS) (9.1% *ML* vs. 9.2% *ML*)
Aggregate Type	Limestone to Gravel with no RAP ➔ ↑*ML* 3.6%
V_a	1% V_a ↑ ➔ ↑*ML* 0.6% (un-aged) & ↑*ML* 0.6 to 2.8% (conditioned or field aged) ↑V_a (7% to 9%) ➔ *MLR* 1.10 (un-aged) & *MLR* 1.09 to 1.22 (conditioned or field aged)
Dust to Binder Ratio (D/P_{be})	0.1 D/P_{be} ↑ ➔ ↑*ML* 2.2%
Binder Content (P_b)	↑P_b from design by factor of 1.1 to 1.2 ➔ ↓*ML* by factor of 0.6 to 0.8 ↓P_b from design by factor of 0.8 to 0.9 ➔ ↑*ML* by factor of 1.5 to 2.0
Field Aging[1]	1 Year ➔ ↑*ML* by factor of 1.16 to 1.40 (average of 1.22)

-- All specimens were SGC compacted and 11.5 cm tall

[1]Specimens were field aged on an asphalt pavement in Columbus, MS with plastic pipe surrounding specimen edges. Tops were directly exposed to the environment and bottoms were in direct contact with the pavement.

Comparing the 2.0% *ML* increase between 1 hour and 8 hours of haul time to the *ML* increases in Table 6.6, the effects of an 8 hour haul time were less than *ML* effects caused by a 6°C increase in high PG binder grade, a change in coarse aggregate type, or a reduction in P_b by a factors of 0.8 to 0.9 (i.e. 0.5% to 1.0% P_b decrease for M14 to M16). The *ML* change produced by 8 hour hauls were of approximately the same magnitude as the inclusion of SBS polymer or a 0.1 increase in dust to effective binder ratio. The only Table 6.6 factor to have a lesser effect on *ML* than 8 hours of hauling was where V_a was increased from 7% to 9%, but the effects of V_a were more pronounced than haul time effects after longer term aging or longer term conditioning had occurred.

6.6 Summary of Short Term Aging Effects

This chapter conducted an investigation of haul time effects of the mixtures used in the Figure 3.1 test section where mixes were hauled for 1.0 to 10.5 hours and subsequently monitored for five years of environmental exposure. Preliminary considerations determined that mixes had consistent volumetrics and were stable over time with no appreciable binder absorption as a result of haul time or after up to 3 years of field aging. Through a four phase analysis of haul time effects, haul time was determined to have secondary effects on mixture behaviors detected using the Cantabro mass loss and Indirect Tensile strength tests when compared to factors such as compacted density or field aging time. There were practically no signs of decreased mixture behavior in mixtures hauled between approximately 2 and approximately 8 hours when evaluated soon after construction, and there were no negative effects of haul time detected after five years of environmental exposure. Overall, the authors did not find evidence to support detrimental effects of increased haul times up to 8 hours in this chapter. There was evidence of haul time effects in some cases, but haul time effects were secondary.

CHAPTER 7 – FIVE YEAR MIXTURE AGING RESULTS

7.1 Overview of Mix Conditioning

This chapter considers the Chapter 3 conditioning protocols and uses mixture tests to pair the damage produced from laboratory conditioning to the damage produced by exposure to non-load associated environmental factors in the Figure 3.1 test section. To complete this objective, the Cantabro Mass Loss (CML), indirect tensile (IDT), and Superpave instrumented indirect tensile (SIDT) tests were used to compare properties of cores collected soon after construction that had been subjected to laboratory conditioning and cores which were collected after 0, 2, 3, 4, or 5 years of environmental exposure.

7.2 Analysis of Mix Conditioning Results

Based on observations from Chapter 6, this chapter: 1) neglected effects of haul times up to 8.5 hours by combining CML and IDT test results by mix (i.e. M14, M15, and M16a); 2) did not consider strip 12 based on the effects of haul time observed after 10.5 hours of hauling in Chapter 6, which is why strips 9 to 11 are designated M16a; 3) considers the observations that moisture induced damage was not observed in the first five years of aging based on there being no stripping inflection points (SIPs) determined in 197 HLWT tests described in Table 5.1.

Prior to matching the effects of laboratory conditioning to environmental exposure, an outlier removal process was completed for CML and IDT test results based on linear regressions between *ML* and V_a or S_t and V_a. All CML and IDT test results from M14, M15, or M16a that were originally presented in Tables 5.3 and 5.4 were considered for outlier removal, and Table 7.1 summarizes the results after outlier removal. Outliers were identified by determining the Cook's distance, that was originally described by Cook (1977), for each data point considered in 63 regressions between *ML* or S_t and V_a. Results where the Cook's distance was greater than four divided by the total number of observations were removed as outliers.

Table 7.1 provides summary statistics (i.e. average (avg) and coefficient of variation (COV)) and regressions between *ML* or S_t and V_a after outlier removal. Coefficients of determination (R^2) and probabilities of non-significance (*p*-value) are provided for each regression. The total number of data points considered (n) and the number of outliers removed (n_o) are also provided. For example, the average S_t of 0 year specimens from M14 was 955 kPa with a COV of 17%, and these values were measured on 52 of the original 53 data points after one outlier was removed. Subsections 7.2.1 and 7.2.2 only consider results which were not identified as outliers in the Table 7.1 outlier removal process.

Table 7.1. Cantabro and Indirect Tensile Test Results after Outlier Removal

Mix	Age or CP	*ML*									S_t								
		n	n_o	Avg (%)	COV (%)	V_a Avg (%)	V_a COV (%)	Regression	R^2	*p*-value	n	n_o	Avg (kPa)	COV (%)	V_a Avg (%)	V_a COV (%)	Regression	R^2	*p*-value
M14	0 year	69	6	31.5	46	10.9	16	*ML* =6.5(V_a) – 39.7	0.65	<0.01	53	1	955	17	10.8	18	S_t =1643 – 63.8 (V_a)	0.58	<0.01
	2 year	55	6	34.7	33	9.2	13	*ML* =7.3(V_a) – 32.6	0.63	<0.01	41	2	1272	12	9.4	10	S_t =2562 – 137.7 (V_a)	0.66	<0.01
	3 year	59	4	32.2	26	9.1	12	*ML* =5.6(V_a) – 18.7	0.58	<0.01	44	1	1359	12	8.9	14	S_t =2057 – 78.0 (V_a)	0.35	<0.01
	4 year	25	2	47.9	42	10.0	18	*ML* =10.1(V_a) – 56.5	0.83	<0.01	24	1	1454	18	9.4	12	S_t =3177 – 183.0 (V_a)	0.67	<0.01
	5 year	48	3	43.2	31	9.9	12	*ML* =5.8 (V_a) – 14.4	0.27	<0.01	40	3	1425	12	9.8	15	S_t =2112 – 69.9 (V_a)	0.35	<0.01
	CP1	20	1	30.3	28	11.1	19	*ML* =3.2(V_a) – 5.3	0.61	<0.01	10	1	1102	3	10.6	9	S_t =2143 – 98.1 (V_a)	0.66	<0.01
	CP2	20	1	32.4	43	10.8	17	*ML* =6.5 (V_a) – 37.5	0.72	<0.01	---	--	---	---	---	---	---	---	---
	CP3	18	1	43.4	37	11.1	16	*ML* =7.1 (V_a) – 35.6	0.63	<0.01	---	--	---	---	---	---	---	---	---
	CP4	16	1	42.5	43	11.3	17	*ML* =7.3 (V_a) – 40.1	0.59	<0.01	12	1	839	17	11.4	19	S_t =1543 – 61.6 (V_a)	0.90	<0.01
	CP5	20	1	47.0	37	11.1	18	*ML* =6.0 (V_a) – 19.0	0.44	<0.01	---	--	---	---	---	---	---	---	---
	CP6	18	2	52.4	37	11.1	18	*ML* =9.1 (V_a) – 49.2	0.83	<0.01	12	1	757	24	10.9	18	S_t =1490 – 67.3 (V_a)	0.54	0.01
	CP7	16	1	51.7	25	11.5	17	*ML* =3.6 (V_a) – 10.1	0.33	0.03	14	0	872	22	10.9	18	S_t =1657 – 72.3 (V_a)	0.54	<0.01
M15	0 year	57	5	20.3	23	9.3	16	*ML* =2.4 (V_a) – 2.0	0.61	<0.01	45	5	1088	14	9.2	15	S_t =2039 – 103.4 (V_a)	0.82	<0.01
	2 year	57	4	22.9	15	8.1	10	*ML* =1.7 (V_a) + 9.3	0.17	<0.01	40	2	1490	12	7.9	10	S_t =2843 – 171.2 (V_a)	0.55	<0.01
	3 year	56	5	22.2	16	7.5	9	*ML* =2.8 (V_a) + 1.3	0.32	<0.01	40	1	1559	11	7.6	20	S_t =2790 – 162.9 (V_a)	0.50	<0.01
	4 year	26	2	30.5	21	7.8	20	*ML* =2.1 (V_a) + 14.2	0.26	0.01	20	0	1627	14	8.3	17	S_t =2340 – 86.1 (V_a)	0.29	0.01
	5 year	48	2	35.0	29	8.3	22	*ML* =4.3 (V_a) – 0.2	0.58	<0.01	40	2	1681	12	8.0	17	S_t =2650 – 121.4 (V_a)	0.62	<0.01
	CP1	19	1	24.9	19	9.0	17	*ML* =2.0 (V_a) + 6.7	0.44	<0.01	12	1	1335	14	9.3	14	S_t =2595 – 135.7 (V_a)	0.90	<0.01
	CP2	21	1	23.3	23	9.1	17	*ML* =2.5 (V_a) + 0.2	0.56	<0.01	---	--	---	---	---	---	---	---	---
	CP3	18	3	24.6	22	8.7	16	*ML* =3.3 (V_a) – 3.8	0.71	<0.01	---	--	---	---	---	---	---	---	---
	CP4	17	2	30.1	42	9.0	18	*ML* =7.1 (V_a) – 33.8	0.85	<0.01	12	1	1049	9	8.6	11	S_t =1752 – 81.6 (V_a)	0.74	<0.01
	CP5	18	2	33.2	34	8.9	14	*ML* =7.6 (V_a) – 34.1	0.70	<0.01	---	--	---	---	---	---	---	---	---
	CP6	18	1	30.1	26	8.7	15	*ML* =4.0 (V_a) – 5.1	0.49	<0.01	14	1	906	18	8.9	16	S_t =1458 – 61.7 (V_a)	0.29	0.06
	CP7	18	1	34.4	28	9.2	16	*ML* =6.0 (V_a) – 21.2	0.83	<0.01	13	0	1105	12	9.2	15	S_t =1872 – 83.6 (V_a)	0.71	<0.01
M16a	0 year	67	4	28.7	42	11.4	19	*ML* =4.2 (V_a) – 19.6	0.61	<0.01	41	2	1035	17	11.4	18	S_t =1918 – 77.2 (V_a)	0.77	<0.01
	2 year	98	6	31.3	33	10.1	16	*ML* =5.1 (V_a) – 19.8	0.60	<0.01	60	1	1495	10	8.8	12	S_t =2177 – 77.4 (V_a)	0.34	<0.01
	3 year	94	6	30.8	40	9.6	19	*ML* =6.1 (V_a) – 28.2	0.79	<0.01	65	0	1474	11	9.8	17	S_t =1982 – 52.0 (V_a)	0.29	<0.01
	4 year	39	2	37.6	42	9.3	19	*ML* =5.9 (V_a) – 17.0	0.41	<0.01	31	3	1533	12	9.0	17	S_t =2383 – 94.1 (V_a)	0.61	<0.01
	5 year	49	3	46.8	38	10.0	18	*ML* =6.6 (V_a) – 19.1	0.46	<0.01	36	2	1511	8	10.4	19	S_t =1696 – 17.8 (V_a)	0.07	0.12
	CP1	12	1	32.3	18	12.1	10	*ML* =4.3 (V_a) – 19.4	0.72	<0.01	11	1	1140	13	11.9	17	S_t =1939 – 67.0 (V_a)	0.83	<0.01
	CP2	10	1	28.1	33	12.1	12	*ML* =6.0 (V_a) – 44.3	0.81	<0.01	---	--	---	---	---	---	---	---	---
	CP3	13	0	40.9	32	11.8	11	*ML* =5.8 (V_a) – 26.8	0.34	0.04	---	--	---	---	---	---	---	---	---
	CP4	15	0	41.4	29	11.5	13	*ML* =4.6 (V_a) – 11.7	0.35	0.02	10	1	907	12	11.9	11	S_t =970 – 5.3 (V_a)	0.00	0.87
	CP5	11	1	45.3	14	12.2	10	*ML* =3.3 (V_a) + 4.6	0.46	0.03	---	--	---	---	---	---	---	---	---
	CP6	12	1	42.2	31	12.1	9	*ML* =1.2 (V_a) + 27.9	0.01	0.77	8	1	782	13	12.1	10	S_t =1569 – 65.1 (V_a)	0.56	0.05
	CP7	13	2	47.0	43	10.9	20	*ML* =8.4 (V_a) – 44.6	0.83	<0.01	9	0	927	22	11.9	14	S_t =2169 – 104.1 (V_a)	0.75	<0.01

7.2.1 Cantabro Mass Loss Results

Table 7.2 provides results from 105 paired *t*-tests where each matched pair considered specimens: 1) with V_a differences of no more than 0.2%, 2) that were from the same mix, and 3) that only differed by mixture condition or field age. The 95% confidence intervals of change in mass loss (ΔML_{CI}) were determined based on a number of specimen pairs considered (n_{pair}) between specimens of a given CP and age combination. In other words, ΔML_{CI} describes the increase in *ML* of field aged specimens that were not laboratory conditioned (ML_f) to the *ML* of specimens which has been subjected to laboratory conditioning (ML_l). For interpretation, tests with an all negative ΔML_{CI} indicate that the laboratory CP produced more damage than the amount of environmental exposure considered, and an all positive ΔML_{CI} indicates that field aging was more severe. No significant difference is detected when ΔML_{CI} contains both negative and positive values, but a ΔML_{CI} which is more centered on zero with a smaller range indicates stronger agreement. For example, 2 years of field exposure matched closest with CP3 in M14 because ΔML_{CI} was more centered on zero for the comparison of CP3 to 2 years of field aging than when compared to 3 years or 4 years of environmental exposure (although there was no statistical difference between CP3 and 3 years or 4 years of aging).

There is a noteworthy difference in the M15 response to laboratory conditioning when compared to the other two mixes. While CPs using hot water followed by FT produced more damage than oven conditioning for all mixes, Table 7.1 indicates that M15 was more susceptible to oxidation and more resistant to moisture conditioning or FT damage than the other two mixtures. These differences are likely due to differences in V_a (see Table 7.1) and moisture infiltration as M15 has lower V_a and lower moisture infiltration. Based on measurements as per Section 3.6.5, the average moisture infiltration (*Inf*) for mixes M14, M15, and M16a were respectively 1.7, 0.5, and 2.7 centimeters per minute.

Table 7.2. Matching Field Aging to Laboratory Conditioning with Cantabro Results

Summary of CP	M14			M15			M16a		
Relative to Field	n_{pairs}	ΔML_{CI} (%)	Conclusion	n_{pairs}	ΔML_{CI} (%)	Conclusion	n_{pairs}	ΔML_{CI} (%)	Conclusion
	14	-5.0 to 1.7	0 years = CP1[a]	15	-7.2 to -2.9	0 years < CP1	11	-6.2 to -0.4	0 years < CP1[a]
	10	7.0 to 16.4	2 years > CP1	13	-1.5 to 2.9	2 years = CP1[a]	10	5.6 to 14.6	2 years > CP1[a]
CP1 = 0 to 2 years	11	7.9 to 13.4	3 years > CP1	10	-2.7 to 3.9	3 years = CP1	7	8.9 to 20.2	3 years > CP1
	12	9.8 to 30.1	4 years > CP1	12	6.3 to 11.8	4 years > CP1	7	12.1 to 38.5	4 years > CP1
	14	11.9 to 21.8	5 years > CP1	13	12.4 to 18.0	5 years > CP1	10	18.3 to 34.0	5 years > CP1
	19	-4.8 to 4.6	0 years = CP2[a]	20	-5.2 to -1.5	0 years < CP2	9	-0.7 to 5.1	0 years = CP2 [a]
	15	10.6 to 20.1	2 years > CP2	15	-0.2 to 4.9	2 years = CP2 [a]	8	7.7 to 18.4	2 years > CP2
CP2 = 0 to 2 years	11	8.0 to 16.7	3 years > CP2	11	0.3 to 4.5	3 years > CP2	5	3.6 to 30.9	3 years > CP2
	11	10.0 to 29.4	4 years > CP2	10	6.8 to 17.6	4 years > CP2	6	22.8 to 38.7	4 years > CP2
	16	10.6 to 21.0	5 years > CP2	15	13.1 to 19.0	5 years > CP2	8	23.0 to 40.0	5 years > CP2
	17	-15.6 to -2.2	0 years < CP3	14	-7.5 to -3.9	0 years < CP3	13	-13.9 to -4.4	0 years < CP3
	12	-3.3 to 10.3	2 years = CP3[a]	13	-1.8 to 2.6	2 years = CP3[a]	13	-7.2 to 5.7	2 years = CP3
CP3 = 2 to 3 years	10	-1.7 to 11.9	3 years = CP3	11	-1.6 to 4.3	3 years = CP3	9	-6.5 to 7.5	3 years = CP3[a]
	10	-0.9 to 19.4	4 years = CP3	9	1.8 to 13.0	4 years > CP4	8	2.3 to 26.3	4 years > CP3
	13	3.5 to 11.6	5 years > CP3	11	11.1 to 16.8	5 years > CP3	12	7.4 to 28.8	5 years > CP3
	14	-16.1 to -4.6	0 years < CP4	15	-15.9 to -5.1	0 years < CP4	5	-25.8 to 0.0	0 years < CP4
	10	-4.2 to 15.9	2 years = CP4	12	-4.2 to 1.3	2 years = CP4	14	-8.6 to 4.0	2 years = CP4
CP4 = 3 years	7	-4.8 to 10.7	3 years = CP4[a]	9	-2.3 to 3.2	3 years = CP4[a]	11	-7.0 to 7.0	3 years = CP4[a]
	10	1.0 to 28.7	4 years > CP4	9	-3.4 to 14.5	4 years = CP4	11	-1.0 to 22.0	4 years = CP4
	13	0.0 to 20.6	5 years = CP4	9	4.3 to 16.6	5 years > CP4	14	11.5 to 27.9	5 years > CP4
	18	-17.3 to -5.1	0 years < CP5	16	-18.6 to -9.0	0 years < CP5	10	-21.2 to -7.9	0 years < CP5
	12	-6.3 to 6.9	2 years = CP5	14	-9.4 to -2.8	2 years < CP5	9	-5.6 to 5.1	2 years = CP5[a]
CP5 = 2 to 4 years	9	-5.9 to 5.5	3 years = CP5[a]	10	-5.9 to -1.3	3 years < CP5	8	-4.6 to 12.5	3 years = CP5
	13	-4.4 to 12.8	4 years = CP5	9	-0.9 to 8.6	4 years = CP5[a]	6	-8.4 to 27.6	4 years = CP5
	15	-7.7 to 10.5	5 years = CP5	12	-4.0 to 12.5	5 years = CP5	9	12.7 to 31.0	5 years > CP5
	14	-24.8 to 13.3	0 years < CP6	16	-14.9 to -8.2	0 years < CP6	11	-19.6 to -0.5	0 years < CP6
	10	-7.0 to 3.0	2 years = CP6	15	-7.4 to -1.7	2 years < CP6	10	-8.2 to 14.7	2 years = CP6
CP6 = 3 to 5 years	9	-10.1 to 4.5	3 years = CP6	12	-7.9 to 0.7	3 years = CP6	8	-11.5 to 18.5	3 years = CP6[a]
	12	-6.3 to 9.7	4 years = CP6	11	-1.7 to 7.6	4 years = CP6[a]	8	4.1 to 36.6	4 years > CP6
	12	-5.3 to 7.0	5 years = CP6[a]	11	2.6 to 14.1	5 years > CP6	11	3.6 to 27.3	5 years > CP6
	13	-25.0 to -8.0	0 years < CP7	17	-16.9 to -10.6	0 years < CP7	9	-30.5 to -7.6	0 years < CP7
	7	-19 to 4.2	2 years = CP7	12	-9.7 to 3.4	2 years < CP7	10	-14.8 to -4.4	2 years < CP7
CP7 = 4 to 5 years	8	-16.3 to 2.1	3 years = CP7	10	-7.1 to -1.0	3 years < CP7	7	-13.0 to 2.2	3 years = CP7
	10	-11.7 to 12.3	4 years = CP7	7	-2.6 to 10.6	4 years = CP7[a]	7	-9.7 to 10.1	4 years = CP7[a]
	12	-10.6 to 7.5	5 years = CP7[a]	12	-0.7 to 11.2	5 years = CP7	9	-1.1 to 20.1	5 years = CP7

[a] closest match between field age and CP for a given mix; n_{pairs} = number of pairs considered; ΔML_{CI} = Confidence Interval of $ML_f - ML_l$

7.2.2 Superpave Indirect Tensile Results

Table 5.5 provides Fracture Energy (FE) data after field aging and CP4, which was the only conditioning protocol considered in SIDT analysis. CP4 noticeably decreased FE_{-10C} and FE_{+20C} for most cases. CP4 reduced FE_{-10C} to levels lower than that seen after 4 years of aging in five of the six test strips. The sixth strip (i.e. strip 3) detected no differences between any of the field ages or conditioning protocols considered with respect to FE_{-10C}. FE_{+20C} was noticeably decreased after CP4 in all strips considered. With respect to FE_{+20C}, CP4 produced less than 2 years worth of environmental exposure in four of the test strips and as much damage as 2 to 4 years of environmental exposure in the other two strips. These observations indicate that CP4 simulated 1 to 4 years of environmental exposure, which is in general agreement with results from CML testing considering the limited SIDT dataset.

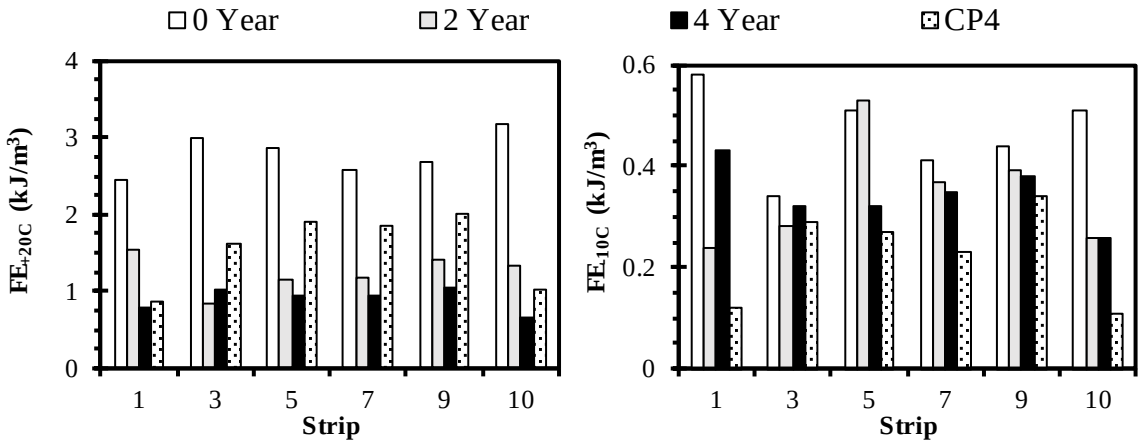

a) 20°C Results *b) -10°C Results*

Figure 7.1. Results of SIDT Testing

7.2.3 Indirect Tensile Results

Figure 7.2 presents normalized S_t for mixtures M14, M15, and M16a after the laboratory conditioning protocols and field aging times considered for IDT testing. Normalized values in Figure 7.2 were determined using the average V_a for all IDT specimens considered by mix and determining the S_t corresponding to those V_a levels using Table 7.1 regressions. For example, 1,005 kPa for S_t of M14 specimens at 0 years was determined using 10.0% V_a and the Table 7.1 regression for S_t.

As shown, S_t increased from the 0 year S_t when considering field ages of 2 to 5 years, and CP1 was the only protocol to produce S_t increases after laboratory conditioning. CP1 produced less than 2 years worth of environmental exposure for M14 and M16a whereas CP1 produced approximately the same S_t as 3 years of environmental exposure for M15. Thus, CP1 simulated between 1 and 3 years of environmental exposure based on S_t results. However, it is concerning that CP4, CP6, and CP7 all reduced S_t with CP7 having the least amount of S_t change of all protocols considered for IDT testing. If IDT testing was suitable to universally consider mixture damage, S_t would have indicated at least a comparable change

after CP7 as the difference imparted by CP1 or CP4. Based solely on S_t, there appears to have been very little to no damage caused by 14 days of exposure to 64°C, which is unrealistic.

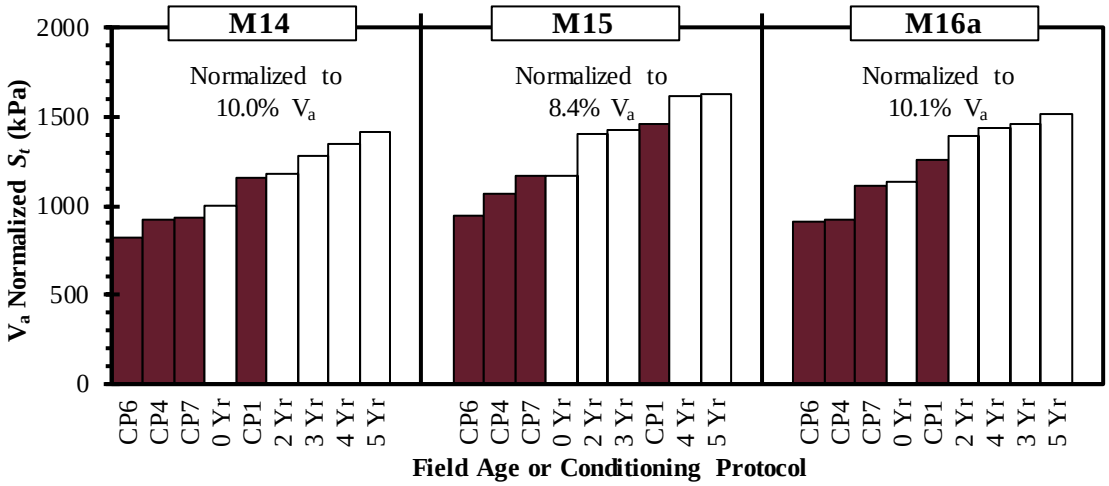

Figure 7.2. Normalized IDT Test Results

7.3 Discussion of Results

The only conditioning protocol evaluated with all three mixture tests (CML, SIDT, and IDT) was CP4. Generally, both CML and SIDT test results collected after CP4 conditioning suggests 1 to 4 years of environmental exposure depending on test method (i.e. increased *ML*, decreased FE_{-10C}, and decreased FE_{+20C}). Alternatively, S_t property changes indicated that CP4 decreased S_t while field aging only increased S_t. Therefore, the remainder of this section considers whether *ML* or S_t is more suitable as a mixture property to compare conditioning protocols to environmental exposure time.

In ideal circumstances, mixture properties used to evaluate changes in mixture integrity should consistently increase or decrease with increased exposure to oxidation, moisture, or freeze-thaw cycles. Air voids should also compound in the same direction as these damage mechanisms. Regressions in Table 7.1 show that *ML* consistently increased with air voids while S_t consistently decreased with increased air voids. Damage from field aging time in years (t_F) was shown in consistently increase both *ML* and S_t as shown in Equations 7.1 and 7.2, which are linear regressions of all non-laboratory conditioned cores used to produce Table 7.1 regressions.

$$ML_{(Tbl\ 7.1)} = 2.75\ (t_F) + 25.4 \qquad p\text{-value} < 0.01 \qquad (7.1)$$

$$S_{t\ (Tbl\ 7.1)} = 102\ (t_F) + 1111 \qquad p\text{-value} < 0.01 \qquad (7.2)$$

The effects of the four laboratory conditioning protocols on *ML* and S_t are demonstrated in Table 7.3 and Figure 7.3. Mixture parameters used to consider damage should always increase or decrease with additional exposure to oxidation, moisture conditioning, or freeze-thaw conditioning (in some cases no change could be acceptable, but indications of property improvement is not).

Eight paired *t*-tests considered the effects of CP1, CP4, CP6, and CP7 on *ML* and S_t (Table 7.3). *ML* *t*-tests combined all Table 7.2 matched pairs for a given conditioning protocol where 0 year cores were considered, and S_t pairs followed the same approach. As an example, 40 Cantabro matched pairs for 0 year to CP1 comparisons were produced (i.e. 14+15+11 from Table 7.2 row 1). As demonstrated in Table 7.3, CP1 and CP4 effects compounded to further increase *ML* when CP7 was conducted, but the effects of CP1 and CP4 conflicted with each other with less damage indicated in CP7 based on S_t results.

Table 7.3. Statistical Inequality of Cantabro Mass Loss and Indirect Tensile Strength

Condition	Description	Cantabro				Indirect Tensile Strength			
		***ML* Effect**	**n_{pairs}**	***p*-value**	**Sig?**	**S_t Effect**	**n_{pairs}**	***p*-value**	**Sig?**
CP1	5 days – 85°C Air (AASHTO R30)	3.4 % ↑	40	<0.01	Yes	168 kPa ↑	27	<0.01	Yes
CP4	14 days – 64°C Water + 1 Freeze-Thaw	10.8% ↑	34	<0.01	Yes	90 kPa ↓	29	<0.01	Yes
CP6	28 days – 64°C Water	13.7% ↑	41	<0.01	Yes	204 kPa ↓	28	<0.01	Yes
CP7	CP1 + CP4	15.9% ↑	39	<0.01	Yes	61 kPa ↓	33	<0.01	Yes

n_{pairs} = number of pairs considered; Sig? = was property effect significant at 95% confidence

The Table 7.3 analysis is presented graphically in Figure 7.3 where mixture test properties of laboratory conditioned cores are plotted on the vertical axis and non-conditioned (i.e. CP0) mixture test properties are plotted on the horizontal axis. The Table 7.3 conclusion is supported by Figure 7.3 equality line slopes. Slopes from Figures 7.3a to 7.3d indicate increased damage based on *ML* results when more severe laboratory conditioning methods were used, and CP7 (i.e. CP1 followed by CP4) indicates the greatest amount of mixture damage. However, IDT test results indicate the least amount of property (i.e. S_t) change based on the equality plot slope in Figure 7.3h when compared to slopes from Figure 7.3e to 7.3h. This suggests that damage mechanisms may counteract one another to indicate less property change or mixture improvement based on S_t. Based on these observations, the collective conditioning protocol assessment in Table 7.4 relies on Cantabro and SIDT assessments with no reliance on IDT assessments.

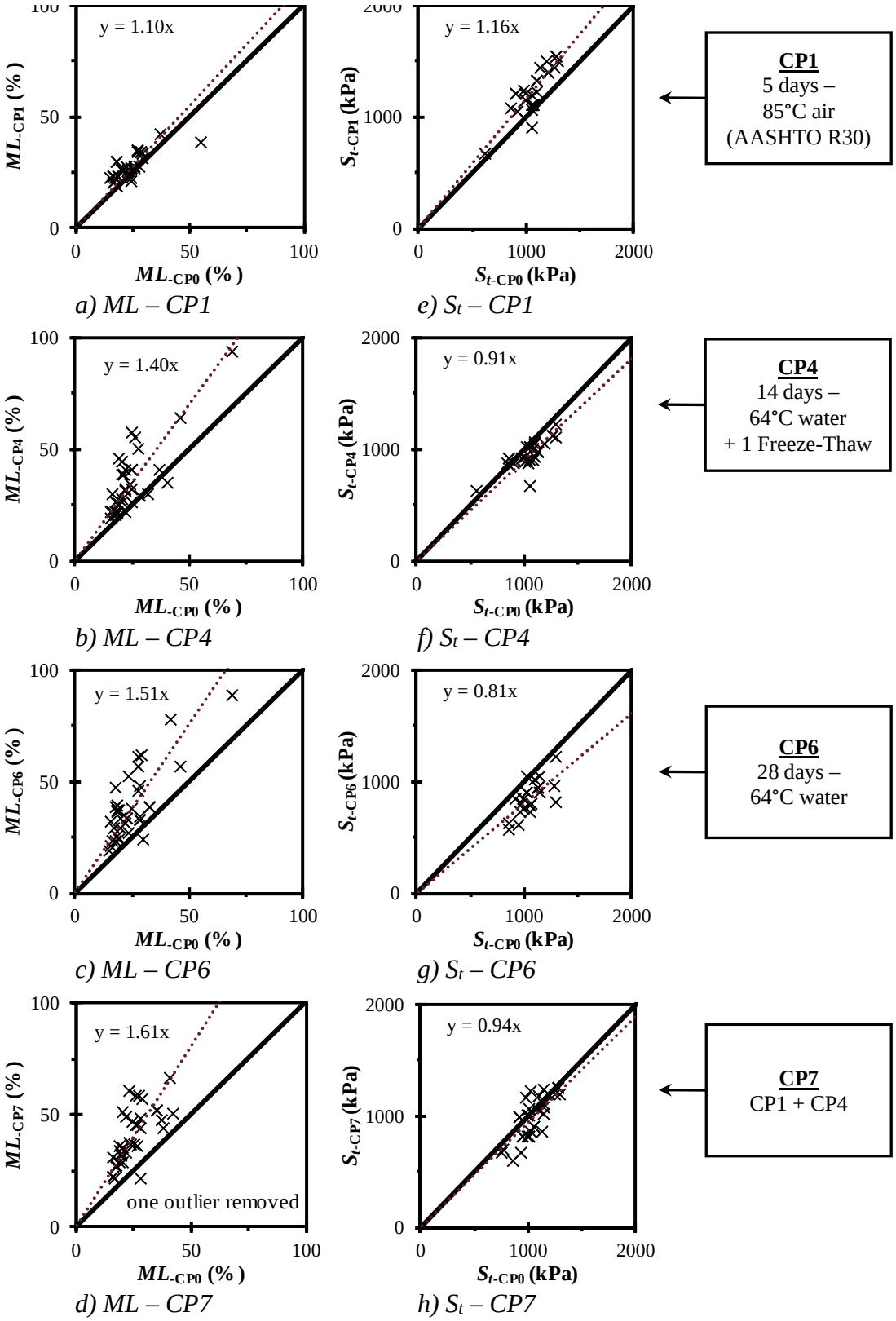

Figure 7.3. Inequality of Cantabro Mass Loss and Indirect Tensile Strength

Table 7.4. Collective Assessment of Conditioning Protocols

Conditioning Protocol	Cantabro Assessment	SIDT Assessment	IDT Assessment	Collective Assessment
CP1	0 to 2 years	---	1 to 3 years	0 to 2 years
CP2	0 to 2 years	---	---	0 to 2 years
CP3	2 to 3 years	---	---	2 to 3 years
CP4	3 years	1 to 4 years	0 years ×	3 years
CP5	2 to 4 years	---	---	2 to 4 years
CP6	3 to 5 years	---	0 years ×	3 to 5 years
CP7	4 to 5 years	---	0 years ×	4 to 5 years

× = Test results indicate behaviors that do not agree with field behaviors.

7.4 Summary of Mix Conditioning

This chapter considered the effects of damage produced in asphalt mixes from laboratory conditioning and matched the resulting damage to damage produced from up to 5 years of non-load associated environmental exposure in the Mississippi climate. Based on the analysis conducted, the Cantabro test consistently indicated increased damage with respect to the three mechanisms considered (i.e. hot air, hot water, and freeze-thaw cycles). Results from non-instrumented indirect tensile testing were shown to produce confounding results in some cases where multiple distress mechanisms had taken place. Thus, the Cantabro test was used to compare mixture conditioning protocols to damage due to non-load associated damage experienced over five years in the north Mississippi climate. Table 7.4 summarizes the overall assessment where laboratory conditioning protocols were matched to environmental effects from field aging.

The guidance in Table 7.4 can be used in a variety of manners. For example, during mixture design, pavements that are in less critical circumstances might be required to meet a given mass loss value for a lesser damaging protocol (e.g. CP1), whereas pavements to be in situations where handling environmental exposure is of more critical importance might be required to meet more stringent protocols (e.g. CP7). Another example might be to pick mixes for a given project that fare better in CP7 than other mixes. This paragraph should be considered examples for MDOT, not recommendations to MDOT. Specific recommendations at the present time are made in Chapter 10.

CHAPTER 8 – BINDER TEST RESULTS

8.1 Overview of Binder Test Results

This study provided a very good opportunity to evaluate binder property changes due to environmental exposure in an asphalt mixture. A dataset where original binders were sampled during paving and evaluated after longer term aging to evaluate binder conditioning levels is rare. This chapter compares binder properties after varying levels of binder conditioning at standard pressure and temperature levels outlined in AASHTO R28 to determine the amount of conditioning time necessary to simulate the binder property changes seen for the Figure 3.1 test section.

8.2. Analysis of Binder Test Results

This section determines the amount of PAV conditioning time (PAVi) necessary to simulate the binder property changes experienced during field aging for the binders used in the Figure 3.1 test section. Figure 8.1 presents relationships between PAVi and the binder properties of interest for the neat PG 67-22 used in M14 and M15 (referred to as B1) and the PG 67-22 modified with 0.5% M1 Evotherm 3G^{TM} (referred to as B2). Trends were predictable ($R^2 > 0.90$ in all cases), and the majority of PAVi relationships were linear. *Pen* (Figure 8.1a) was the only exception with *Pen* following an exponential relationship with PAVi. In many cases PAVi effects were more pronounced in B1 than in B2 (i.e. for $T_c(DSR_{25})$, $T_c(BBR_m)$, and ΔT_c), which indicates that that additive decreased the effects of aging.

Table 8.1 relies on the Figure 8.1 regressions to determine PAVi to produce binder properties similar to those seen during field aging. To account for binder property changes resulting from the inclusion of RAP and other mixture production factors, mixture offsets were determined in the fourth column of Table 8.1 by subtracting the AASHTO T240 conditioned material property for binders B1 or B2 from the average 0 year property measured on FCB samples by mix. For example, the *P*en mixture offset of -11 dmm for M14 was determined by averaging the FCB values with no longer term aging (23, 27, 29, and 25 dmm from Tables 5.8 and 5.9) and subtracting the T240 conditioned ARB *Pen* for B1 (37 dmm from Table 5.10). This same process was completed for all mixture offsets in Table 8.1, and mixture offsets were added to the end of Figure 8.1 regressions to uniformly shift them to consider the effects of B1 and B2 being incorporated in mixes M14, M15, and M16. As an example, the -11 dmm offset for M14 *Pen* was added to $Pen = 30.9e^{-0.016(PAVi)}$ to produce $Pen = 30.9e^{-0.016(PAVi)} - 11$ and subsequently solved for PAVi (see Table 8.1 column 5). Table 8.1 column 5 regressions were then used in conjunction with FCB properties measured in Tables 5.6, 5.8, and 5.9 to determine PAVi needed to experience the same amount of property change as field aging or CP4 (the only mixture conditioning protocol considered for binder properties). This approach produced negative PAVi in some cases, and negative PAVi values were replaced with zeros based on the understanding that field aging and the CP4 conditioning protocol do not improve binder properties.

Had the test section considered in this report been constructed with the intention of considering PAV effects as opposed to being used in an emergency paving demonstration, large quantities of all raw materials would have been obtained and a comprehensive mixture offset would have been determined. Since this was impossible with the test section used for this report,

the approximate (but believed reasonable by the authors) difference between T240 conditioned ARB and 0 year FCB sample properties was used.

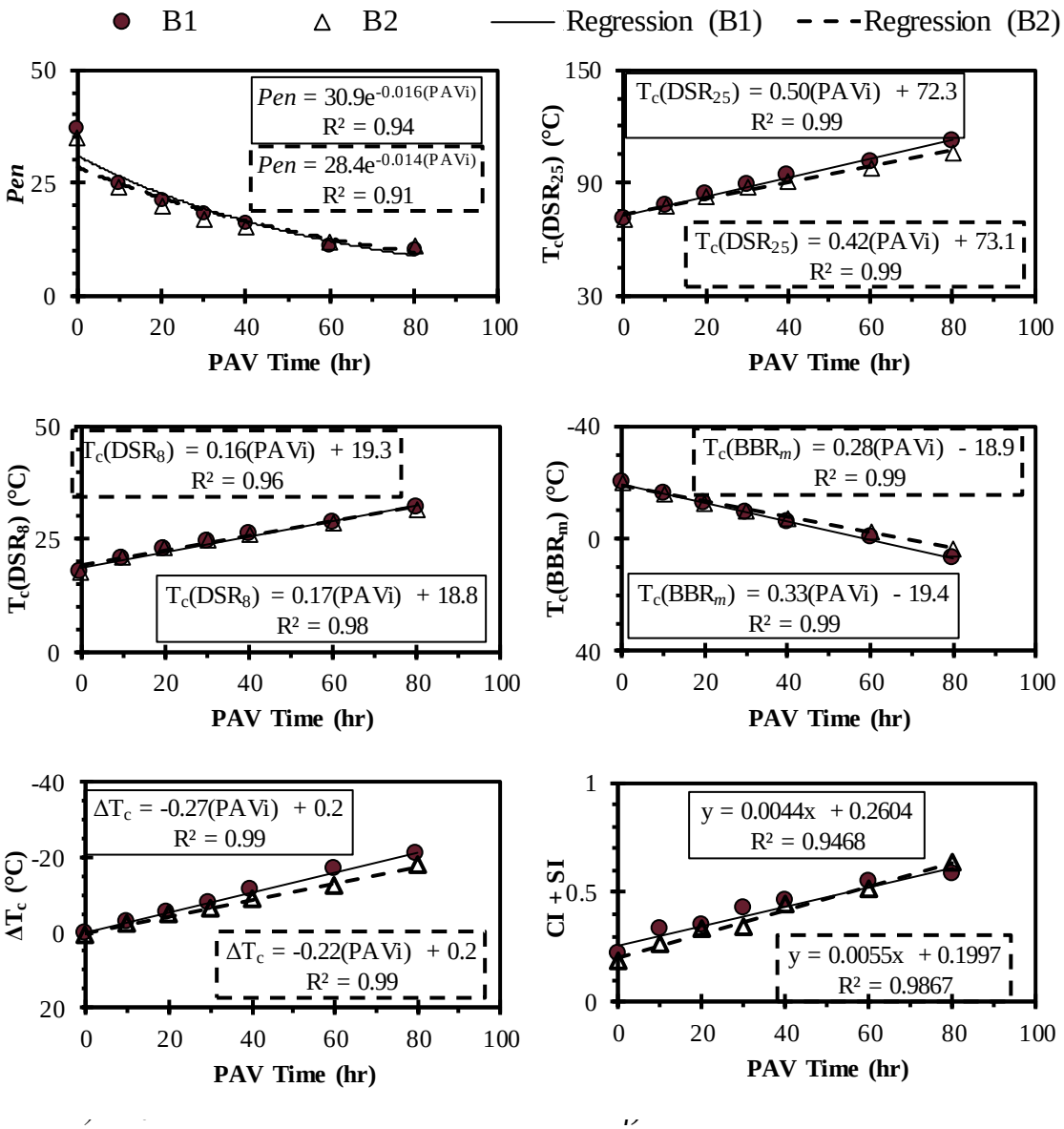

Figure 8.1. Pressure Aging Vessel Time Behaviors for As-Received Binder

.

Table 8.1. PAV Times (PAVi) in hours to Simulate Binder Changes in Mixtures

Binder Property	Mix	Figure 8.1 Regression	Mixture Offset	Regression Plus Offset Solved for PAVi (Modified Fig. 8.1 Regression)	Test Strip	2 Year PAVi		4 Year PAVi		CP4 PAVi	
						FCB_0	FCB_5	FCB_0	FCB_5	FCB_0	FCB_5
Pen (dmm)	M14	$Pen = 30.9e^{-0.016(PAVi)}$	-11	$PAVi = \ln[(Pen+11)/30.9](-1/0.016)$	1	11	0	24	6	0	0
					3	8	0	24	2	0	0
	M15	$Pen = 30.9e^{-0.016(PAVi)}$	+2	$PAVi = \ln[(Pen-2)/30.9](-1/0.016)$	5	18	0	77	41	21	30
					7	45	6	77	49	27	30
	M16	$Pen = 28.4e^{-0.014(PAVi)}$	-1	$PAVi = \ln[(Pen+1)/28.4](-1/0.014)$	9	37	6	68	15	22	12
					10	41	15	68	22	29	22
$T_c(DSR_{25})$ (°C)	M14	$T_c(DSR_{25}) = 0.50(PAVi)+72.3$	+8.3	$PAVi = (T_c(DSR_{25})-80.6)(1/0.50)$	1	14	0	27	8	0	0
					3	19	5	32	6	3	4
	M15	$T_c(DSR_{25}) = 0.50(PAVi)+72.3$	+2.9	$PAVi = (T_c(DSR_{25})-75.2)(1/0.50)$	5	13	0	35	15	7	6
					7	24	2	40	21	11	10
	M16	$T_c(DSR_{25}) = 0.42(PAVi)+73.1$	+3.9	$PAVi = (T_c(DSR_{25})-77.0)(1/0.42)$	9	21	0	40	4	5	1
					10	28	10	45	10	10	6
$T_c(DSR_8)$ (°C)	M14	$T_c(DSR_8) = 0.17(PAVi)+18.8$	+1.8	$PAVi = (T_c(DSR_8)-20.6)(1/0.17)$	1	28	0	44	16	0	0
					3	28	15	45	6	0	2
	M15	$T_c(DSR_8) = 0.17(PAVi)+18.8$	-1.1	$PAVi = (T_c(DSR_8)-17.7)(1/0.17)$	5	14	0	63	32	12	12
					7	36	1	70	36	16	21
	M16	$T_c(DSR_8) = 0.16(PAVi)+19.3$	-0.8	$PAVi = (T_c(DSR_8)-18.5)(1/0.16)$	9	33	0	69	11	15	10
					10	48	33	77	21	21	13
$T_c(BBR_m)$ (°C)	M14	$T_c(BBR_m) = 0.33(PAVi)–19.4$	+0.2	$PAVi = (T_c(BBR_m)+19.2)(1/0.33)$	1	15	0	29	14	2	0
					3	14	6	34	5	2	4
	M15	$T_c(BBR_m) = 0.33(PAVi)–19.4$	-4.0	$PAVi = (T_c(BBR_m)+23.4)(1/0.33)$	5	15	0	42	23	13	14
					7	27	5	48	30	16	17
	M16	$T_c(BBR_m) = 0.28(PAVi)–18.9$	-1.8	$PAVi = (T_c(BBR_m)+20.7)(1/0.28)$	9	21	0	46	5	11	6
					10	28	15	52	9	13	8
ΔT_c (°C)	M14	$\Delta T_c = -0.27(PAVi)+0.2$	-2.9	$PAVi = (\Delta T_c+2.7)(-1/0.27)$	1	10	0	17	8	3	0
					3	9	3	18	3	3	1
	M15	$\Delta T_c = -0.27(PAVi)+0.2$	-2.2	$PAVi = (\Delta T_c+2.0)(-1/0.27)$	5	11	0	19	3	4	3
					7	12	0	24	15	6	3
	M16	$\Delta T_c = -0.22(PAVi)+0.2$	-2.7	$PAVi = (\Delta T_c+2.5)(-1/0.22)$	9	12	0	23	0	5	0
					10	15	2	25	0	2	2
CI+SI	M14	(CI+SI) =0.004(PAVi)+0.26	+0.33	$PAVi = ((CI+SI)-0.59)(1/0.004)$	1	0	0	52	25	2	2
					3	25	---	42	5	7	0
	M15	(CI+SI) =0.004(PAVi)+0.26	+0.37	$PAVi = ((CI+SI)-0.63)(1/0.004)$	5	12	0	62	0	2	2
					7	35	0	100	30	15	5
	M16	(CI+SI) =0.006(PAVi)+0.20	+0.40	$PAVi = ((CI+SI)-0.61)(1/0.006)$	9	10	0	15	0	0	5
					10	14	0	39	0	2	0

8.3 Discussion of Binder Test Results

Table 8.2 provides a summary of the Table 8.1 analysis where the range and averages of PAVi necessary to simulate 2 years or 4 years of binder aging are provided. As shown, the average PAVi to re-create property changes seen after 2 or 4 years of field aging was 21 hours and 45 hours respectively when considering FCB_0 binders collected from the pavement surface. The PAVi to re-create 2 or 4 years of aging when considering binders collected from 5.0 to 6.3 cm below the pavement surface was 3 hours and 14 hours.

Table 8.2. Summary of PAV Times (PAVi) in hours to Simulate Field Aging

Binder Property	2 Year PAVi				4 Year PAVi			
	FCB_0		FCB_5		FCB_0		FCB_5	
	Range	Average	Range	Average	Range	Average	Range	Average
Pen	8 to 45	27	0 to 15	5	24 to 77	56	2 to 49	23
$T_c(DSR_{25})$	13 to 28	20	0 to 10	3	27 to 45	37	4 to 21	11
$T_c(DSR_8)$	14 to 48	31	0 to 33	8	44 to 77	61	6 to 36	20
$T_c(BBR_m)$	14 to 28	20	0 to 15	4	29 to 52	42	5 to 30	14
ΔT_c	9 to 15	12	0 to 3	1	17 to 25	21	0 to 15	5
CI+SI	0 to 35	16	0 to 0	0	15 to 100	52	0 to 30	10
Collective	*0 to 48*	*21*	*0 to 33*	*3*	*15 to 100*	*45*	*0 to 49*	*14*

Figure 8.2 uses the average PAVi values presented in Table 8.2 and compares the PAVi in hours needed between FCB_0 and FCB_5 binders. Based on the slopes of linear regressions that were forced through the origin, one year of aging was best simulated by 3.1 PAVi hours at depth (i.e. 5 cm below the pavement surface) and by 11.1 PAVi hours at the pavement surface. Considering the 20 hour conditioning time provided in AASHTO R28-12, 20 hours of PAVi in the FCB_5 regression would simulate around 6.5 years of field aging. This is within the 5 to 10 year range suggested in AASHTO R28-12. Thus, the PAVi rate at depth seems to be in reasonable agreement with simulating 5 to 10 years of binder aging.

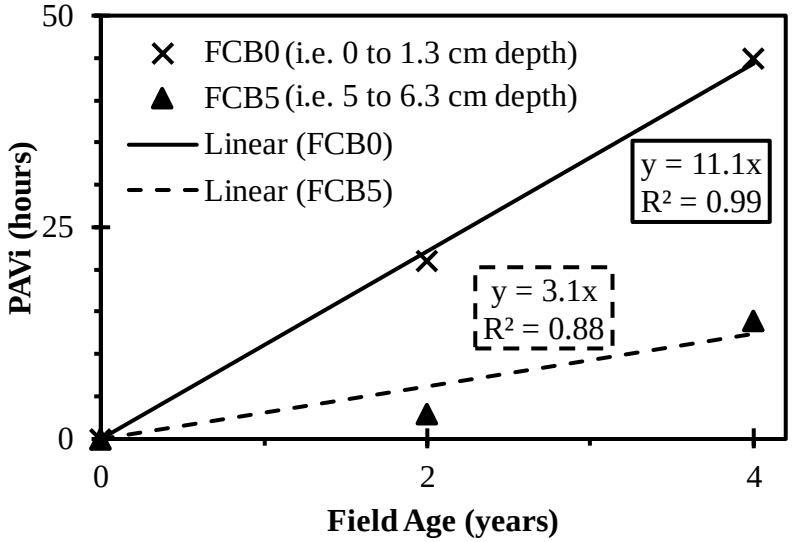

FIGURE 8.2. Relationships Between Field Age and PAVi with Depth.

8.4 Summary of Binder Test Results

Based on the analysis and discussion presented in this chapter, 2 and 4 years of field aging were best replicated by 21 hours and 45 hours of PAV conditioning for binders collected from the top 1.3 cm of the pavement surface. The same field aging times were best simulated by 3 hours and 14 hours of PAV conditioning for binders collected from 5.0 to 6.3 cm below the pavement surface for the same pavement. These rates correspond to PAV conditioning times of 11 hours per year of field aging and 3 hours per year of field aging for binder materials placed at pavement surfaces and 5 cm below pavement surfaces, respectively.

CHAPTER 9 – MIXTURE AGING RESULTS FOR YEAR SIX

9.1 Overview of Year Six Field Aging Results

Scheduling and overall progress of this work made it possible to collect 165 cores after six years of field aging when the original plan was to cease monitoring of the test section after five years. Of these 165 cores, 36 were stored for potential testing of binder properties outside the scope of this report, 24 were tested for HLWT properties (Section 9.2), and 105 were tested via CML (Section 9.3). This data was kept separate from the primary experiments in Chapters 5 to 8 since there is a possibility that this data might be used in conjunction with additional monitoring beyond six years.

9.2 Year Six Hamburg Test Results

Figure 9.1 plots HLWT year 6 results versus those obtained at year 5. The cores tested at year 6 were often at higher air void levels than those at year 5. In retrospect, more closely aligning air voids between years 5 and 6 would have provided more clarity in HLWT results. Figure 9.1 provides modest evidence that HLWT resistance may have decreased between years 5 and 6, which is interesting considering the consistency over time shown in Table 5.1 over the first five years. Figure 9.1 indicated there could be some value in monitoring the Figure 3.1 test section for additional time to determine if any non-linearity in properties with time can be observed.

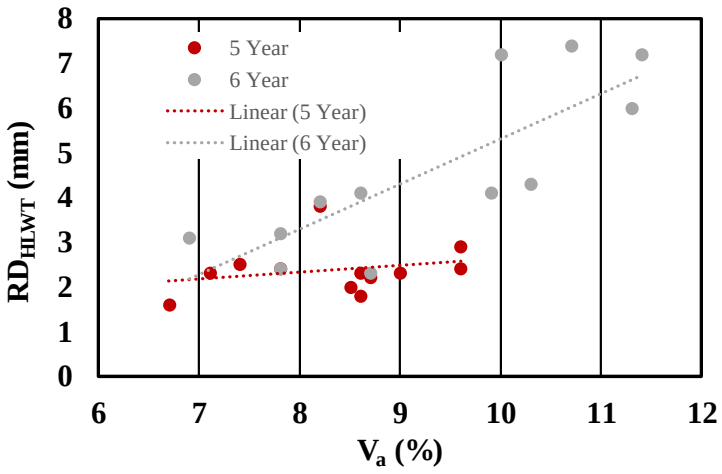

Figure 9.1. Years Five and Six HLWT Test Results

9.3 Year Six Cantabro Test Results

Table 9.1 is an excerpt of Table 7.1 where CML data from 0 to 5 years is provided alongside the newly added year 6 data. As in Chapter 7, Table 9.1 provides summary statistics (i.e. average (Avg) and coefficient of variation (COV)) and regressions between *ML* and V_a after outlier removal. Coefficients of determination (R^2) and probabilities of non-significance (*p*-value) are provided for each regression. The total number of data points

considered (n) and the number of outliers removed (n_o) are also provided. The remainder of this chapter only considers results which were not identified as outliers in the Table 9.1 outlier removal process.

Table 9.1. Cantabro Test Results For Six Years After Outlier Removal

Mix	Age or CP	*ML* n	n_o	Avg (%)	COV (%)	V_a Avg (%)	V_a COV (%)	Regression	R^2	*p*-value
M14	0 year	69	6	31.5	46	10.9	16	*ML* =6.5(V_a) – 39.7	0.65	<0.01
	2 year	55	6	34.7	33	9.2	13	*ML* =7.3(V_a) – 32.6	0.63	<0.01
	3 year	59	4	32.2	26	9.1	12	*ML* =5.6(V_a) – 18.7	0.58	<0.01
	4 year	25	2	47.9	42	10.0	18	*ML* =10.1(V_a) – 56.5	0.83	<0.01
	5 year	48	3	43.2	31	9.9	12	*ML* =5.8 (V_a) – 14.4	0.27	<0.01
	6 year	30	2	60.3	29	9.1	12	*ML* =12.3(V_a) – 52.1	0.59	<0.01
M15	0 year	57	5	20.3	23	9.3	16	*ML* =2.4 (V_a) – 2.0	0.61	<0.01
	2 year	57	4	22.9	15	8.1	10	*ML* =1.7 (V_a) + 9.3	0.17	<0.01
	3 year	56	5	22.2	16	7.5	9	*ML* =2.8 (V_a) + 1.3	0.32	<0.01
	4 year	26	2	30.5	21	7.8	20	*ML* =2.1 (V_a) + 14.2	0.26	0.01
	5 year	48	2	35.0	29	8.3	22	*ML* =4.3 (V_a) – 0.2	0.58	<0.01
	6 year	30	1	37.4	18	8.1	11	*ML* =4.5 (V_a) +1.04	0.29	<0.01
M16a	0 year	67	4	28.7	42	11.4	19	*ML* =4.2 (V_a) – 19.6	0.61	<0.01
	2 year	98	6	31.3	33	10.1	16	*ML* =5.1 (V_a) – 19.8	0.60	<0.01
	3 year	94	6	30.8	40	9.6	19	*ML* =6.1 (V_a) – 28.2	0.79	<0.01
	4 year	39	2	37.6	42	9.3	19	*ML* =5.9 (V_a) – 17.0	0.41	<0.01
	5 year	49	3	46.8	38	10.0	18	*ML* =6.6 (V_a) – 19.1	0.46	<0.01
	6 year	45	1	61.9	35	9.9	13	*ML* =9.4 (V_a) – 31.1	0.30	<0.01

Figure 9.1 plots *ML* versus field age for all non-outlier data points from mixes M14, M15, and M16a. Figure 9.1 has scatter, and a considerable amount of this scatter can be attributed to this plot neglecting effects of varying mixes or air voids. Figure 9.1 is intended to be an overall view of the data, where future efforts can refine the trends. Figure 9.1, however, is very useful in showing that the slope of the *ML* to years in the field (t_F) increased from 2.75 (equation 7.1 where 5 years of data were included) to 3.87, which is a very noticeable increase by adding only one year of data. Figure 9.1 suggests that *ML* increased more rapidly between year 5 and year 6.

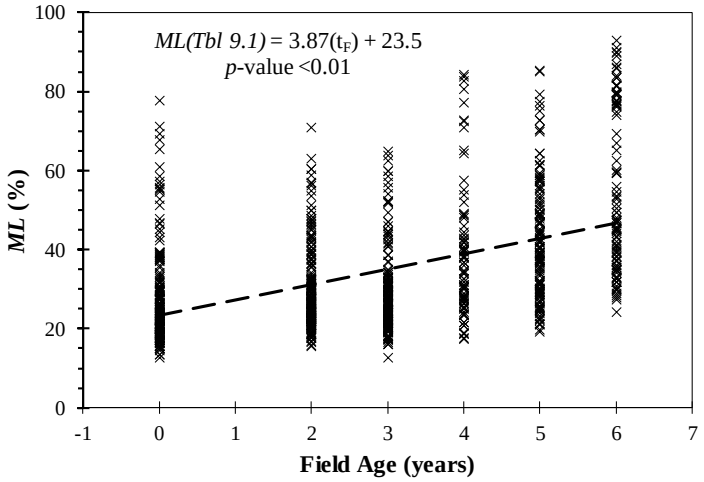

Figure 9.2. Cantabro Mass Loss Versus Time for Six Year Period

Table 9.2 provides results from 21 paired *t*-tests that were conducted in an identical manner to the matched pair *t*-tests presented in Table 7.2. The *ML* of specimens collected after 6 years of field aging was consistently greater than all conditioning protocols considered. Table 9.2 aligns with all mixture collected after six years of field aging that suggests there is value in continuing to monitor this test section to determine if the rate of damage from environmental effects continues to progress as suggested from years 5 to 6, or if damage levels over time trend back toward those observed through five years of aging.

Table 9.2. Comparing 6 Year Cantabro Results to Laboratory Conditioned Results

M14			**M15**			**M16a**		
n_{pairs}	ΔML_{CI} (%)	**Conclusion**	n_{pairs}	ΔML_{CI} (%)	**Conclusion**	n_{pairs}	ΔML_{CI} (%)	**Conclusion**
7	33.5 to 55.7	6Year > CP1	12	9.2 to 17	6Year > CP1	6	27.6 to 61.5	6Year > CP1
11	34.4 to 51.3	6Year > CP2	12	11.9 to 18.8	6Year > CP2	5	24.3 to 70.1	6Year > CP2
8	27.9 to 45.1	6Year > CP3	11	11.2 to 17.5	6Year > CP3	7	34.5 to 52.5	6Year > CP3
7	32.7 to 50.7	6Year > CP4	11	10.5 to 17.7	6Year > CP4	10	23.3 to 50.1	6Year > CP4
9	18.4 to 32.6	6Year > CP5	11	6.3 to 10.9	6Year > CP5	6	28.1 to 47.4	6Year > CP5
6	15.0 to 47.6	6Year > CP6	12	6.8 to 11.2	6Year > CP6	7	11.8 to 63.6	6Year > CP6
7	13.6 to 40.8	6Year > CP7	12	4.7 to 11.0	6Year > CP7	9	10.3 to 35.8	6Year > CP7

CHAPTER 10 - SUMMARY, CONCLUSIONS, AND RECOMMENDATIONS

10.1 Summary

This report focused on characterization of the Columbus, MS test section described in Chapter 3 with emphasis on mechanisms known to relate to non-load associated damage due to environmental exposure. The main objective of this report was to characterize the effects of short and longer term aging on this test section. This objective was met through an investigation using predominately field cores with characterization of binder aging to a lesser extent.

Chapter 4 presented an investigation where the density effects of moisture remaining in field cores after field aging were characterized, and the resulting observations were considered in the treatment of all field aged cores considered in Chapters 5 to 9. Chapter 5 contains the results of all non-density related material tests conducted in this report through five years of aging, and results from Chapter 5 are used as needed in Chapters 6 to 8. Chapter 6 presents an analysis of the effects of haul time on mixture and binder properties. Chapter 7 considers a combination of seven conditioning protocols and matches the effects of laboratory conditioning to the effects of environmental exposure on mixture properties. Chapter 8 presents a binder conditioning investigation where the exact binders used in test section construction were sampled the day of paving and subjected to varying levels of pressure aging vessel conditioning before matching the effects of laboratory conditioning to the effects of environmental exposure on asphalt binder properties. Chapter 9 explored mixture properties after six years of aging.

A comprehensive assessment of mixture conditioning protocols to simulate environmental exposure in Mississippi had not been conducted prior to this effort. The contents of this report demonstrate a series of approaches to consider paving material property changes over time in Mississippi, and the next two sections provide conclusions and recommendations from these efforts.

10.2 Conclusions

Multiple technical points documented throughout this report could be considered as conclusions, but many have been omitted from this chapter to provide more emphasis for primary points of the study. The overall conclusion of this study is that the Cantabro Mass Loss test can be used in conjunction with mixture conditioning protocols to evaluate the resistance of various paving mixtures to non-load associated environmental effects in the Mississippi climate. Emphasis was also placed on binder conditioning protocols by way of the Pressure Aging Vessel (PAV) for comparison to binder properties.

Because the effects of extended haul times up to 8.4 hours had secondary effects when compared to density or longer-term field aging, all strips of like mixture with haul times of 8.4 hours or less were considered equal for mixture conditioning. Mixture conditioning protocols consisting of hot air, hot water, and freeze-thaw cycles produced damage levels which were comparable to less than 2 years of field aging (i.e. 5 days in 85°C air) up to damage levels comparable to 5 years of environmental exposure (i.e. 5 days in

85°C air followed by 14 days in 64°C water and one freeze-thaw cycle) based on comparisons to field aged test results using the Cantabro Mass Loss test.

Binder conditioning efforts identified multiple factors which could impact decisions relative to binder conditioning protocols used for performance graded binders in Mississippi pavements. First, the effects of pavement depth were substantial with binders aged within the top 1.3 cm of the test section experiencing property changes at roughly three times the rate of property change for binder sampled from 5.0 to 6.3 cm below the pavement surface. Secondly, the 20 hour PAV protocol described in AASHTO R28-12 seemed on track to simulate 2 years of binder property changes at the surface or 6.5 years of binder property changes at depth. The binder property changes experienced at depth were on track to be within the 5 to 10 years of pavement life suggested in AASHTO R28-12.

10.3 Recommendations

This report led to four recommendations, which align with the overall body of work in Volumes 1 to 3 of this report series.

1. MDOT should only rely on ASTM D7227 to remove moisture induced during short exposure periods such as sawing or density measurement, and should not rely (without verification) on this method to remove moisture induced during field aging over time. Chapter 4 provides recommended guidance for obtaining proper densities of cores taken after years of environmental exposure.
2. MDOT should consider the guidance in Table 7.4 for how to condition and test laboratory specimens to estimate field aging time in Mississippi. Cantabro testing is recommended for primary assessment, with Fracture Energy used as secondary information. Indirect tensile testing is not recommended for use in this capacity. The default recommendation is to use CP7 for conditioning with CML testing.
3. MDOT should consider the data presented in Chapter 8 (Table 8.2 and Figure 8.2 in particular) when considering any changes to binder conditioning methods used for acceptance tests. RTFO and PAV conditioning are topics of national attention at the present time, and Chapter 8 should be used by MDOT for guidance when deciding matters related to binder grading.

CHAPTER 11 – REFERENCES

Alam, M.M., Tandon, V., Nazarian, S., Tahmoressi, M. (1998). "Identification of Moisture Susceptible Asphalt Concrete Using Modified Environmental Conditioning System," *Transportation Research Record: Journal of the Transportation Research Board*, 1630, pp. 106-116.

Allen, W.L., Terrel, R.L. (1994*). Field Validation of the Environmental Conditioning System*. Report SHRP-A-396, Strategic Highway Research Program, Washington, D.C.

Al-Omari, A., Tashman, E., Masad, E., Cooley, A., Harman, T. (2002). "Proposed Methodology for Predicting HMA Permeability," *Journal of the Association of Asphalt Paving Technologists*, 71, pp. 30-58.

Anderson, M., King, G., Hanson, D., and Blankenship, P. (2011). "Evaluation of the Relationship Between Asphalt Binder Properties and Non-Load Related Cracking," *Journal of the Association of Asphalt Paving Technologists,* 80, pp. 615-661.

Aschenbrener, T. (1995). "Evaluation of Hamburg Wheel-Tracking Device to Predict Moisture Damage in Hot Mix Asphalt," *Transportation Research Record: Journal of the Transportation Research Board*, 1492, pp. 193-201.

Azari, H. (2010). *Precision Estimates of AASHTO T283: Resistance of Compacted Hot Mix Asphalt to Moisture-Induced Damage*, NCHRP Web-Only Document 166, National Cooperative Highway Research Program, Washington, D.C.

Bae, A., Mohammad, L.N., Cooper, S.B., King, W. (2012). "Evaluation of Various Test Devices for the Measurement of Aggregates and Asphalt Mixtures' Specific Gravity," *Journal of Testing and Evaluation*, 40(1), pp. 1-8.

Bahia, H.U., Anderson, D.A. (1995). "The Pressure Aging Vessel (PAV): A Test to Simulate Rheological Changes Due to Field Aging," *Physical Properties of Asphalt Cement Binders*, ASTM STP 1241, Philadelphia, pp. 67-88.

Bateman, J.H., Lehmann, H.L. (1929). "The Effect of the Mixing Temperature on the Physical Properties of an Oil Asphalt in a Sheet Asphalt Mixture," *Proceedings Part II*, American Society for Testing Materials, pp. 943-953.

Beitchman, B.C. (1959). "Infrared Spectra of Asphalts," *Journal of Research of the National Bureau of Standards*, 63A (2), pp. 189-193.

Bell, C.A., AbWahab, Y., Cristi, M.E., Sosnovske, D., (1994a). *Selection of Laboratory Aging Procedures for Asphalt-Aggregate Mixtures,* Report SHRP-A-383, Strategic Highway Research Program, Washington, D.C.

Bell, C.A., Weider, A.J., Fellin, M.J. (1994b). *Laboratory Aging of Asphalt-Aggregate Mixtures: Field Validation*, Report SHRP-A-390, Strategic Highway Research Program, Washington, D.C.

Bell, C.A., Sosnovske, D. (1994). *Aging: Binder Validation*, Report SHRP-A-384, Strategic Highway Research Program, Washington, D.C.

Bennert, T. (2016). "Discussion of: Moving Forward from performance-Based Design to True Balanced Mixture Design in New Jersey," *Journal of the Association of Asphalt Paving Technologists*, 85, pp. 853-856.

Benson, P.E. (1976). *Low Temperature Transverse Cracking of Asphalt Concrete Pavements in Central and West Texas*, Report 175-2F, Cooperative Research Project, Texas Transportation Institute and State Department of Highways and Public Transportation.

Brown, E.R. (1990). "Density of Asphalt Concrete—How Much is Needed?," *Transportation Research Record: Journal of the Transportation Research Board*, 1282, pp. 27-32.

Buchanan, M.S. (2000). "An Evaluation of Selected Methods for Measuring the Bulk Specific Gravity of Compacted Hot Mix Asphalt (HMA) Mixes," *Journal of the Association of Asphalt Paving Technologists*, 69, pp. 608-634.

Buchanan, M.S. (2016). "Optimized Mix Design Approach: Contractor's Perspective," *Journal of the Association of Asphalt Paving Technologists*, 85, pp. 819-838.

Buttlar, W.G., Roque, R., Kim, N. (1996). "Accurate Asphalt Mixture Tensile Strength," *Proceedings of the 4th Materials Engineering Conference: Materials for a New Millennium*, Washington, D.C., pp. 163-172.

Cook, R. D. (1977). "Detection of Influential Observation in Linear Regression." *Technometrics,* Vol. 19 (1), pp. 15-18.

Cooley Jr., L.A., Kandhal, P.S., Buchanan, M.S., Fee, F., Epps, A. (2000). *Loaded Wheel Testers in the United States: State of the Practice*, Transportation Research E-Circular Number E-C016, Transportation Research Board, Washington, D.C.

Coons, R.F. and Wright, P.H. (1967). "An Investigation of the Hardening of Asphalt Recovered from Pavements of Various Ages." *Journal of the Association of Asphalt Paving Technologists*, Atlanta, GA, Vol. 37, 510-528.

Copas, T.L., Pennock, H.A. (1979). *Relationship of Asphalt Cement Properties to Pavement Durability*, NCHRP Synthesis 59, National Cooperative Highway Research Program, Washington, D.C.

Cox, B.C., Howard, I.L. (2015a). *Cold In-Place Recycling Characterization and Framework and Design Guidance for Single or Multiple Component Binder Systems*, Report No. FHWA/MS-DOT-RD-15-250-Volume 2, Mississippi Department of Transportation, Jackson, MS., pp. 184.

Cox, B.C., Howard, I.L., Ivy, J. (2015b). *Evaluation of Approaches to Improve Longitudinal Joints in Mississippi Overlay Projects*, Report No. FHWA/MS-DOT-RD-15-250-Volume 3, Mississippi Department of Transportation, Jackson, MS., pp. 159.

Cox, B.C., Smith, B.T., Howard, I.L., James, R.S. (2017). "State of Knowledge for Cantabro Testing of Dense Graded Asphalt," *Journals of Materials in Civil Engineering*, 29(10), 04017174, DOI: 10.1061/(ASCE)MT.1943-5533.0002020.

Crouch, L.K., Copeland, A.R., Walker, C.T., Maxwell, R.A., Duncan, G.M., Goodwin, W.A., Badoe, D.A., Leimer, H.W. (2002). "Determining Air Void Content of Compacted Hot-Mix Asphalt Mixtures," *Transportation Research Record: Journal of the Transportation Research Board*, 1813, pp. 39-46.

Epps, J.A., Hand, A., Seeds, S., Schulz, T., Alavi, S., Ashmore, C., Monismith, C.L., Deacon, J.A., Harvey, J.T., Leahy, R. (2002). *Recommended Performance-Related Specification for Hot-Mix Asphalt Construction: Results of the Westrack Project*, Report NCHRP 455, National Cooperative Highway Research Program, Washington, D.C.

Epps, J.A., Monismith, C.L. (1969). "Influence of Mixture Variables on the Flexural Fatigue Properties of Asphalt Concrete," *Journal of the Association of Asphalt Paving Technologists*, 38, pp. 423-464.

Epps-Marin, A., Arambula, E., Yin, F., Cucalon, L.G., Chowdhury, A., Lytton, R., Epps, J., Estakhri, C., Park, E.S. (2014). *Evaluation of the Moisture Susceptibility of WMA Technologies*, Report NCHRP 763, National Cooperative Highway Research Program, Washington, D.C.

Finn, F.N. (1967). *Factors Involved in the Design of Asphalt Pavement Surfaces*, Report NCHRP 39, National Cooperative Highway Research Program, Washington, D.C.

Glaser, R.R., Loveridge, J.L. (2012). "Low Temperature Kinetics of Asphalt Binders," *American Chemical Society Division of Petroleum Chemistry*, 57(1).

Glover, C.J., Davison, R.R., Domke, C.H., Ruan, Y., Juristyarini, P., Knorr, D.B., Jung, S.H. (2005). *Development of a New Method for Assessing Asphalt Binder Durability with Field Validation*, Report No. FHWA/TX-05/1872-2, Texas Department of Transportation, Austin, TX.

Griffin, R.L, Miles, T.K., Penther, C.J., Simpson, W.C. (1957). "Sliding Plate Microviscometer for Rapid Measurement of Asphalt Viscosity in Absolute Units," *ASTM Special Publication No. 212*, pp. 36-48.

Heithaus, J.J., Johnson, R.W. (1958). "A Microviscometer Study of Road Asphalt Hardening in the Field and Laboratory," *Journal of the Association of Asphalt Paving Technologists*, 27, pp. 17-34.

Hekmatfare, A., Shah, A., Huber, G., McDaniel, R., Haddock, J.E. (2015). "Modifying Laboratory Mixture Design to Improve Field Compaction," *Road Materials and Pavement Design*, 16(2), pp. 149-167.

Highway Research Board. (1953). *The WASHO Road Test Part 1: Design, Construction, and Testing Procedures,* HRB Special Report 18, Publication National Academy of Sciences – National Research Council, Washington, D.C.

Highway Research Board. (1962). *The AASHTO Road Test Report 2 Materials and Construction,* HRB Special Report 61B, Publication National Academy of Sciences – National Research Council, Washington, D.C.

Howard, I.L., Payne, B.A., Bouge, M., Glusenkamp, S., Baumgardner, G.L., Hemsley, J.M. (2012). *Full Scale Testing of Hot-Mixed Warm-Compacted Asphalt for Emergency Paving*, Report SERRI 70015-011, U.S. Department of Homeland Security Science and Technology Directorate, pp. 125.

Howard, I.L., Doyle, J.D. (2014). "Investigating the Consistency of Asphalt Density Measurement Methods Over a Wide Range of Air Voids," *Journal of Testing and Evaluation*, 42(3), pp. 749-760.

Howard, I.L., Baumgardner, G.L., Jordan III, W.S., Menapace, A.M., Mogawer, W.S., Hemsley, J.M. (2013). "Haul Time Effects on Unmodified, Foamed, and Additive-Modified Binders Used in Hot-Mix Asphalt," *Transportation Research Record: Journal of the Transportation Research Board*, 2347, pp. 88-95.

Howard, I.L., Baumgardner, G.L., Monismith, C.L. (2016). "Debating Cracking Performance Methods—Overview of Current Methods and State of Practice," *Journal of the Association of Asphalt Paving Technologists,* 85, pp. 777-806.

Hubbard, P., Field, F.C. (1926). "A Study of Certain Factors Affecting the Stability of Asphalt Paving Mixtures," *Proceedings of the American Society for Testing Materials*, 26, pp. 557-601.

Hubbard, P., Gollomb, H. (1937). "The Hardening of Asphalt with Relation to Development of Cracks in Asphalt Pavement," *Journal of the Association of Asphalt Paving Technologists,* 9, pp. 165-194.

Hughes, C.S. (1986). "Density Testing," *Journal of the Association of Asphalt Paving Technologists*, 55, pp. 607-614.

Hveem, F.N. (1943). "Quality Tests for Asphalts — A Progress Report," *Journal of the Association of Asphalt Paving Technologists*, 15, pp. 111-152.

Hveem, F.N. (1955). "Pavement Deflections and Fatigue Failures," *Highway Research Board Bulletin: Design and Testing of Flexible Pavement*, 114, pp. 43-87.

Hveem, F.N., Zube, E., Skog, J. (1962). "Proposed New Tests and Specifications for Paving Grade Asphalts," *Journal of the Association of Asphalt Paving Technologists*, 32, pp. 271-327.

Isola, M., Chun, S., Roque, R., Zou, J., Koh, C., Lopp, G. (2014). "Development and Evaluation of Laboratory Conditioning Procedures to Simulate Mixture Property Changes Effectively in the Field," *Transportation Research Record: Journal of the Transportation Research Board*, 2447, pp. 74-82.

Jacques, C., Daniel, J.S., Bennert, T., Reinke, G., Norouzi, A., Ericson, C., Mogawer, W., Kim, Y.R. (2016). "Effect of Silo Storage Time on Characteristics of Virgin and RAP Asphalt Mixtures," *Transportation Research Record: Journal of the Transportation Research Board*, 2573, pp. 76-85.

Jemison, H.B., Davison, R.R., Glover, C.J., Bullin, J.A. (1991). "Evaluation of Standard Oven Tests for Hot-Mix Plant Aging," *Transportation Research Record: Journal of the Transportation Research Board*, 1323, pp. 77-84.

Kandhal, P.S., Koehler, W.C. (1984). "Significant Studies on Asphalt Durability: Pennsylvania Experience," *Transportation Research Record: Journal of the Transportation Research Board*, 999, pp. 41-50.

Kari. (1982). "Effect of Construction Practices on the Asphalt Properties of the Mix," *Proceedings of the 27th Annual Conference of the Canadian Technical Asphalt Association*, Edmonton, Canada, pp. 310-334.

Kemp, G.R., Predoehl, N.H. (1981). "A Comparison of Field Laboratory Environments on Asphalt Durability," *Journal of the Association of Asphalt Paving Technologists*, 50, pp. 492-537.

Kim, Y., Wen, H. (2002). "Fracture Energy from Indirect Tension Testing," *Journal of the Association of Asphalt Paving Technologists*, 71, pp. 779-793

Koh, C., Roque, R. (2010). "Use of Nonuniform Stress-State Tests to Determine Fracture Energy of Asphalt Mixtures Accurately," *Transportation Research Record: Journal of the Transportation Research Board*, 2181, pp. 55-66.

Lang, F.C., Thomas, T.W. (1939). "Laboratory Studies of Asphalt Cements," *Bulletin of the University of Minnesota Engineering Experiment Station*, 55(15), Minneapolis, MN.

Lee, D.Y. (1977). "Asphalt Durability Correlation in Iowa," *Highway Research Record: Journal of the Highway Research Board*, 468, pp. 43-60.

Lottman, R.P., (1978). *Predicting Moisture-Induced Damage to Asphaltic Concrete*, NCHRP Report 192, National Cooperative Highway Research Program, Washington, D.C.

Lottman, R.P. (1982a). "Laboratory Test Method for Predicting Moisture-Induced Damage to Asphalt Concrete," *Transportation Research Record: Journal of the Transportation Research Board*, 843, pp. 88-95.

Lottman, R.P., (1982b). *Predicting Moisture-Induced Damage to Asphaltic Concrete: Field Evaluation*, NCHRP Report 246, National Cooperative Research Program, Washington, D.C.

Lund, J.W., Wilson, J.E. (1984). "Evaluation of Asphalt Aging in Hot Mix Plants," *Journal of the Association of Asphalt Paving Technologists*, 53, pp. 1-18.

Lund, J.W., Wilson, J.E. (1986). "Field Verification of Asphalt Aging in Hot Mix Plants," *Journal of the Association of Asphalt Paving Technologists*, 55, p. 92-119.

Lytton, R.L., Uzan, J., Fernando, E.G., Roque, R., Hiltunen, D., Stoffels, S. (1993). *Development and Validation of Performance Prediction Models and Specifications for Asphalt Binders and Paving Mixes*, Report SHRP-A-357, Strategic Highway Research Program, Washington, D.C.

Mirza, M.W., Witczak, M.W. (1995). "Development of a Global Aging System for Short and Long Term Analysis of Asphalt Cements," *Journal of the Association of Asphalt Paving Technologists*, 64, pp. 393-430.

Mohammad, L.N., Cooper, S.B.III (2016). "Implementation of a Balanced Asphalt Mixture Design Procedure: Louisiana's Approach," *Journal of the Association of Asphalt Paving Technologists*, 85, pp. 857-876.

Molenaar, A., Scarpas, A., Liu, X., Erkens, S. (2002). "Semi-Circular Bending Test; Simple but Useful?," *Journal of the Association of Asphalt Paving Technologists*, 71, pp. 794-815.

Monismith, C.L., Popescu, L., Harvey, J. (2004). "Performance-Based Pay Factors for Asphalt Concrete Construction; Comparison with a Currently Used Experience-Based Approach," *Journal of the Association of Asphalt Paving Technologists*, 73, pp. 147-194.

Moore, D. S. and GcCabe, G. (2005). *Introduction to the Practice of Statistics*, W. H. Freeman, New York.

Petersen, J.C. (1986). "Quantitative Functional Group Analysis Using Differential Infrared Spectrometry and Selective Chemical Reactions — Theory and Applications," *Transportation Research Record: Journal of the Transportation Research Board*, 1096, pp. 1-11.

Petersen, J.C., Robertson, R.E., Branthaver, J.F., Harnsberger, P.M., Duvall, J.J., Kim, S.S., Anderson, D.A., Christiansen, D.W., Bahia, H.U., Dongre, R., Antle, C.E., Sharma, M.G., Button, J.W., Glover, C.J. (1994). *Binder Characterization and Evaluation Volume 4: Test Methods*, Report SHRP-A-370, Strategic Highway Research Program, Washington, D.C.

Roque, R., Buttlar, W.G. (1992). "The Development of a Measurement and Analysis System to Accurately Determine Asphalt Concrete Properties Using the Indirect Tensile Mode," *Journal of the Association of Asphalt Paving Technologists*, 61, pp. 304-332.

Roque, R., Buttlar, W.G., Ruth, B.E., Tia, M., Dickson, S.W., Reid, B. (1997). *Evaluation of SHRP Indirect Tension Tester to Mitigate Cracking in Asphalt Pavements and Overlays*, Report No. B-9885, Florida Department of Transportation, Tallahassee, FL.

Rowe, G. M. (2011). Prepared Discussion of Anderson et al. (2011). *Journal of the Association of Asphalt Paving Technologists*, 80, pp. 649-662.

Santucci, L.E., Allen, D.D., Coats, R.L. (1985). "The Effects of Moisture and Compaction on the Quality of Asphalt Pavements," *Journal of the Association of Asphalt Paving Technologists*, 54, pp. 168-208.

Smith, B.T., Moore, R.A., and Howard, I.L. (2017). "Density Observations from a Full-Scale Untrafficked Test Section with Guidance for Dryback Methods," *Transportation Research Record: Journal of the Transportation Research Board*, 2630, DOI: 10.3141/2630-17.

Tandon, V., Kambham, B.S., Bonaquist, R., Solaimanian, M. (2004). "Results of Integrating Simple Performance Tests and the Environmental Conditioning System," *Transportation Research Record: Journal of the Transportation Research Board*, 1891, pp. 140-152.

Tandon, V., Nazarian, S. (2001). *Modified Environmental Conditioning System: Validation and Optimization*, Report No. TX-1/1826-1F, Texas Department of Transportation, Austin, TX., pp. 68.

Terrel, R.L., Al-Swailmi, S. (1994). *Water Sensitivity of Asphalt-Aggregate Mixes: Test Selection*, Report SHRP-A-403, Strategic Highway Research Program, Washington, D.C. pp. 183.

Vallerga, B.A., Monismith, C.L., Granthem, K. (1957). "A Study of Some Factors Influencing the Weathering of Paving Asphalts," *Journal of the Association of Asphalt Paving Technologists*, 26, pp. 126-148.

West, R., Rodezno, C., Julian, G., Prowell, B., Frank, B., Osborn, L.V., and Kriech, T. (2014). *Field Performance of Warm Mix Asphalt Technologies.* NCHRP Report 779, National Cooperative Highway Research Program, Washington, D.C.

Williams, K.L., Howard, I.L., Cooley, L.A. (2011). *The Effects of Coarse Aggregate Cleanliness and Moisture Content on Asphalt Concrete Compactability and Moisture Susceptibility*, Report No. FHWA/MS-DOT-RD-11-208, Mississippi Department of Transportation, Jackson, MS.

Wright, P.H., Paquette, R.J. (1966). "Hardening of Asphalt in Hot Bituminous Mixes During the Hauling Process," *Highway Research Record: Journal of the Highway Research Board*, 132, pp. 11-28.

Yin, F., Arambula-Mercado, E., Martin, A.E., Newcomb, D., Tran, N. (2016). "Long-Term Aging of Asphalt Mixtures," *Journal of the Association of Asphalt Paving Technologists*, 85, pp. 01-34.

Yin, F., Martin, A.E., Arambula, E., Newcomb, D.E. (2015). "Short-Term Aging of Asphalt Mixtures," *Journal of the Association of Asphalt Paving Technologists*, 84, pp. 333-368.

Zhang, Z., Roque, R., Birgisson, B., Sangpetngam, B. (2001). "Identification and Verification of a Suitable Crack Growth Law," *Journal of the Association of Asphalt Paving Technologists*, 70, pp. 206-241.

Zhou, F., Scullion, T. (2016). "Development and Implementation of Balanced Mix Design in Texas," *Journal of the Association of Asphalt Paving Technologists*, 85, pp. 839-852.

Zou, J. Roque, R., Chun, S., Lopp, G. (2013). "Long-term field evaluation and analysis of top-down cracking for superpave projects," *Road Materials and Pavement Design*, 14(4), pp. 831-846.